2009-12-21

Materials for Sustainable Constructions

Rosella Mafalda Ferraro
University of Miami, r.ferraro@miami.edu

UNIVERSITY OF MIAMI

MATERIALS FOR SUSTAINABLE CONSTRUCTIONS

By

Rossella Mafalda Ferraro

A DISSERTATION

Submitted to the Faculty
of the University of Miami
in partial fulfillment of the requirements for
the degree of Doctor of Philosophy

Coral Gables, Florida

December 2009

UNIVERSITY OF MIAMI

A dissertation submitted in partial fulfillment of
the requirements for the degree of
Doctor of Philosophy

MATERIALS FOR SUSTAINABLE CONSTRUCTIONS

Rossella Mafalda Ferraro

Approved:

_____ Antonio Nanni, Ph.D. Professor of the Civil, Architectural and Environmental Engineering	_____ Terri A. Scandura, Ph.D. Dean of the Graduate School
_____ Ronald Zollo, Ph.D. Professor of Civil, Architectural and Environmental Engineering	_____ Brian Metrovich, Ph.D. Assistant Professor of Civil, Architectural and Environmental Engineering
_____ Fabio Matta, Ph.D. Research Assistance Professor of Civil, Architectural and Environmental Engineering	_____ Nestore Galati, Ph.D. Design Engineer Structural Group Baltimore, Maryland

FERRARO, ROSSELLA MAFALDA (Ph.D., Civil Engineering)
Materials for Sustainable Constructions (December 2009)

Abstract of a dissertation at the University of Miami.

Dissertation supervised by Professor Antonio Nanni.
No. of pages in text. (123)

White cement has currently received increasing attention due to potential for use in sustainable concrete structures. Based on the U.S. Green Building Council certification practice, the LEED Green Building Rating System for New Construction and Major Renovation (LEED-NC) considers that the reflective quality of white surfaces may help to improve lighting efficiency and reduce temperature fluctuations, resulting in lower heating and cooling with reduction of related energy costs. In addition to the environmental impact, white concrete represents a valuable tool for the aesthetic acceptability of a structure, and can also offer important practical benefits in terms of safety (i.e., light reflection in the dark). In this thesis white concrete was combined with off-white rice husk ash and with a glass fibers reinforced polymer to obtain an innovative composite system able to: a) reduce the energy used for the production of the primary materials, b) decrease the temperature fluctuation in the building resulting in less energy needed for heating and cooling, and c) increase the life of the structure and thereby reduce energy usage for material disposal. It is evident that in applications where aesthetics is the driver, a great deal of attention needs to be devoted to the concrete mixture, but also to durability properties. To further improve the durability of white

concrete, novel methodologies were introduced to study the corrosion mechanism of steel embedded in concrete and its effect on the color degradation of white surface. This study demonstrates the validity of the sustainable system made by white cement, OWRHA, and GFRP, and of the methodology introduce to evaluate corrosion and color degradation of reinforced concrete.

To Lella & Salvatore with unconditioned love

ACKNOWLEDGEMENT

My Ph.D. years at the University of Miami had mentorship from numerous outstanding individuals from both within the university and outside of it. It is to these individuals that took part in my study, that my heartfelt gratitude and thanks go out to, for without their help, this thesis would not have made it to this point.

First and foremost I would like to express my sincere gratitude to my advisor, Dr. Antonio Nanni, for the continuous support of my Ph.D. study and research, for his patience, motivation, enthusiasm, and immense knowledge. His guidance helped me continuously during my research and writing of this thesis. I could not have imagined having a better mentor for my study.

Besides my advisor, I would like to thank the other members of my thesis committee: Dr. Roland Zollo, Dr. Fabio Matta, Dr. Brian Metrovich, and Dr. Nestore Galati for their encouragement, insightful comments, and challenging questions.

I would like to thank the faculty members of the Civil, Architectural and Environmental Engineering Department, and in particular Dr. Carol Hays, for her constant support, and Dr. James Giancaspro for challenging me in a way that only through time I could realize.

I would like to extend my gratitude to the National Science Foundation for the financial support in the form of SBIR Phase II funding and the Grant Number for the project NSF 0724463.

The contribution of materials and help from Artistic Stones Inc. (Miami, Florida), is gratefully acknowledged.

Dr. Clarissa Ferraris from the National Institute of Standards and Technology (NIST) is acknowledged for the help and assistance with the determination of the particle size distribution.

I gratefully thank Dr. Rajan Vempati for taking intense academic interest in this study as well as providing valuable suggestions that improved the quality of this study.

My special thanks goes to my friend Antonio. He never let me down when I needed his expertise in structural engineering, he encouraged me to grow and to expand my thinking. I was lucky to have such a good friend and partner at work.

Thank you to Alexander who was a true friend, an amazing person, and my personal psychologist for my doctoral paranoia. He helped me to concentrate on completing this dissertation and provided mental support during the course of this work. Without his help and encouragement, this study would not have been completed.

Dozens of people have helped and taught me immensely at the green-orange U of M. The graduate students of the CAE department, for sharing time, knowledge and experience with me throughout these three years; my undergraduates, Seana Campbell, Daniela Delgado, Ali Haji, Philip Hopkins, Ryan Goolabsingh, who helped me to understand my bent for teaching; the ASCE student chapter at UM for showing me the enthusiasm and firmness that they constantly put in the preparation of their regional conferences; the staff of the College of Engineering; and in particular Mrs. Carole Kavooras, who has been a source of love and chocolate since I met her.

My keen appreciation goes to Derek Schesser for his valuable assistance in the lab. Without his help, the lab work would have never been accomplished on time and in such good quality.

To my best friends Manuela, Valentina, Sara, and Raffaele goes my gratitude. They were always with me with their love, even from so far away.

Thanks to my roommate Jessica for many evenings filled with wine and interesting discussions, for the introduction to American traditions and to share with me her deep experiences of life.

Last, but not least, I thank my family: my parents, Lella and Salvatore, for giving me life in the first place, for educating me with aspects from science, for unconditional support and encouragement to pursue my interests, even when the interests went beyond boundaries of language, field and geography. Thanks to Spartacus, who woke me up in the middle of the night, who bit my favorite shoes, and gave me some of the happiest moments I had in Miami.

There are some supporting people that I might have forgotten: exhaustion plays havoc on memory. My humblest apologies for anyone I have forgotten!

TABLE OF CONTENTS

LIST OF FIGURES

LIST OF TABLES

Chapter 1

1. INTRODUCTION

1.1. PREFACE

The strong impact that buildings have on quality of environment, resource use, human health and global economy is one of the main drivers that helped the concept of sustainable construction become more and more popular during the last decade. By intellectually integrating building materials and methods, a sustainable building may meet users' needs, reduce impact on future generations, and promote environment quality, economic vitality, and social benefits [1]. Sustainable development means making a conscious choice every time: looking at its implications in terms of resources, waste, recycling, and the building's value as part of an area or frontage, and not just as a capital asset or liability. Integrating green building materials for new construction and innovative repair material systems into building projects can help reduce the environmental impacts associated with the extraction, transport, processing, fabrication, installation, reuse, recycling, and disposal of these source materials [2].

This project started with a partnership with a relatively small company named ChK Group INC, located in Plano, Texas. Their mission statement is to produce profitable products form solid inorganic industrial wastes (such as rice hulls and fly ash) and to develop eco-friendly and low-cost technologies for remediation of environmental

pollutants. With these objectives and the support of NSF resources, Chk Group demonstrated in a pilot-scale experiment the possibility to manufacture off-white rice hull ash (OWRHA) using a rotary furnace. The possibility to have an eco-friendly off-white hull ash, with no graphitic carbon, generated the idea to combine this green material with white cement and glass fibers reinforced polymer (GFRP) to make a durable white concrete. White concrete is an attractive architectural material widely used around the world. With the inclusion of pigments or additives to the mixture constituents, white cement allows for a broad spectrum of colors from bright whites and pastels to saturated colors in the final concrete product [3]. White concrete has currently received increasing attention due to its potential for use in sustainable concrete structures [4]. Based on the U.S. Green Building Council certification practice, the LEED Green Building Rating System for New Construction and Major Renovation (LEED-NC) considers that the reflective quality of white surfaces may help to improve reflective lighting efficiency and to reduce temperature fluctuations, resulting in lower heating and cooling with a reduction of resulting energy costs [5]. In addition to the environmental impact, white concrete represents a valuable tool for the acceptability of a structure, and can also offer important practical benefits in the transportation infrastructure in terms of traffic safety, particularly in overcast and rainy days. It is evident that in applications where aesthetics is the driver, a great deal of attention needs to be devoted to the concrete mixture, but also to the durability properties. To further improve the durability of white concrete the corrosion mechanism of steel embedded in concrete and its effect on the color degradation of white surface was studied.

Many studies have been conducted on corrosion of steel, considered the most important durability problem of reinforced concrete (RC) [6-7]. Corrosion of steel in concrete is often caused by exposure to chloride mainly from application of deicing salts or from exposure to marine environment. Chloride salts are highly soluble in water and dissolved ions penetrate concrete, either by convection or by diffusion, due to a concentration gradient between the environment and the concrete itself. Oxidation of steel reinforcement bars is due to an electrochemical process that results in concrete damage caused by the production of expansive FeO_2. In this reaction oxygen takes electrons from iron atoms, causing iron to go into the solution, and chloride ions are the catalysts, which represents the critical component in the corrosion process. Chloride ions are uniquely able to react with ferrous ions (iron in solution) after they are liberated from the rebar, allowing them to travel some distance before precipitating as iron hydroxide. After the ferrous ions are finally deposited, they oxidize further by reacting with oxygen. The product of the reaction is highly insoluble hydrated ferric oxides, with a volume much larger than that of the original iron in the rebar. The chloride ions are then released to return to the rebar and continue the corrosion cycle.

Some ion products are protective when they are thin and remain stable, e.g. ferrous hydroxide $Fe(OH)_2$ or "green rust". On the other hand, these are products which do not stop corrosion growth with time. The reduction of the steel cross area and simultaneous rust swelling induces a reduction of bond between steel and concrete. The primary corrosion product of iron is $Fe(OH)_2$ (or more likely $FeO \cdot nH_2O$), and can react with oxygen and water and yield to other products having different colors, such as red-

brown ($Fe(OH)_3$), green ($Fe_2O_3 \cdot FeO$) or black (Fe_3O_4) [8-9]. The strong pigmentation of these products inevitably affects the aesthetical of the white concrete.

A physical and chemical protection of the steel can considerably increase the durability of RC structures in terms of structural and aesthetic properties. The physical protection is made by the concrete itself. By reducing the porosity of the concrete and increasing the cover on the steel, the system provides electrochemical stability for the embedded bars. The steel can also be chemically protected by organic or metal coatings which increase the durability and the bond between reinforcement and concrete. Another way to avoid corrosion in RC structures is to use GFRP bars instead of steel. When correctly applied, composites can result in significant benefits related to both overall cost and durability. Other advantages include high strength and stiffness to weight ratios, resistance to corrosion and chemical attack, controllable thermal expansion, damping characteristics, and electromagnetic neutrality. In order to eliminate the corrosion problem and improve the mechanical properties of white concrete, it was considered to reinforce white concrete with GFRP and partially replace white portland cement with a pozzolanic material.

Previous studies recognized that the use of pozzolanic materials as a partial replacement to Portland cement is an effective means for improving the properties of concrete in terms of strength and durability. Pozzolans are materials that react with $Ca(OH)_2$ (C-H) generated during the hydration of cement to produce calcium-silicate-hydrate phase (C-S-H). It is well established that C-H is the weakest link in the strength chain of concrete. These crystals can be massive in size, but their inter-planar strength is low. The advantage of adding pozzolan in cement or concrete is that $Ca(OH)_2$ is

consumed in the pozzolanic reaction, and in its place additional C-S-H phase is formed, which is the primary binder in concrete. Thus, not only does the permeability of concrete decrease as a result of a denser matrix, but its strength does too. The lower permeability impedes the permeation of chemical solution in concrete; thereby, increasing its durability. Hence, the low impermeability-high strength concrete is designated as high performance concrete (HPC) [10]. The demand for Supplementary Cementing Materials (SCMs) used in the production of HPC, both in US and globally, is annually growing. A big part of the market is driven by high rise buildings, highway construction, and infrastructures built in severe environmental conditions, e.g. petrochemical plants and marine structures [11].

The competing SCMs products in the market are Silica Fume (SF) and metakaolin. Silica Fume is a byproduct generated by the ferrosilicon industry. The color of the ash is grey and is difficult to handle because of the ultrafine particle size. Besides, the presence of toxic metals is a concern. Therefore, the blended-SF cannot be used for architectural purposes. Furthermore, with the recent declining steel production the production of SF (a byproduct) has decreased significantly. Metakaolin is produced by heating high quality kaolinite at 1022°F, and the product is white in color with a particle diameter of 1.5 μm. The black rice hull ash (BRHA) byproducts from power and fuel usage plants are commercially available, but contain high graphitic-C with black color. Most of the previous work has been focused on rice hull ash with 3% or more graphitic-C. This graphitic-C decreases air entrainment resulting in poor freeze-thaw characteristics. For this reason, there is a very limited market for BRHA containing graphite C. Before Vempati et al. [12], no available technologies to either decrease or

eliminate the graphitic C content of the end product and produce off-white rice hull ash were available.

Vempati et al. [12-13] demonstrated the manufacturing of off-white rice hull ash introducing a new technique. Built on this novelty, this research project began. OWRHA is the product of rice husk, manufactured with a continuous process in a rotary furnace designed expressly for this application. The principal advantages of OWRHA are its off-white color with no graphitic carbon and absence of crystalline SiO_2 and toxic metals. Therefore, the product is not only environmental friendly but can also be used to make off-white concrete. The use of OWRHA can reduce material cost due to cement saving, increase the environmental benefit related to the disposal of waste materials, and reduce the carbon oxidation emission. Additionally, because of the color properties, OWRHA can be combined with white concrete and be used for architectural design, sustainable construction and safety application.

The aim of this thesis is to introduce a new composite system for sustainable construction, consisting of WPC and OWRHA. This study demonstrates that, because of the pozzolanic activity of OWRHA, this system has higher durability and strength than conventional white concrete. Furthermore, the system maintains its light reflective properties thanks to the low level of carbon in OWRHA which does not modify the color of the mixture. After demonstrating the pozzolanic activity of OWRHA, a study of the corrosion and color deterioration was conducted. Two original methodologies of testing were introduced in this thesis. The first methodology was designed to determine the occurrence of the first crack in concrete due to the corrosion of embedded steel. The second methodology was introduced to address the need of scientifically measure the

whiteness of the concrete and the color changes due to its degradation. The system OWRHA/WPC was also integrated with GFRP to demonstrate the high durability of this composite system.

1.2. OBJECTIVE

In this thesis, the characterization of an innovative sustainable material system, made by white concrete and off-white rice husk ash, is presented. The main objectives of this thesis are:

1. Realize a novel material for sustainable construction. The composite system is assumed to be able to: a) reduce the energy used for the production of the primary materials, b) decrease the temperature fluctuation in the building resulting in less needed energy for heating and cooling, and c) increase the life of the structure and thereby reduce the energy usage for material disposal.
2. Integrate different techniques to create a methodology which enables an accurate identification of the beginning of the corrosion process in concrete. This technique would also allow to better determine the influence that concrete quality has on the corrosion process.
3. Create a methodology to evaluate the color of concrete and its variation, applying technologies used in other disciplines. The methodology would consent to identify the phenomena that affect the degradation of the whiteness of the concrete due to composition and conditioning.

1.3. RESEARCH SIGNIFICANCE

White concrete is increasing in popularity thanks to its performance in the area of sustainable construction and safety applications. Additionally, previous studies have shown that one of the benefits of incorporating rice husk ash in concrete is the enhancement of the strength and resistance to chloride diffusion. In these studies, it has been proven that the incorporation of RHA reduces the chloride penetration and the chloride-induced corrosion initiation period of steel reinforcement. This thesis proposes to combine these two materials in order to obtain a strong, durable and sustainable product. The knowledge produced in this thesis on the use of OWRHA and its effects on strength, porosity, and corrosion resistance would be beneficial to future applications of this innovative material.

Because of the benefits related to the color and the reflectivity of white concrete, this project also focuses its attention on color analysis. The whiteness of the concrete, and its variation due to composition of mix design and environment conditions are investigated. This thesis may lead to the development of a more scientific methodology to evaluate the color durability needed to define the influencing parameters of the lightening reflectance deterioration.

The innovative material system consisting in WPC and OWRHA has the potential to reduce the energy waste related to production, maintenance and demolition of concrete structure, and become a certificate material for sustainable construction.

1.4. OUTLINE

In order to assess the effectiveness of the material system presented in this thesis, the manuscript is articulated in three studies:

Study I: This study presents the physical and chemical properties of a new generation RHA of off-white color, carbon neutral, and no crystalline SiO_2 and toxic metals. The effects on the mechanical properties of a mixture, using off-white rice hull ash (OWRHA) as partial replacement of white cement, are also investigated. The study was developed in two phases. In the first phase, physical and chemical properties of OWRHA are studied in order to define the pozzolanic activity of the material produced using the procedure developed by Vempati et al. [12]. The investigation included X-ray Diffraction (XRD), Fourier Transform Infrared Spectroscopy (FTIR), Thermogravimetric Analysis (TGA), and Scanning Electron Microscopy (SEM). In the second phase, studies on concrete specimens are conducted. This phase is mainly concerned with the effect of different OWRHA dosages in various curing periods on the compressive and splitting tensile strength.

Study II: This study presents the results of an experimental investigation on the strength, porosity, and corrosion resistance of white concrete blended with off-white rice husk ash (OWRHA). The process of corrosion is studied by means of accelerated corrosion tests with impressed voltage (ACTIV). Acoustic emission, visual inspection, and corrosion current measurements are used to follow the corrosion development. Compression, durability and accelerated corrosion tests are conducted on white portland cement specimens with different percentages of OWRHA. For all series, three mixtures with different WPC/OWRHA proportions, including the control specimen, were prepared

and tested. The water to binder ratio of 0.44 was maintained constant in order to reduce the variables and focus on the effect of OWRHA. Different OWRHA contents of 0, 7.5 and 15% by mass replaced the cement in the mixture. The first series is used to evaluate the compressive strength of the three mixtures at 7, 28, and 90 days. The second series is used to investigate the porosity and the coefficient of water absorption of each mixture at different ages. In the third series, reinforced concrete prisms are subjected to accelerated corrosion tests with impressed voltage (ACTIV). The time of initiation of the first crack is evaluated as measurement of the specimen's relative resistance against chloride attack and reinforcement corrosion. This parameter is evaluated by means of the results obtained with three different techniques: visual inspection, acoustic emission, and corrosion current measurement.

Study III: In this study the color performance of concrete using white cement and rice husk ash (RHA) as its partial substitute was analyzed. Variation with composition and environmental exposure of concrete color is investigated. The study is developed in two phases. In the first phase the color of each mixture component, used in phase II, is studied. Furthermore, the influence that the amount of carbon present in the ash has on the powder and on the hardened concrete color, is analyzed. The color of rice husk ashes produced with the same methodology developed from Vempati et al. [13], but with different time of processing, is tested. The time of processing is the main parameter governing the percentage of residual carbon in the ash. In this phase, the samples are tested in the form of powder and hardened concrete incorporating different percentage of RHA. In the second phase, concrete beams with and without reinforcement were cast from three batches containing different amounts of RHA and were exposed to different

environments. A new methodology to condition the samples and monitor color and pH of the concrete is introduced.

Chapter 2

2. Study I: Carbon Neutral Off-White Rice Husk Ash as a Partial White Cement Replacement

2.1. Background

Rice husk as an agricultural residue, constitutes the largest (about 20%) and most worthless by-product of the rice milling industry. About 70 million tons of rice husk ash (RHA) is produced annually worldwide [24], and since the husk does not biodegrade or burn easily [25] it is considered an environmental nuisance. When burned, the ash of rice husk contains the highest proportion of silica among all the plant residues, nearly 20% silica in amorphous form [26]. Under controlled combustion conditions, this by-product can produce amorphous silica with high reactivity [21-28] studied the properties of mortars containing different percentage of RHA and noted not only an increase in compressive strength, but also a reduction in absorption characteristics and in oxygen permeability. Cost reduction, performance, durability and environmental concerns are the primary characteristics that can make RHA a valid alternative to Portland cement [29-31].

Until the 1970's, production of RHA was by uncontrolled combustion and for this reason the product was usually crystalline and poor in pozzolanic properties [32]. After

Mehta [22] described the effect of pyroprocessing parameters on the pozzolanic reactivity of RHA, Pitt [34] designed a fluidized-bed furnace for controlled combustion of RHA. By controlling temperature and atmosphere a highly reactive RHA was obtained. Today, RHA generated by the processes that are on the market contains 3% or more with graphitic carbon which determines the dark pigmentation of the material, restricting its utilization in architectural applications where color is the driver. This leads to excessive demand from water and chemical admixtures in order to maintain appropriate slump and air content [35-36]. There have been some attempts to produce amorphous SiO_2 from rice husk using different techniques, but none of these methods has successfully produced commercial-scale off-white amorphous SiO_2 with less than 1% amorphous carbon [37-39]. Vempati et al. [12] developed a new continuous production process of manufacturing RHA in which the rotary tube furnace was maintained in aerobic conditions and temperature at 700ºC with a residence time of 40 min to obtain off white RHA with carbon content less than 0.3%. This carbon neutral ash is off-white color with no graphitic carbon, no crystalline SiO_2 and toxic metals, and therefore considered environmentally friendly. The reduction of carbon in portland cement concrete is not the only reason that makes this material sustainable. Based on the U.S. Green Building Council certification practice, the LEED Green Building Rating System for New Construction and Major Renovation (LEED-NC) [5] considers that the reflective quality of white surfaces may help to improve lighting efficiency and reduce temperature fluctuations, resulting in lower heating and cooling of the structure and related energy costs. The off-white rice husk ash (OWRHA) can be combined with white cement to obtain off-white concrete for sustainable constructions.

The objective of this research is to provide information on the utilization of the OWRHA as a partial cementitious binder substitute with reference to pozzolanic activity and strength of hardened concrete. Different mixtures were tested in order to evaluate the favorable percentage of replacement of white portland cement (WPC) with OWRHA. The results are also compared to experimental values of RHA available in the literature.

2.2. EXPERIMENTAL INVESTIGATION

The study was developed in two phases. In the first phase, physical and chemical properties of OWRHA were studied in order to define the pozzolanic activity of the material produced using the procedure developed by Vempati et al. The investigation included X-ray Diffraction (XRD), Fourier Transform Infrared Spectroscopy (FTIR), Thermogravimetric Analysis (TGA), and Scanning Electron Microscopy (SEM). In the second phase, studies on concrete specimens were conducted. This phase was mainly concerned with the effect of different OWRHA dosage in varied curing periods on the compressive and splitting tensile strength.

2.3. PHASE I

2.3.1. MATERIALS

2.3.1.1 OWRHA

OWRHA was manufactured by burning rice husk procured from a rice mill plant located at Jonesboro, AK. The continuous process of manufacturing off white RHA with <0.3% amorphous carbon is summarized as follows. A rotary tube furnace set to maintain an aerobic condition and temperature at 700ºC was used. The residence time of the rice hulls in the furnace was 40 min. Unground OWRHA was used after determining that its particle size was comparable to that of white portland cement (WPC). Generally, reactivity of cementitious materials is also favored by increasing the fineness of the pozzolanic materials [40-42]; however, [21] demonstrated that a high degree of fineness of RHA grindings should be avoided since this material gains its pozzolanic activity mainly from the internal surface area of the particles. The main chemical components of OWRHA as used in this project are summarized in Table 2-1. The total percentage composition of iron oxide (Fe_2O_3 = 0.13%) Silicon dioxide (SiO_2 = 94.8%) and Aluminum Oxide (Al_2O_3 = 0.52) was found to be 95.45%. The value is considerably above the required value of 70% minimum for pozzolans (ASTM C 618).

2.3.2. PARAMETERS AND RESULTS

2.3.2.1 X-RAY DIFFRACTION (XRD)

The mineralogy of OWRHA was obtained with a Philips X'pert System diffractometer (Philips Electrical Co., Almelo, Netherlands). Using about 0.0053 oz, the XRD patterns were recorded with a diffraction angle of 5- 40 2θ at a scan rate of 3 min^{-1} using Ni-filtered CuKα (1.584Å) radiation. The X-ray diffraction pattern (Fig. 2-1) showed a pattern which is typical for amorphous solids [43]. The broad smooth hump between 15° 2θ and 35° 2θ indicates that pyrolysis converted the ordered crystalline cellulose structure into a random amorphous structure. Previous studies have shown that RHA with most of its silica in an amorphous form, as in this case, is highly reactive and can considerably improve the strength and durability of concrete.

2.3.2.2 FOURIER TRANSFORMATION INFRARED SPECTROSCOPY (FTIR)

OWRHA was characterized by infrared spectroscopy. The FTIR spectrum of OWRHA was collected in the transmission mode using a Perkin Elmer 2000 (Perkin Elmer, Massachusetts, USA). 0.0105 Oz of KBr was mixed with 0.00021 oz of the sample, and 128 scans were collected and averaged. The FTIR spectrum of OWRHA is presented in Fig. 2-2. The FTIR study showed the presence of -O-Si-O- vibrations attributable to asymmetrical stretching bands which occurred around 1220 cm^{-1} and 1080 cm^{-1} in the form of shoulder and broad bands respectively. Symmetrical stretching band

occurred at 773 cm^{-1}, and Si-O bending band at 466 cm^{-1}. Free water band were observed at 3436 cm^{-1}. The position of these bands confirmed that the material was amorphous SiO_2.

2.3.2.3 THERMOGRAVIMETRY

Thermogravimetric analysis of OWRHA was calculated using a TGA-HP (TA Instruments, Delaware, USA). The analysis was carried out by heating the sample from ambient to 1742°F at a rate of 36°F per minute while under a nitrogen atmosphere. The total weight loss over the temperature range was then calculated using Universal Analysis software (TA Instruments, Delaware, USA). The TGA indicated that the loss of ignition of OWRHA is ~0.03% (Fig. 2-3), which demonstrates the absence of residual combustible carbon, reducer of the pozzolanic activity.

2.3.2.4 PARTICLE SIZE DISTRIBUTION

Particle size distribution of WPC and OWRHA was determined using a laser diffraction particle size analyzer Malvern (Malvern Instruments, Worcestershire, UK). The particle size distribution curves shown in Fig. 2-4 suggest that WPC and OWRHA have comparable particle size distribution. The particle density was $6.24x10^{-3}$ oz/in^3 for both materials and the specific surface area is 903 ft^2/lbs for OWRHA and 1172 ft^2/lbs for WPC. Previous study showed that the high fineness of RHA had a greater pozzolanic

reaction and the small particles could also fill in the voids of the mortar mixture, thus increasing the compressive strength and durability of the mortar (Rukzon and Chindaprasirt 2006; Rukzon et al. 2009). Therefore, if unground OWRHA can increase the properties of the concrete, then finer particles (higher grinding time) may further improve the final product.

2.3.2.5 SCANNING ELECTRON MICROSCOPY (SEM)

The SEM analysis was performed on WPC and OWRHA to study the microgeometry of the material. The particles were imaged using Environmental SEM (ESEM) system (Philips XL30 ESEM-FEG, Philips Electrical Co., Almelo, Netherlands). Scanning Electron micrographs of the material were taken in the variable pressure secondary electron (VPSE) mode with the following instrument parameters: electron beam energy and probe current were 5 KV and 170 A, respectively, with a variable working distance. The SEM image reveals that OWRHA consists of irregular-shaped particles with porous cellular surface (Fig. 2-5) typical of unground RHA [46]. The basic cellular structure comes from the organic material from which OWRHA is derived and is responsible for the high surface area of the material even when the particles size in not fine [47].

2.3.3. PHASE I CONCLUSIONS

From the characterization of OWRHA carried in Phase I it can be stated that this product has proven to be an effective pozzolanic material with high amorphous silica content and high specific surface area. The effect of OWRHA as supplementary cementitious material for white Portland cement is evaluated in Phase II.

2.4. PHASE II

2.4.1. MATERIALS

2.4.1.1 AGGREGATES

Clean river sand with specific gravity 2.55 and fineness modulus of 2.49 was used as fine aggregate. Locally available well ground limestone of size greater than 0.16 in. and less than 0.47 in., with specific gravity of 2.6, was used as coarse aggregate.

2.4.1.2 WHITE PORTLAND CEMENT

White Type I Portland cement conforming to ASTM C 150 – 07 was utilized. The cement had a specific gravity of 3.15 and a fineness of 812,745 ft^2/lbs. The main chemical components of the WPC used are presented in Table 2-1.

2.4.1.3 SUPERPLASTICIZER

High-range water reducing admixture (Adva 140M, Grace Construction Product, Maryland, USA) was used to maintain a constant consistency, expressed as a constant slump without any additional amount of mixing water and without any direct effect on the compressive strength of the concrete. This superplasticizer is based on polycarboxylate technology and meets the requirements of ASTM C494 as a Type A and F, and ASTM C1017 Type I.

Following the industry practice, a typical slump for ordinary decorative application would be in the 4 to 5 in. range, and this value was adopted as the target in the study of the different mixtures tested.

2.4.1.4 MIX DESIGN AND SPECIMENS

Three mixtures with different WPC/OWRHA proportions, including the control one, were prepared and tested for the mechanical characterization of the concrete. The water to binder ratio of 0.44 was maintained constant in order to focus on the effect of OWRHA. Different OWRHA contents of 0, 7.5, and 15% by mass of cement, replaced an equal weight of cement in the mix. Blended cements were prepared by replacing WPC with OWRHA in dry conditions. The mixtures were thoroughly homogenized and kept in polyethylene containers. The three batches were coded as W0, W7.5 and W15, where the digits represent the percentage of OWRHA in the blended cement. The mix proportions are presented in Table 2-2.

Eighteen cylinders of 4 in. diameter and 8 in. height were cast from each batch and used for compressive strength testing (9) and splitting tensile strength testing (9). For each batch and age three cylinders were tested in compression and three in splitting. Even though the sample size is limited and does not allow for complete statistical analysis and generalization, it remains valid for relevant considerations on properties trends. The specimens were cast, compacted and cured according to the ASTM C 192. Compressive strength was determined as per ASTM C39M after 7, 28 and 90 days of moist curing at 68°F and RH of 95%. Splitting tensile strength tests were conducted as per ASTM 496M after 28 days of moist curing at 68°F and RH of 95%. A SATEC MKIII-C with 400 kips capacity was used for both tests.

2.4.2. PARAMETERS AND RESULTS

2.4.2.1 MECHANICAL PROPERTIES

Table 2-3 shows the average compressive strength of concrete mixed with different percentages of OWRHA (0, 7.5, and 15% by weight) at different ages. Fig. 6 shows the data of each sample tested and the average value is reported with a dash line. The compressive strength of OWRHA blended concrete containing 7.5 and 15% are comparable and higher than the control mix at all ages.

The test data indicate that the splitting tensile strengths of control mix and concrete incorporating OWRHA are comparable (Fig. 2-7). As reported in

Table **2-4**, at 28 days, the 15% OWRHA blended concrete shows an increase of the splitting tensile strength of ~9% respect to the control concrete. Only very low increase (~2%) was demonstrated for the 7.5% blend. Table 2-5 shows normalized experimental values for compression and tensile strength of rice hull ash (RHA) blended concrete in the literature [48-50]. The literature was selected choosing mix design with about the same w/c ratio (~0.4) and the same percentage of replaced cement of the one tested in this research, but with a high-r carbon content (-CC) in RHA. For the batch W7.5 it was not possible to find any previous work with the same percentage of replacement, so the comparison was made using 10% RHA blended cement. The comparison shows that white cement, blended with OWRHA, has mechanical properties comparable to concrete made with RHA with carbon content higher than 0.03.

2.5. CONCLUSIONS

From the results obtained it can be concluded that:

1. Because of the high amorphous silica and specific surface area, OWRHA is an effective pozzolanic material, employable as SCM.
2. A percentage of WPC as high as 15% by weight can be replaced with OWRHA without any adverse effect on strength properties.
3. The compressive strength of OWRHA blended white concrete increases with cement replacement percentage and specimen age.

4. The comparison of the results obtained from OWRHA blended white concrete with literature related to RHA demonstrates that the compressive and splitting tensile strength are not negatively affected by the use of this byproduct.

Table 2-1 Chemical composition (% by mass)

Element Composition	White Portland Cement Type I	OWRHA (1112°F for 180 min)
SiO_2	23.06	94.8
Al_2O_3	4.46	0.52
Alkalis	2.37	2.92
C	-	0.24
P_2O_5	-	1.09
Fe_2O_3	0.25	0.13
MnO	-	0.39
CaO	66.6	-
SiO_3	3	-
MgO	0.26	-

Table 2-2 Mix proportions

Mix Design	OWRHA (%)	Quantities (kg/m^2)					Water/Cement
		Cement	OWRHA	Sand	Coarse aggregates	Water	
W0	0	470	0				
W7.5	7.5	435	35	1193	468	211	0.45
W15	15	400	70				

Table 2-3 Average concrete compressive strength of tested concrete at different ages

Mix No.	Symbol	Average compressive strength			Average compressive strength			Average compressive strength		
		psi	Normalized	COV	psi	Normalized	COV	psi	Normalized	COV
		7 days			28 days			90 days		
1	W0	4003	100	3%	5236	100	2%	5511	100	0.4%
2	W7.5	4061	101	1%	5947	113	1%	6440	117	1%
3	W15	4235	106	1%	6034	115	1%	6614	120	1%

Table 2-4 Average splitting tensile strength of tested concretes at 28 days

Mix No.	Symbol	Average splitting tensile strength		
		psi	Normalized	COV
		28 days		
1	W0	653	100	4%
2	W7.5	667	103	2%
3	W15	711	109	1%

Table 2-5 Comparison of the results of the present study with experimental values of rise hull ash (RHA) in the literature

% of cement replaced with RHA	Investigator	Normalized compressive strength			Normalized splitting tensile strength
		7 days	28 days	90 days	28 days
10	Sarawathy/Song (2007)	112	103	-	104
	Ganesan et al. (2008)	103	111	117	103
	Sakr (2006)	108	111	114	-
	Zhang/Malhotra (1996)	108	106	111	130
	Rodriguez de Sensale (2006)	-	-	-	102
7.5	Present Study	101	113	117	103
15	Sarawathy/Song (2007)	116	103	-	110
	Ganesan et al. (2008)	108	113	119	109
	Sakr (2006)	118	112	115	-
	Zhang/Malhotra (1996)	-	-	-	-
	Rodriguez de Sensale (2006)	-	-	-	-
	Present Study	106	115	120	109

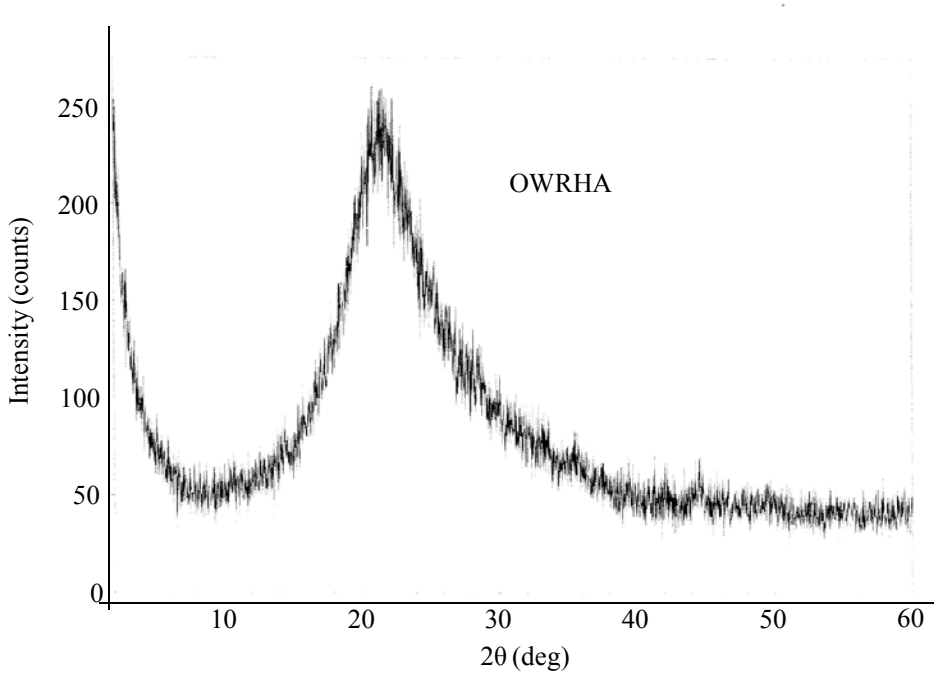

Fig. 2-1 X-Ray diffractogram of OWRHA

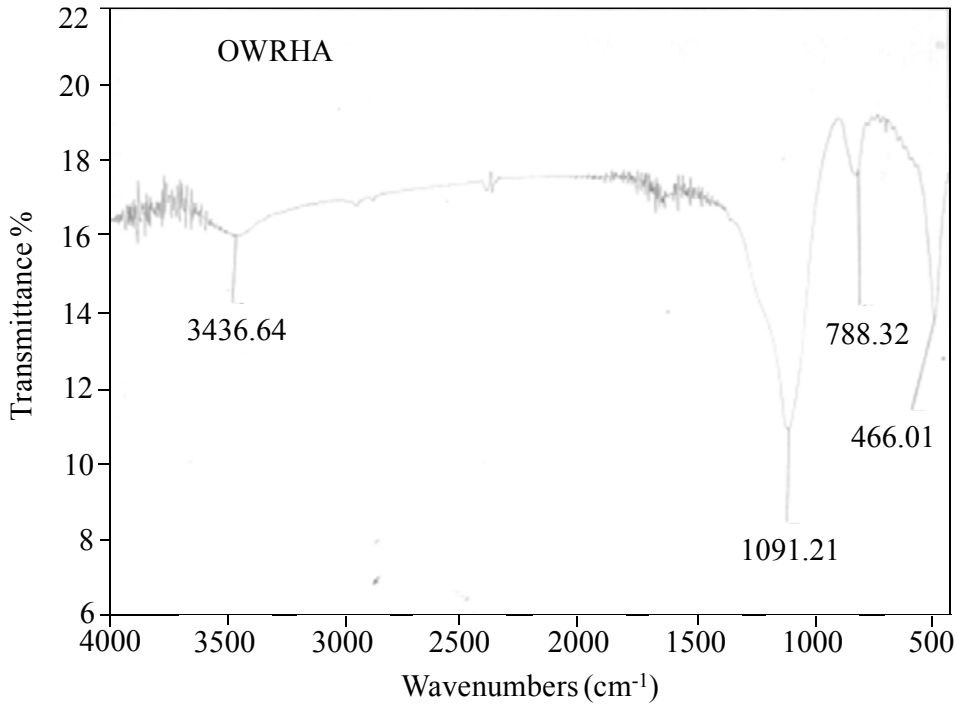

Fig. 2-2 FTIR of OWRHA

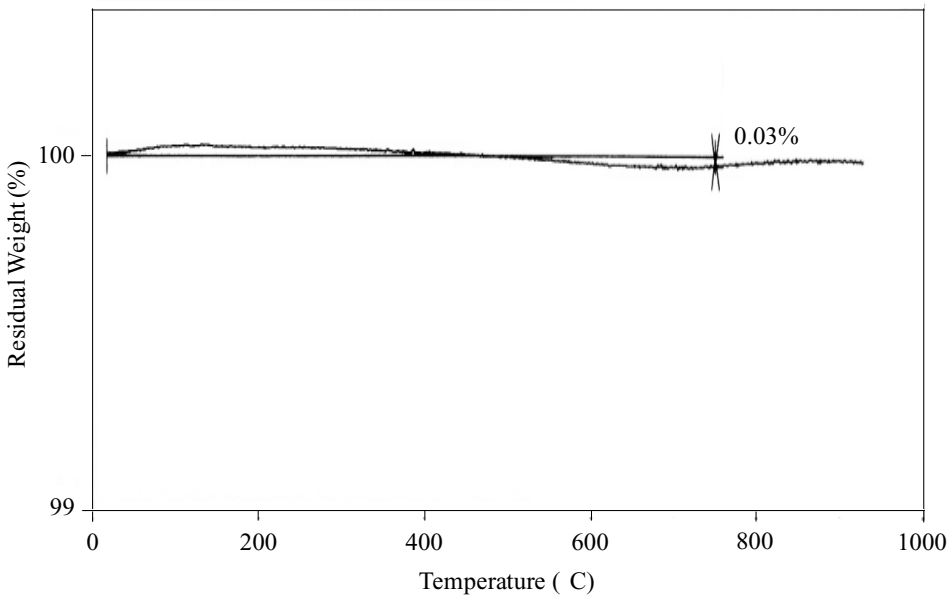

Fig. 2-3 – Thermogravimetric analysis of OWRHA

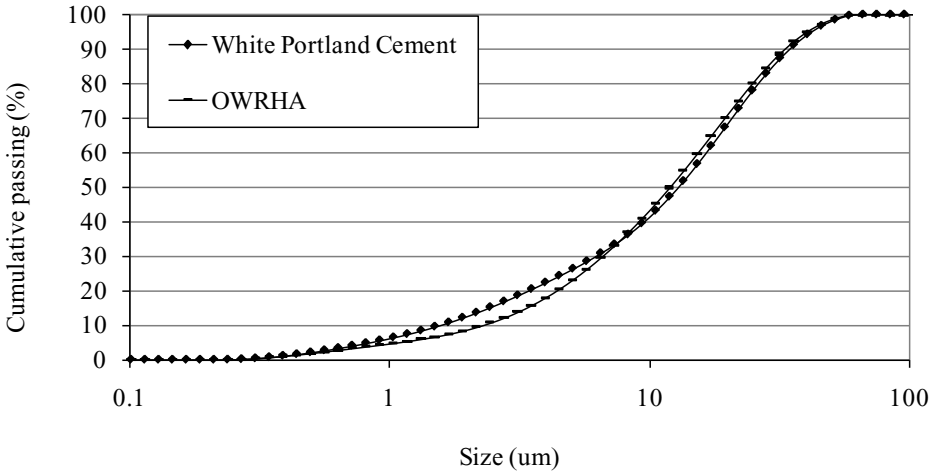

Fig. 2-4 – Particle size distribution of OWRHA and WPC

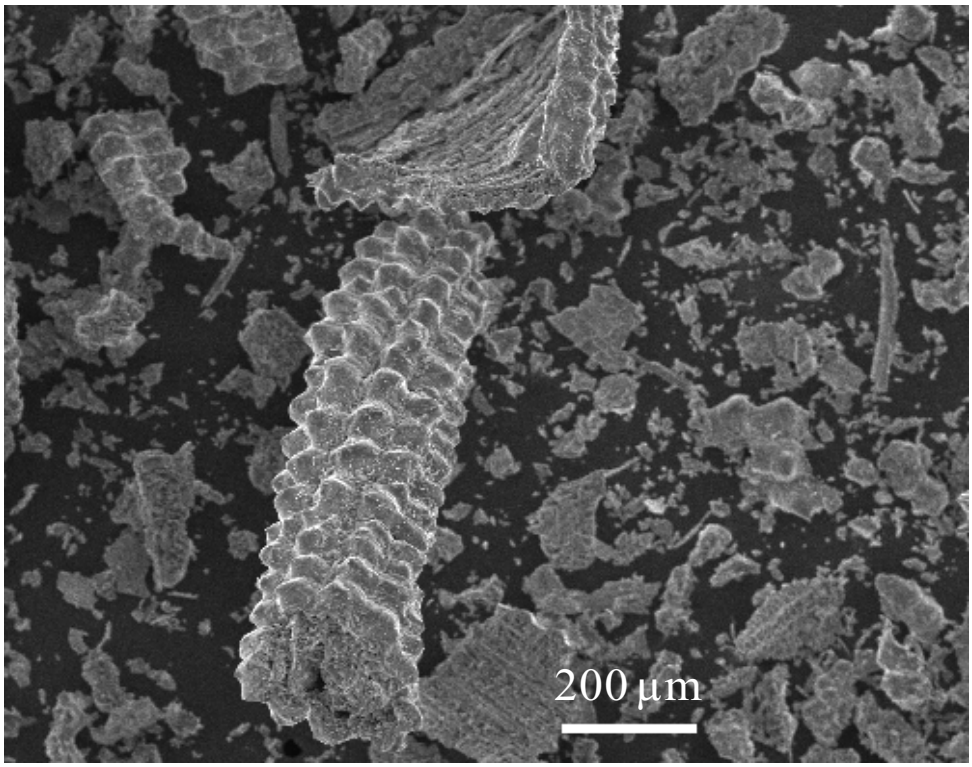

Fig. 2-5– SEM of OWRHA

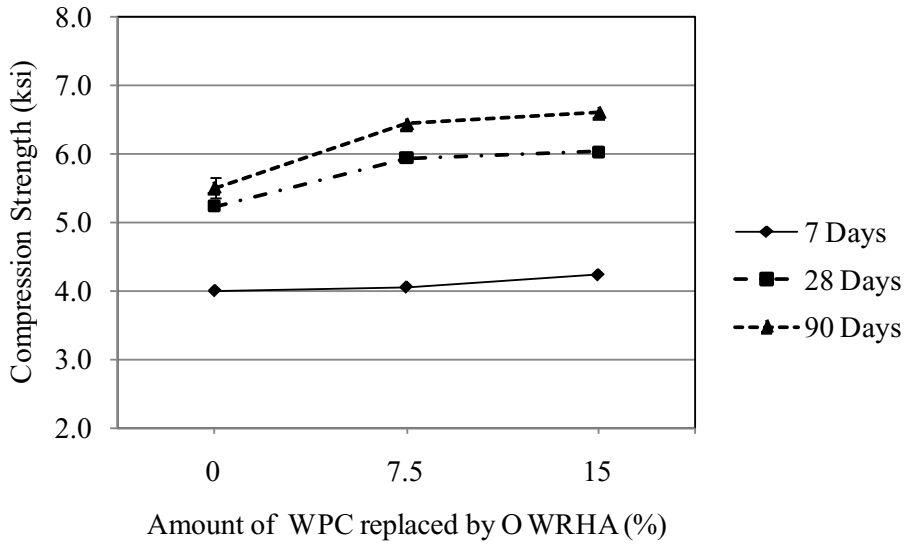

Fig. 2-6– Compressive strength (MPa) vs. percentage of OWRHA at different ages

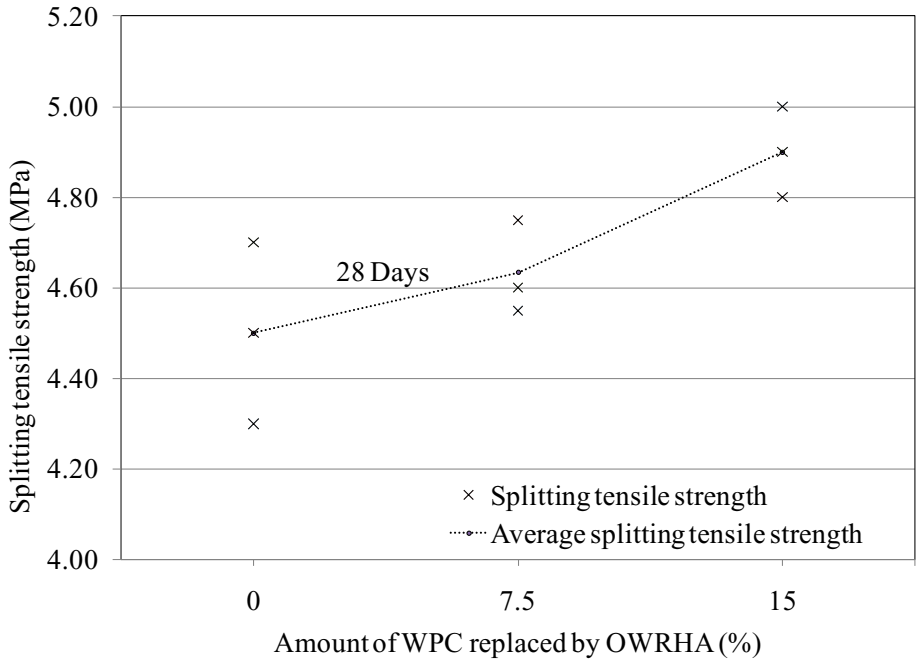

Fig. 2-7– Splitting tensile strength (MPa)[1] vs. percentage of OWRHA at 28 days

[1] 1 MPa = 145 psi

Chapter 3

3. Study II: Corrosion Study of Rice Husk Ash Blended Concrete

3.1. Background

Steel reinforced concrete (RC) is the most widely used construction material. Many studies have been conducted on the corrosion of steel, considered the most important durability problem of reinforced concrete [51-52]. Previous works have demonstrated that the high pH of the concrete, due to the cement hydration, sustains electrochemical stability conditions for the embedded steel bars, and that the concrete itself creates a physical barrier that delays the ingress of aggressive agents and the onset of the corrosion process [53-55]. Concrete is a porous material and therefore protection of the steel is not always effective. Mixture design, quality of the constituents, and care exercised during casting and curing of the concrete are the main variables that determine the quality of the concrete and therefore the protection of the steel.

Corrosion of the steel reinforcement is frequently caused by exposure to chloride mainly from application of deicing salts or from exposure to marine environments [56]. Chloride salts are highly soluble in water. The ions dissolved in water penetrate concrete, either by convection or by diffusion, due to a concentration gradient between the

environment and the concrete. Steel oxidation and the production of expansive products due to an electrochemical process result in damage to the concrete caused by the corrosion of reinforcement. Oxygen is the reactant, which takes electrons from iron atoms, causing iron to go into the solution, while the chloride ion is the catalyst, and represents the critical component in the corrosion process. Chloride ions are uniquely able to react with ferrous ions (iron in solution) after they are liberated from the rebar, allowing them to travel some distance before precipitating as iron hydroxide. When the ferrous ions are finally deposited, they oxidize further by reaction with oxygen and become highly insoluble hydrated ferric oxides, with a volume much larger than that of the original iron in the rebar. This expansion pressure induces tensile stresses in concrete around the reinforcing bar, and the continuous increase of pressure eventually causes cracking through the concrete cover. The chloride ions are then released to return to the rebar and continue the corrosion cycle [57-59].

A recent study commissioned by the Federal Highway Administration states that the cost of corrosion in the USA consumes about $286 billion per year [60]. To overcome this problem, new solutions have been introduced, including the use of supplementary cementitious materials (SCMs). Previous studies recognized that, because of their pozzolanic properties, SCMs as a partial replacement to portland cement are an effective means for improving the properties of the concrete. Pozzolans are materials that react with $Ca(OH)_2$ (C-H) generated during the hydration of cement to produce calcium-silicate-hydrate phase (C-S-H). It is well established that C-H is the weakest link in the strength chain of concrete [61] as these crystals can be massive in size, but their inter-planar strength is low (145 ÷ 218 psi). The advantage of adding pozzolan to cement or

concrete is that $Ca(OH)_2$ is consumed in the pozzolanic reaction, and in its place additional C-S-H phase is formed as the primary binder in concrete. Thus, not only does the permeability of concrete decrease as a result of a denser matrix, but its strength does too. The lower permeability impedes the permeation of chemical solutions in concrete, thereby increasing its durability [62-63].

Significant research has been directed towards the utilization of rice husk ash (RHA) as SCM [63-64]. Rice husk is a major agricultural waste, constituting the largest (about 20%) and most worthless by-product of the rice milling industry. About 70 million tons of RHA is produced annually worldwide [24], and since the husk does not biodegrade or burn easily [25], it is considered as an environmental nuisance. The burned ash of rice husk contains the highest proportion of silica among all the plant residues: nearly 20% silica in amorphous form [26], and under controlled combustion conditions, this by-product can produce an amorphous silica with high reactivity [22]. Spite et al. [27] studied the properties of mortars containing different percentages of RHA and noted an increase in compressive strength, and a reduction in absorption characteristics and in oxygen permeability. Cost reduction, performance, durability, and environmental concerns are the primary characteristics that can make RHA a competitive additive to portland cement [29-31].

Until the 1970s, the production of RHA was by uncontrolled combustion, and for this reason the product was usually crystalline and with a considerable amount of unburned carbon (~30%), resulting in a poor pozzolanic activity [21]. After Mehta [21] described the effect of pyroprocessing parameters on the pozzolanic reactivity of RHA,

Pitt [23] designed a fluidized-bed furnace for controlled combustion of RHA, which allowed for the control of temperature and atmosphere, and to obtain a highly reactive RHA. Nowadays, RHA produced with commercially available equipment contains 3% or more of graphitic carbon, which determines the dark pigmentation of the material. This restricts its utilization to architectural applications where color is the driver, and leads to excessive demand from water and chemical admixtures in order to maintain appropriate slump and air content [35-36]. There have been some attempts to produce amorphous SiO_2 from rice husk using different burning techniques, but none of these methods has successfully produced commercial-scale off-white amorphous SiO_2 with less than 1% amorphous carbon [37-39]. In 2006, Vempati et al. [65] developed a new continuous production process to manufacture RHA. The rotary tube furnace was maintained in aerobic conditions and at a temperature of 1292ºF with a residence time of 40 min to obtain off white RHA with carbon content less than 0.3%.

The purpose of this study is to examine the effect on the concrete strength and durability of the RHA produced using the procedure developed by Vempati et al. [65]. This carbon neutral ash is off-white in color, with no graphitic carbon, no crystalline SiO_2 and toxic metals, and is legitimately considered environmentally friendly. In this work, white portland cement (WPC) and off-white rice husk ash (OWRHA) were blended in different ratios to evaluate the effect of OWRHA on concrete in terms of strength, porosity and corrosion resistance.

3.2. EXPERIMENTAL INVESTIGATION

Compression, durability and accelerated corrosion tests were conducted on WPC specimens with different percentages of OWRHA. For all series, three mixtures with different WPC/OWRHA proportions, including the control one, were prepared and tested. The water to binder ratio of 0.44 was maintained constant in order to reduce the variables and focus on the effect of OWRHA. Different OWRHA contents of 0, 7.5 and 15% by mass of cement replaced the cement in the mixture. The first series was used to evaluate the compressive strength of the three mixture at 7, 28, and 90 days. The second series was used to investigate the porosity and the coefficient of water absorption of each mixture at different ages. In the third series, RC prisms were subjected to accelerated corrosion tests with impressed voltage (ACTIV). The time of initiation of the first crack was evaluated as a measure of the relative resistance to chloride attack and corrosion of the reinforcement. This parameter was studied by means of the results obtained with three different techniques: visual inspection, acoustic emission, and corrosion current measurement.

3.3. MATERIALS

The concrete mixtures were made using the following materials and mix proportions.

3.3.1. WHITE PORTLAND CEMENT

White Type I Portland cement conforming to ASTM C 150 – 07 was utilized. Its physical properties and chemical composition are given in Table 3-1.

3.3.2. OWRHA

OWRHA was manufactured by burning rice husk procured from a rice mill plant located in Jonesboro, AK (USA). To manufacture OWRHA with less than 0.3% amorphous carbon, a rotary tube furnace was used to maintain the process in aerobic conditions at a temperature of 1392ºF and residence time of 40 min.

After confirming that the particle size of OWRHA was comparable to that of white Portland cement (WPC), unground OWRHA was employed in this stage of the project shows the particle size distribution of the two binders. Typically, reactivity of cementitious materials is also favored by increasing in fineness of the pozzolanic material [66-73]; however, Mehta20 [21] demonstrated that a high degree of fineness of RHA's grinding should be avoided since this material gains its pozzolanic activity mainly from the internal surface area of the particles. The main chemical components of OWRHA as used in this project are summarized in Table 3-1. The value of the total percentage composition of iron oxide, silicon dioxide, and aluminum oxide was found to be 95.45%, which is considerably above the required value of 70% minimum for pozzolans (ASTM C 618).

3.3.3. Fine and Coarse Aggregates

The fine aggregate was clean river sand with a specific gravity of 2.55 and fineness modulus of 2.49. The coarse aggregate was ground limestone of size greater than 0.15 in. and less than 0.5 in. with a specific gravity of 2.60.

3.3.4. Superplasticizer

High-range water reducing admixture (Adva 140M, Grace Construction Product, Maryland, USA), was used to maintain a constant workability, expressed as a constant slump without any additional amount of mixing. This superplasticizer is based on polycarboxylate technology and meets the requirements of ASTM C494 as a Type A and F, and ASTM C1017 as Type I.

Following the industry practice, a typical slump for ordinary architectural concrete application would be in the range of 4÷5 in. This value was adopted as the target of the different mixtures tested in the study.

3.4. Mix Design and Specimens

Three different proportions of concrete mixes, including the control mixture, were prepared with a water/cement ratio of 0.44. Blended cements were prepared by replacing WPC with OWRHA in dry conditions. The mixtures were thoroughly homogenized and

kept in polyethylene containers. The mix proportions and the designations are presented in Table 2-1.

Plain concrete cylinders 6 in. in diameter and 12 in. in height were used to determine the compressive strength of each batch. The specimens were cast in two layers, compacted and cured according to ASTM C 192. For the durability test, plain concrete blocks specimens of cross section 4 in. by 4 in. and height 2 in. were used for this investigation. The samples were cast, compacted using a vibrating table, and moist cured at 68°F with a RH of 95%. For the corrosion test, concrete prism of cross section 2 in. by 2 in. and height 6 in., with on embedded one #2 steel rebar 6 in. long were used. The steel was positioned such that, centered from the sides, it protruded from the top surface of the prism by 0.5 in., and was spaced 0.5 in. from the bottom (Fig. 3-3). The exposed area of the steel bar was protected with an epoxy resin coating. The concrete prisms were cast in two layers, vibrated and covered for 24 hours with a plastic sheet. Following this period, the specimens were demolded and cured in distilled water to prevent chloride contamination.

3.5. PARAMETERS AND RESULTS

3.5.1. COMPRESSIVE STRENGTH

In order to determine the mechanical properties of each batch, compression tests were performed. The compressive strength of each batch was determined in accordance with ASTM C 39 after 7, 28 and 90 days of curing. After casting, the specimens were left

covered with a plastic sheet for 24 hours, and then moist cured for the designated time. For each batch and age, three cylinders were tested in compression. Even though the sample size is limited and does not allow for complete statistical analysis and generalization, it remains valid for considerations on property trends.

Table 3-3 reports the average and the normalized value with respect to the 0% OWRHA batch, of compressive strength of the three batches tested at 7, 28 and 90 days of moisture curing. The experimental results reveal that the incorporation of either 7.5 or 15% of OWRHA does not adversely affect the strength of concrete. The strength of OWRHA concrete increases with the blending percentage and with the age of the concrete. The incorporation of OWRHA improves the strength of concrete at all ages, which means that OWRHA has good reactivity, and the pozzolanic reaction starts rapidly.

3.5.2. EFFECTIVE POROSITY

The percentage of water absorption is considered a measure of the pore volume (porosity) in hardened concrete, which is occupied by water under suturated condition. The values of the water absorption of the three batches were measured after 7, 28 and 90 days of moisture curing, following the ASTM C642. After curing, the specimens were desiccated in an oven at 221°F ± 41°F for 48 hours to evaporate the moisture content in the concrete. After removing the samples from the oven, they were allowed to cool in dry air to a temperature of about 171°F, and their mass was determined. The procedure was repeated two or more times, until the difference between two successive mass

measurements was less than 0.5% of the smaller value. The first measure obtained represents the mass of the oven-dried sample in air (A). The second measure taken was the mass of the surface-dry sample in air after immersion and boiling (C). The sample was placed in a suitable receptacle, covered with tap water and boiled for 5 hours. After the designated time, the sample was left in water 14 hours in order to allow a natural cooling down. At a temperature of 68 ÷ 77°F, the sample was removed from the water, superficially dried with a towel and weighed. The last measure taken was the apparent mass of the sample in water after immersion and boiling (D). The mass was measured while each sample was suspended to a wire and completely submerged in water. Using the values obtained during the test, the effective porosity was calculated as follows:

$$Porosity(\%) = \frac{(C - A)}{(C - D)} \quad \textbf{(1)}$$

Where

A = Mass of oven-dried sample in air

C = Mass of the surface-dry sample in air after immersion and boiling

D = Apparent mass of sample in water after immersion and boiling

For each batch, three samples were tested. The average porosity evaluated on three samples for each batch at 7, 28 and 90 days of curing is shown in Fig. 3-2. At all ages, the concrete containing OWRHA has a lower porosity than the control one. It is inferred that the integration of particles of OWRHA produces segmentation of large pores

and increases the nucleation site for precipitation of hydration products in the concrete [21]. The porosity in all batches decreases with age as a result of the hydration of cementitious materials.

It is well known that a relationship exists between the compressive strength of concrete and its porosity. As the porosity of concrete increases, the compressive strength decreases in an essentially linear fashion [66-71]. Based on the assumption that the influence of porosity plays the role of one of the main factors affecting the compressive strength of hardened concrete, this two parameters were plotted in Fig. 3-4. The figure shows that porosity and strength of OWRHA concrete follows the typical trend of concrete incorporating SCM [72].

3.5.3. COEFFICIENT OF WATER ABSORPTION

The coefficient of water absorption is used as a measure of water permeability [74]. Following ASTM C642, this parameter is evaluated through the rate of water uptake of dry concrete in a period of 60 minutes. The samples were dried in the oven at a temperature of 430°F ± 40°F for 48 hours, then removed and placed in a sealed container to cool down for three days. After this period, the sides of the sample were coated with transparent epoxy resin in order to ensure the flow in one direction. Then each sample was immersed vertically in 0.2 in. of water in an open polyethylene container for the designated period of time. After one hour, the quantity of water absorbed was calculated.

The coefficient of water absorption (Ka) for each batch at 7, 28 and 90 days of moisture was determined as follows:

$$Ka = \left(\frac{Q}{A}\right)^2 \times \frac{1}{t} \quad \textbf{(2)}$$

Where:

Q = Quantity of water absorbed by the oven-dried specimen in time t (ft^3)

t = Time of exposition (3600 sec)

A = Total surface area of concrete through which water penetrates (ft^2)

The test was conducted on three samples for each batch and age. Table 3-4 presents the coefficient of water absorption of the OWRHA blended concrete specimens at 7, 28 and 90 days. In addition to the coefficient of water absorption, the table shows the normalized values with the respect to the 0% OWRHA concrete and the COV. It is observed that the coefficient of water absorption for the OWRHA blended concrete at all replacement levels is less than that of the 0% benchmark concrete. The coefficient decreases with time, and at 90 days, for all three mixtures, the values are about 25% smaller than the values at 7 days. This confirms that prolonged curing results in a reduction of permeable voids for the OWRHA concrete, in agreement with the results available in the literature [31].

3.5.4. ACCELERATED CORROSION EXPERIMENTS

After 28 days of water curing, the prisms were subjected to accelerated corrosion testing with impressed voltage. The impressed voltage technique is an accelerated corrosion conditioning method that can provide valuable information on the permeation characteristics of the concrete. The RC specimens illustrated in Fig. 5 were immersed in a 5% NaCl solution. The embedded steel rebar is acts as the anode with respect to an external stainless steel electrode, which serves as cathode by applying a constant potential of 12 V to the system using a DC source, as described in Fig. 4. The corrosion current was recorded every 6 hours.

The condition of the sample was continuously monitored and time of development of the first crack was recorded. To evaluate the time of initial crack formation, three methods were applied: visual inspection, measurement of the corrosion current, and acoustic emission (AE) monitoring. In the first case, the samples were inspected at one hour intervals to identify if any crack of 0.02– 0.04 in. width. In the second case, the anodic current flow was recorded by means of an ampere-meter. In the third case, an AE sensor was attached on the top surface of the specimen to detect acoustic signals resulting from the cracking of the concrete. The AE instrumentation consists of a piezoelectric transducer with operating frequency range of 40–100 kHz, and a portable digital data acquisition system (SAMOS AE System from Physical Acoustics Corporation – PAC) connected to a laptop computer. The transducer is a resonant R6 type from piezo-electric disks (PAC), measuring 0.75 in diameter and 0.88 in. high, and with an operating frequency range of 35 – 100 kHz. This sensor is designed to be high

sensitivity and for general purpose. Cyanoacrylate was used as the coupling agent between the AE sensor and the concrete surface. The characteristic parameters recorded during the tests were: AE amplitude, energy, and duration. Amplitude of 45 dB was initially set as a threshold to eliminate noise. Nine samples for each concrete batch were tested following the procedure as described.

After a first evaluation of the data recorded, the data were filtered by raising the amplitude threshold to 75 dB to disregard any events that were not associated with crack formation. Fig. 3-6 (a) shows the graph of amplitude versus time of the crack initiation for a representative sample (No. 1, batch W7.5, labeled as "W7.5-1"). This event is characterized by an amplitude of 94 dB, an energy of 579, and a duration of 1729 μs; these numbers are considered representative for corrosion cracks in concrete [68-69]. The waveform of the hit highlighted in Fig. 3-6 (a), is plotted in Fig. 3-6 (b). Previous work showed that this type of waveform may be associated with the accumulation of the corrosion product at the interface between steel reinforcement and surrounding concrete, which exerts expansion pressure in the concrete [76-77]. This leads to the formation of the crack that generates the AE burst, as shown in the photograph in Fig. 3-6 (c). The results of the AE tests carried on the three mixtures are presented in Table 3-5,and show that the time associated with the cracking event increases with the incorporation of OWRHA.

Table 3-5 shows the deviation of the average corrosion currents with the time for the three different concretes tested. It is known that the corrosion current is function of the overall system resistance. The resistance of the system is the sum of: 1) the overall cathodic interfacial resistance, 2) the electrolytic concrete resistance, 3) the overall

anodic interfacial resistance, and 4) the electronic steel resistance [82]. A reduction in the micro-corrosion cell, represented by the porosity of the sample, determines a decrease in the corrosion current from the beginning of the test. The results show that the corrosion current decreases at increasing percentages of OWRHA, in agreement with the porosity results previously presented. Assuming that the concrete is free of any damage, the corrosion current is primarily governed by the porosity of the material. However, when cracking occurs, the electrolytic concrete resistance locally decreases, and a rapid increment in the current value is detected in the circuit, as detailed in Fig. 3-6 (c). The application of this concept allows the evaluation of the initiation of the crack by means of the corrosion current. The results show that the time of first crack detected with the rapid increment of the corrosion current, increases with the incorporation of OWRHA in the mixture.

The visual inspection conducted throughout the test allowed to detect the crack for all the samples. The results presented in Table 3-5 confirm that the initiation of the crack is delayed with the incorporation of OWRHA in the concrete mixture.

In order to stress the correlation of data obtained from current measurements and the AE Fig. 3-6 (a) and (d) shows the results for sample W7.5-1. The two diagrams are plotted as a function of time expressed in hours. Table 3-5 shows the average results, the normalized value with the respect to the 0% OWRHA concrete, and the COV of the three test methodologies for each batch. It can be noticed that the time of initiation of the crack taken with the three methods is consistent also considering that data were collected at one hour intervals. For all the samples tested, the AE sensor detected the crack formation more effectively compared to the other two methodologies. The use of acoustic emission

could be employed for an early detection of cracks in concrete, but more in depth implementation should be conducted to validate this possibility.

The correlation among the three test methodologies showed that the first cracking for the WPC samples starts after about 46 hours with a standard deviation of 1.6. The use of 7.5% OWRHA concrete extends this time to 74 hours with standard deviation of 1.7, which increases to 153 hours with standard deviation of 0.1 when using 15% OWRHA concrete. A more impermeable concrete delays the permeation of Cl^- ions, reducing the corrosion current and extending the time of damage occurrence [78-79]. It can be concluded that the specimens produced with OWRHA exhibit enhanced durability with respect to corrosion of the steel reinforcement.

3.6. CONCLUSION

Based on this research on the use of OWRHA as supplementary cementitous material for white concrete production, for values of replacement of WPC of 7 and 15% by weight, the following conclusions are drawn:

1. The compressive strength of OWRHA blended white concrete increases with the percentage of cement replacement and age.
2. The porosity and the coefficient of water absorption of the concrete decrease with the increase in percentage of OWRHA.
3. The resistance to corrosion under ACTIV conditioning is significantly improved in comparison to that of all portland cement concrete. The pore refinement and the impermeability of the concrete (responsible of the permeation of Cl^- ions)

play an important role in the corrosion resistance of the RC incorporating OWRHA.

4. The three methodologies implemented for to determine the occurrence of the first crack under ACTIV conditioning (visual inspection, corrosion current measurement, and AE monitoring) showed excellent correlation. In particular, AE monitoring efficiently detects early cracking that results from corrosion of the steel reinforcement.

Table 3-1–Physical and chemical compositions of WPC and OWRHA

	WPC	OWRHA
Specific gravity	3.15	2.3
Loss of ignition, %	N/A	0.003
SiO2, %	23.06	94.8
Al2O3, %	4.46	0.52
CaO, %	66.6	N/A
MgO, %	0.26	N/A
SO3, %	3	N/A
MnO, %	N/A	0.39
Fe2O3, %	0.25	0.13
Alkalis	2.37	2.92
C	N/A	0.24
P2O5	N/A	1.09

Table 3-2– Mix proportions for concrete samples

Code	OWRHA (%)	Quantities lb/ft^3					Water/Cementitious
		Cement	OWRHA	Sand	Coarse aggregates	Water	
W0	0	29.4	0				
W7.5	7.5	27.2	2.2	74.5	29.2	13.2	0.44
W15	15	24.9	4.3				

Table 3-3– Average concrete compressive strength at different ages

Code	Average compressive strength			Average compressive strength			Average compressive strength		
	ksi	Normalized	COV	ksi	Normalized	COV	ksi	Normalized	COV
	7 days			28 days			90 days		
W0	4.01	100	3%	5.23	100	2%	5.51	100	0.4%
W7.5	4.06	101	1%	5.94	113	1%	6.43	117	1%
W15	4.23	106	1%	6.03	115	1%	6.61	120	1%

Table 3-4–Coefficient of water absorption of concrete at increasing percentage of OWRHA

Code	Average coefficient of water absorption x 10^{-11} ft^2/s			Average coefficient of water absorption x 10^{-11} ft^2/s			Average coefficient of water absorption x 10^{-11} ft^2/s		
		Normalized	COV		Normalized	COV		Normalized	COV
	7 days			28 days			90 days		
W0	46.2	100	1%	11.4	100	3%	11.6	100	2%
W7.5	43.1	93	4%	11.2	98	2 %	10.5	90	2.5%
W15	44.4	96	2%	11.5	101	4.5%	10.4	89	1%

Table 3-5–ACTIV test results* of concrete at increasing percentage of OWRHA

Code	Visual Inspection	Time of discontinuity in Corrosion Current	AE Event Time	AE parameters Wave	
				Amplitude	Duration
	[h]	[h]	[h]	[dB]	[μs]
W0	46 ± 2	45 ± 4	45 ± 2	91 ± 4	1665 ± 200
W7.5	74 ± 2	75 ± 3	73 ± 2	89 ± 5	1744 ± 231
W15	153 ± 3	155 ± 4	153 ± 5	90 ± 3	1730 ± 230

* = average of 9 samples

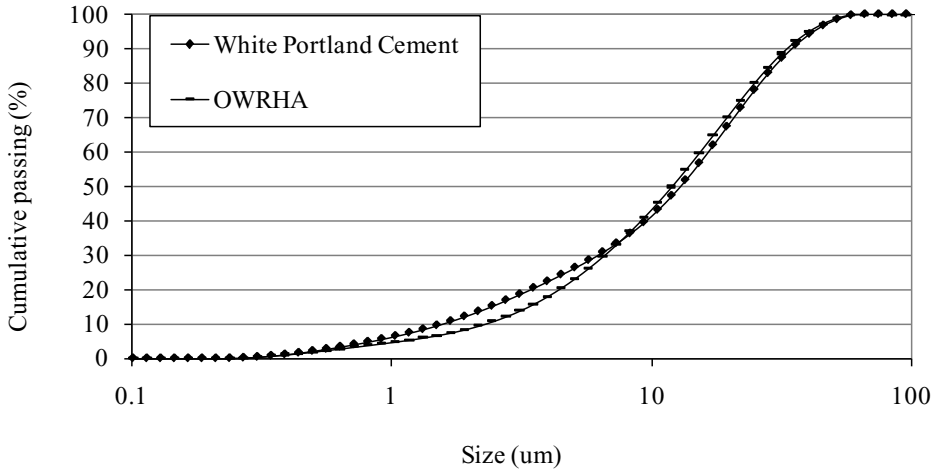

Fig. 3-1–Particle size distribution of OWRHA and WPC

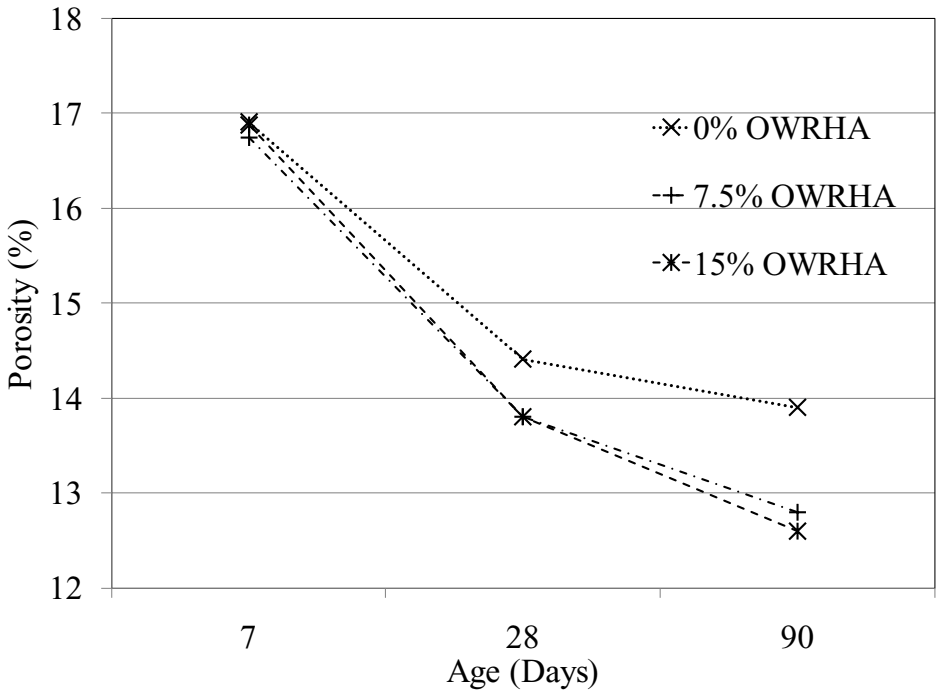

Fig. 3-2–Porosity (%) versus concrete age at increasing percentage of OWRHA

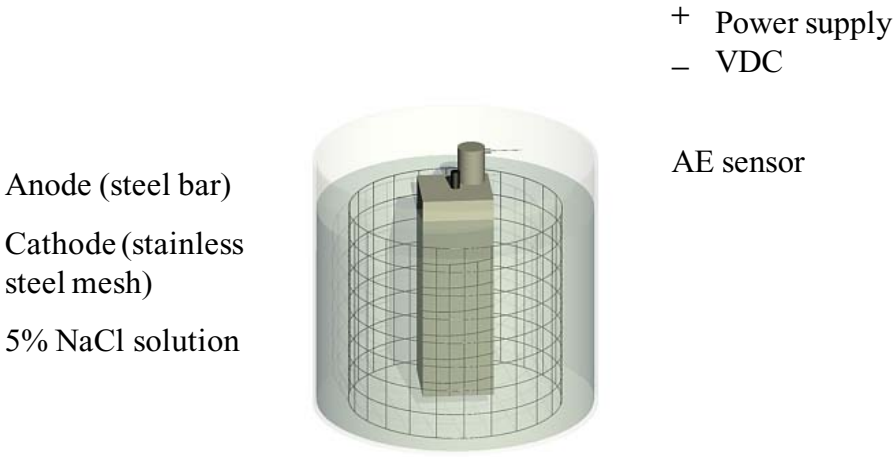

Fig. 3-3– ACTIV test set up

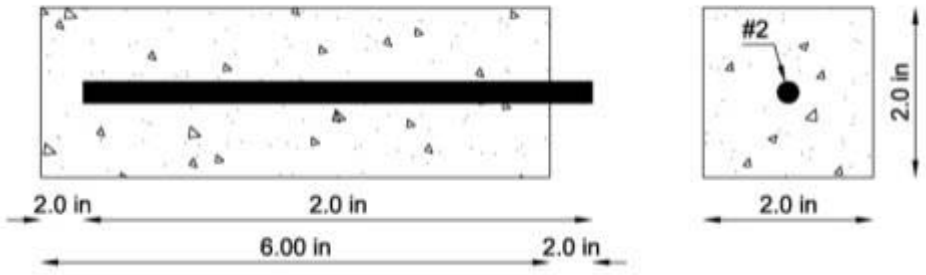

Fig. 3-4–Schematic of ACTIV RC sample

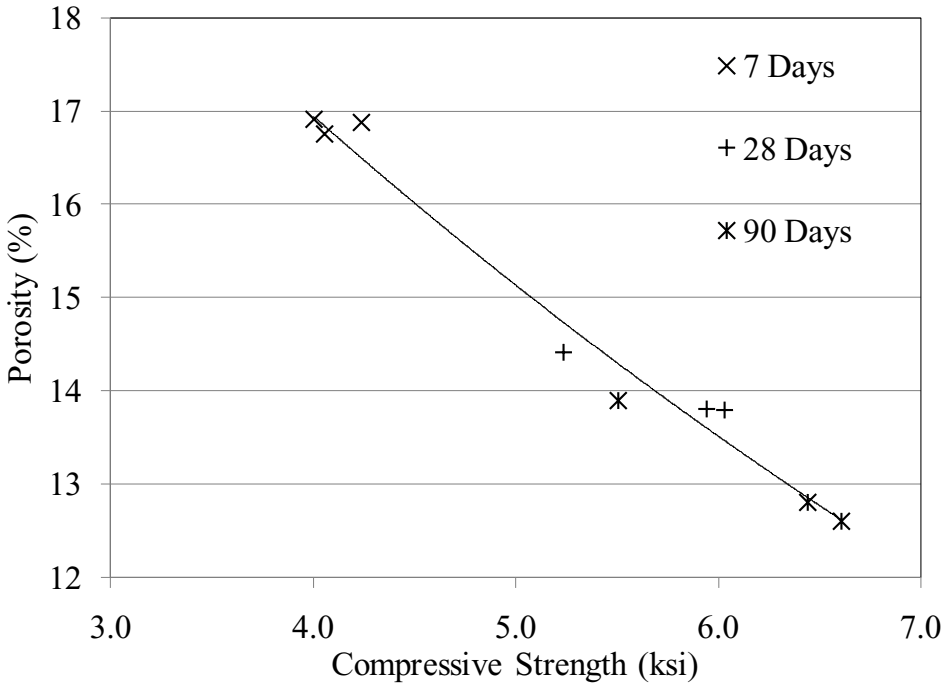

Fig. 3-5–Porosity versus concrete compressive strength at different ages

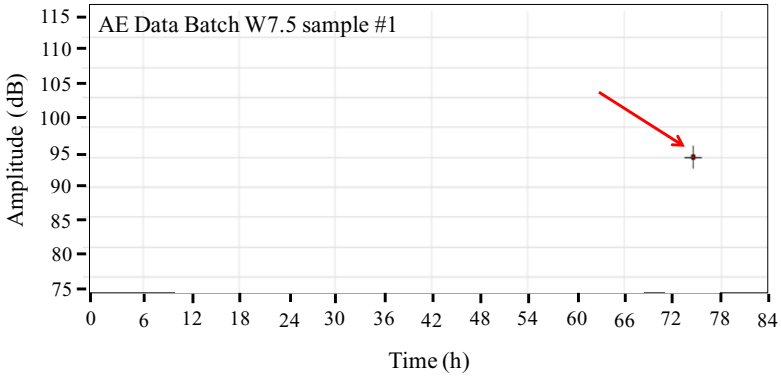

(a)

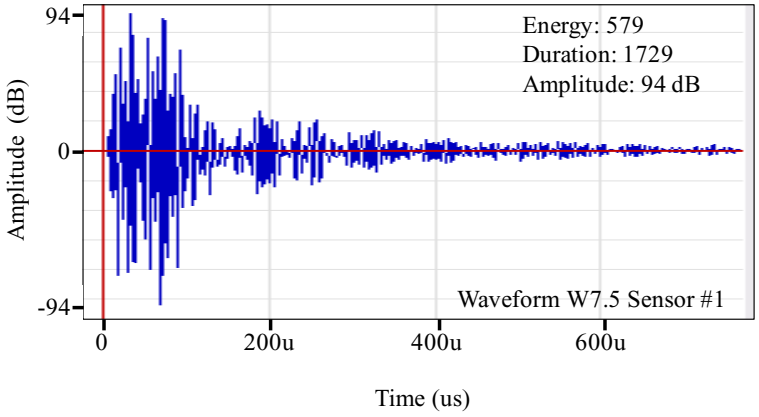

(b)

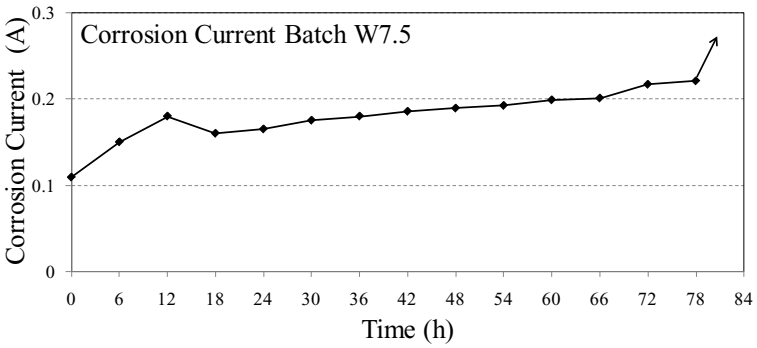

(c)

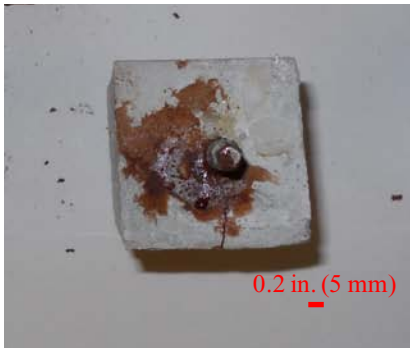

(d)

Fig. 3-6– ACTIV data correlation for representative sample (W7.5-1): (a) AE data expressed in amplitude versus time; (b) waveform of the event in (a); (c) Photograph of crack detected by visual inspection; and (d) Plot of measured corrosion current during testing time; (d)

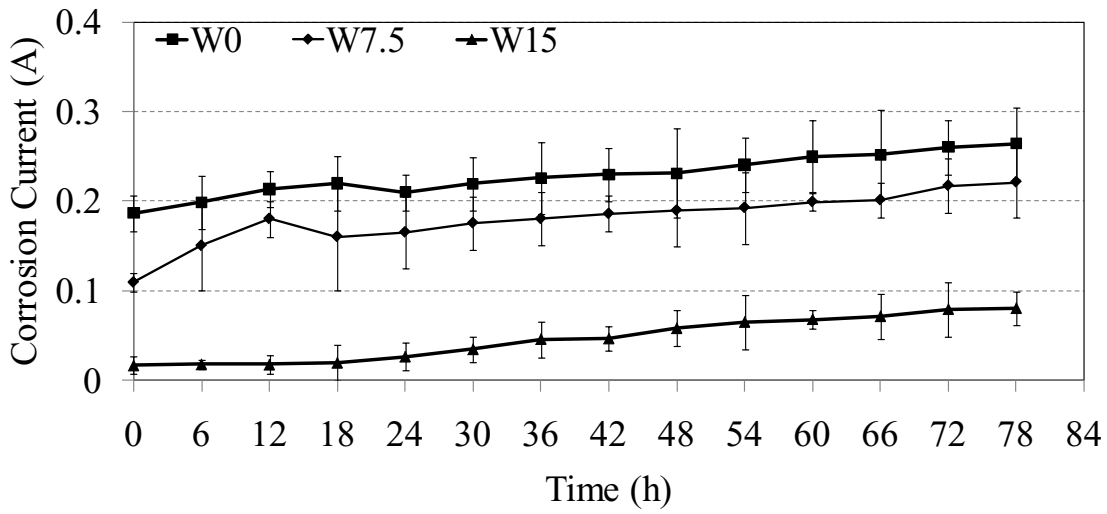

Fig. 3-7–Corrosion current versus time of WPC at increasing percentage of OWRHA

Chapter 4

4. Study III: Color Degradation Analysis of Rice Husk Ash Blended White Concrete

4.1. Background

White cement has currently received increasing attention due to its potential for use in sustainable concrete structures. Based on the U.S. Green Building Council certification practice, the LEED Green Building Rating System for New Construction and Major Renovation (LEED-NC) considers that the reflective quality of white surfaces may help to improve lighting efficiency and reduce temperature fluctuations, resulting in lower heating and cooling with a reduction of related energy costs [83]. In addition to the environmental impact, white concrete represents a valuable tool for the aesthetic acceptability of a structure, and can also offer important practical benefits in terms of safety (i.e., light reflection in the dark).

From an economical stand point, white concrete represents a valuable investment over the long and short term. Painting is eliminated when permanent color is intrinsic to the concrete mixture, and maintenance becomes minimal [84]. With its high reflectance, white floors and ceilings can reduce the load of utility cost, and in industrial and workplace settings, the reflectivity of the surfaces may reduce errors, accidents, and optimizes productivity and performance.

The durability of white concrete can be improved by incorporating by-products such as rice husk ash (RHA) to the mix design as a partial replacement to cement. Rice husk consists of about 40% cellulose, 30% lignin, and 20% ash. Rice husk does not biodegrade or burn easily [85] and, additionally, due to its abrasive character and almost negligible digestible protein content, it is not suitable for use as animal food. For these reasons, rice husk is a major agricultural waste, constituting the largest (about 20%) and most worthless by-product of the rice milling industry. Significant research has been directed towards the utilization of rice husk ash as Supplementary Cementitious Material (SCM) [17-19]. The burned ash of rice husk contains the highest proportion of silica among all the plant residues (nearly 20% silica in amorphous form [20]), and under controlled combustion conditions, this by-product can produce amorphous silica with high reactivity [21]. Until the 1970s, the production of RHA was by uncontrolled combustion, and for this reason the product was usually crystalline and with a considerable amount of unburned carbon (~30%) resulting in a poor pozzolanic activity [22]. After Mehta [21] described the effect of pyroprocessing parameters on the pozzolanic reactivity of RHA, Pitt [23] designed a fluidized-bed furnace for controlled combustion of RHA which allowed for the control of temperature and atmosphere, and to obtain a highly reactive RHA. Today, RHA generated by the processes available on the market contains 3% or more of graphitic carbon which determines the dark pigmentation of the material. This prevents its utilization in applications where color is the driver, and leads to excessive demand for water and chemical admixtures in order to maintain appropriate slump and air content [85-86].

There have been some attempts to produce amorphous SiO_2 from rice husk using different burning techniques, but none of these methods has successfully produced commercial-scale off-white amorphous SiO_2 with less than 1% amorphous carbon [12-15]. In 2006, Vempati et al. [12] developed a new continuous production process of manufacturing RHA. A rotary tube furnace is maintained in aerobic conditions and at temperature of 700ºC with a residence time of 180 min to obtain off white RHA with carbon content less than 0.3%. This carbon neutral ash is off-white in color, with no graphitic carbon, no crystalline SiO_2, and toxic metals, and is therefore considered environmentally friendly and employable as SCM for white concrete.

The awareness of the advantages of white concrete comes with the need of a scientific to characterize "whiteness" for the construction industry. The current literature in the civil engineering field lacks information and a rigorous methodology for color analysis. Conversely, because of the direct connection between the appearance of the product and its organoleptic properties, effective and suitable procedures are followed in food engineering to address and define such properties [90-92]. This knowledge has become a great resource for this study.

Several color scales have been used to describe color. The most frequently adopted is the CIE L*a*b* color scale (CIELab [93]). The CIELab color scale may be used on any object whose color may be measured. It provides a standard scale for comparison of color values and is used extensively in many industries.

In 1976, CIE (Commettee Internationale d'Eclairage) recommended the use of CIELab. CIE Publication 15.2 (1986), Section 4.2 [93], contains details on this color

scale. Its intent is to provide a standard, approximate and uniform color scale so that color values could be easily compared for any type of application. In a uniform color scale, the difference between points plotted in the color space corresponds to visual differences between the colors plotted. The CIELab scale is rendered as a three-dimensional diagram as illustrated in Fig. 4-1. The vertical L* axis reaches a maximum of 100, which represents a perfectly reflecting diffuser (white); the minimum for L* is zero, which represents black. The a* and b* axes have no specific numerical limits. Positive a* is red and negative a* is green; positive b* is yellow and negative b* is blue.

Delta values are also associated with this color scale. ΔL*, Δa*, and Δb* indicate how much the benchmark and sample differ from one another in the L*, a* and b* reference system. These delta values are often used for quality control of formula adjustment. The total color difference ΔE*, may also be calculated as a single value which takes into account the difference between the L*, a*, and b* coordinates of the sample and benchmark. As on aggregate, ΔE* does not indicate which parameter is out of tolerance. The measures were taken by means of a spectrophotometer with details about the instrumentation to be provided in th e following section.

To the best of the author's knowledge, no studies on the influence of the composition and/or exposure to different environments on the whiteness of concrete are available in the open literature. In this research, the variation of the whiteness of white concrete with respect to composition and environmental exposure is investigated. Three mixtures of white concrete with different percentages of off-white rice husk ash and different types of reinforcement were tested for the evaluation of the factors influencing color degradation. The choice of the environments was governed by the intention of

covering representative scenarios for a reinforced concrete structure. Furthermore, the different percentages of rice husk ash selected are meant to demonstrate the effect on color and corrosion resistance that this by-product may have on white concrete.

4.2. EXPERIMENTAL INVESTIGATION

The study was subdivided into two phases. In Phase I, the color of each mixture component was studied. This included white portland cement (WPC), RHA, and fine and coarse aggregates. It did not include the liquid admixture. Furthermore, the influence of the percentage of carbon present in the ash both in the powder form and the hardened concrete color was studied. The color of rice husk ashes produced with the methodology developed from Vempati et al. [12], at different times of processing, was evaluated. The time of processing is the main parameter governing the percentage of residual carbon in the ash. In this phase, samples of powder and hardened concrete incorporating different percentage of RHA were tested.

In Phase II, concrete beams with and without reinforcement were cast from three batches containing different amounts of RHA and were exposed to different environments. During conditioning, their color together with the pH of the concrete were periodically monitored.

4.3. MATERIALS

4.3.1. WHITE PORTLAND CEMENT

White Type I Portland cement (WPC) conforming to ASTM C 150 – 07 was utilized. The cement had a specific gravity of 3.15 and a fineness of 813 ft^2/lbs. The particle size distribution is shown in Fig. 4-2. The main chemical components of the WPC are 23.06% SiO_2, 4.46% Al_2O_3, 2.37% alkalis, 0.25% Fe_2O_3, 66.6% CaO, 3% of SiO_3, and 0.26% MgO.

4.3.2. RICE HUSK ASH

Eight types of rice husk ash were tested in phase I. The RHA was manufactured by burning rice husk procured from a rice mill plant located in Jonesboro, AK. The RHA was manufactured with a continuous process using a rotary tube furnace under aerobic condition at a temperature of 1292ºF. The residence time of the rice husk in the furnace is the primary variable responsible for the final carbon content in the ash. Table 4-1 summarizes the residence time and the respective carbon content for each of the RHA samples tested.

The composition of each sample was analyzed showing that iron oxide (Fe_2O_3 ~ 0.13%), silicon dioxide (SiO_2 ~ 94.8%), and aluminum oxide (Al_2O_3 ~ 0.52) constituted of about 95%. This value is considerably above the required value of 70% minimum for pozzolans (ASTM C 618).

The particle distribution of all the RHA samples is reported in Fig. 4-2. Nomenclature of the RHA samples was based on the residence time, expresses in minutes, of the rice hush in the furnace. For example R180 stands for RHA processed with residence time of 180 minutes. Unground RHA was used in this project, after determining that its particle size was comparable to that of WPC. Generally, reactivity of cementitious materials is favored by increasing their fineness [87-42]; however, Mehta [21] demonstrated that a high degree of RHA fineness should be avoided since this material gains its pozzolanic activity mainly from the internal surface area of the particles. The source of high surface area in RHA is in the microporouse structure of individual particles shown in the SEM picture in Fig. 4-3.

4.3.3. AGGREGATES

Clean river sand with specific gravity 2.55 and fineness modulus of 2.49 was used as fine aggregate. Locally available well ground limestone of size greater than 0.16 in. and less than 0.47 in. with a specific gravity of 2.6, was used as coarse aggregate.

4.3.4. SUPERPLASTICIZER

High-range water reducing admixture (Adva 140M, Grace Construction Product, Maryland, USA) was used to maintain a constant workability, expressed as a constant slump without any additional amount of mixing water and without any direct effect on

the compressive strength of the concrete. This superplasticizer is based on a polycarboxylate technology and meets the requirements of ASTM C494 as a Type A and F, and ASTM C1017 Type I.

Following the industry practice, a typical slump for ordinary architectural concrete application would be in the 4 to 5 in. range. This value was adopted as the target in the study of the different mixtures tested.

4.4. PHASE I

4.4.1. SPECIMENS

The color analysis of the constituent materials in the form of powder was conducted on 0.176 lbs for each powder sample. Eleven powder samples were tested, consisting of 8 RHA, 1 WPC, 1 fine aggregate, and 1 coarse aggregate powdered at the same size of the fine sample.

The color analysis of the mortar was carried on 18 batches. Each RHA type was used for two batches, one replacing 7.5% by mass of cement, and the other 15%. A batch with 100% white cement was used as a benchmark. A water-to-binder ratio of 0.44 was maintained constant for all mixture. The batches were hand mixed using the same procedure and tools, and placed in plastic molds with 4 in. diameter and 0.6 in. height. After the vibrating and trowel finishing, the molds were covered with a plastic sheet for 24 hours. Following this period, the specimens were demolded and moist cured at 68°F with a RH of 95% for 28 days.

4.4.2. PARAMETERS AND RESULTS

Color was measured using a spectrophotometer (MiniScan XE Plus by HunterLab, US). Spectrophotometers use an optical mechanism to break down light entering the instrument into its component parts and measuring them in an objective manner. Fig. 4-4 illustrates how this device operates. The light generated by the source (B) is collected from the external target (A) that the user is attempting to characterize. This light is then passed through a set of optics (C) that focuses and projects it onto a diffraction grating (D). The grating acts like a prism and deflects light with different wavelengths at different angles. As such, the resulting pattern can be projected onto a set of sensors (E) that can measure the light at specific intervals. Each sensor can measure the quantity of light in a specific area of the spectrum. This allows the device to acquire the data to identify the components of the light, from which a color profile is generated.

The instrument was programmed to use 65°/0° geometry, D25 optical sensor, 2° observer for color interpretation, and was calibrated using white (L = 93.42; a = 0.84; b = 0.93) and black reference tiles (L = 0.21; a = 0.11; b = 0.06). The color values were expressed as L* (whiteness / darkness), a* (redness / greenness), and b* (yellowness / blueness). The total color difference at time t, ΔE*, which indicates the magnitude of color change after conditioning, was computed as follows:

$$\Delta E^* = \sqrt{(L^* - L_0)^2 + (a^* - a_0)^2 + (b^* - b_0)^2} \quad (2)$$

Where:

L* and L_0 = whiteness / darkness of specimen at time t and time 0, respectively

a* and a_0 = redness / greenness of specimen at time t and time 0, respectively

b* and b_0 = yellowness / blueness of specimen at time t and time 0, respectively

ΔE* represents the distance of two points (the benchmark and the specimen measurements) in a three-dimensional space. Five color measurements were taken from each sample and the mean value with the standard deviation were reported.

For the powder, eighty grams were placed in a clear glass cup of 2.26 in. diameter and manual pressure was applied to compact flatten the powder. The color of the powder was measured through the bottom of the glass sample cup by tapping the cup a couple of times on a hard surface to tighten up the powder. The effects of the absorbance of the glass surface on the measurements values were eliminated by calibrating the device with the glass over a white standard reference material.

The color measurements of the hardened mortars were taken directly on the surface in five randomly chosen locations. For each location the average of five readings was recorded as one measurement and the standard deviation was calculated. Therefore each mixture is represented by twenty-five color measurements.

The average color measurements for each mixture, expressed in terms of L*, a*, b*, and ΔE* are shown in where the color of WPC is the benchmark. Fig. 4-5 shows the trend (linear relationship) of the whiteness in terms of L* of the powder samples with different percentage of residual carbon content. The whiteness of the RHA decreases with

the increase in carbon content. In particular, L*, for the sample with carbon content higher than 0.10%, is even lower than half of the white concrete L*. In order to select the most appropriate RHA among the four (R90, R120, R150, and R180) sample with L* closer to white concrete L* the hardened mortar was analyzed. Fig. 4-6 presents the data relative to the hardened mortar color. The graphic shows that the incorporation of RHA in white concrete reduces L* of the mortar, at all levels of replacement and/or carbon content. The whiteness decreases not only with the amount of carbon content, but also with the percentage of RHA used. The lines in Fig. 4-6 converge to a point where the amount of carbon content in the RHA is zero. In this case the color is comparable to the WPC, and the percentage of RHA would not have any substantial effect on the final mixture color. This justifies the convergence of the two trend lines.

In order to select the most appropriate RHA to use in phase II an interval of acceptability was defined. The minimum of the interval was defined using the minimum L* value found for the constituent of the concrete (Table 4-1) which is 86.55, (coarse aggregates), and the maximum is the value of the WPC. The only sample that for both percentages of replacement falls in the defined range is R180, and it was then used in Phase II.

4.5. PHASE II

4.5.1. MIX PROPORTION AND SPECIMENS

In Phase II, three configurations of white concrete specimens were cast: steel reinforced, glass fibers reinforced polymers (GFRP) reinforced, and unreinforced concrete. Three mix designs were used for each configuration. The three different proportions of concrete mix, including the control mixture, were prepared with a water-to-cementitious materials ratio of 0.44. Blended cements were prepared by replacing WPC with OWRHA in dry conditions. The mixtures were thoroughly homogenized and kept in polyethylene containers. The mix proportions and the designations are presented in Table 4-2, with W0 used as a benchmark.

Fifteen concrete beams, 2 x 4 x 12 in., per each mix design, were cast. After the concrete was vibrated and troweled, the molds were covered with plastic sheet for 24 hours. After 24 hours, the molds were stripped and the specimens were cured for 28 days at 68°F with a RH of 95%. The beams were reinforced with one #3 steel (Grade 50) or GFRP bar positioned at 0.5 in from the bottom. The GFRP bars had a tensile strength of 120 ksi and a modulus of elasticity of 5.9 ksi. Previous research demonstrated that the use of GFRP reinforcement is a valid alternative to eliminate the problem of corrosion in reinforced concrete [94]. This study uses GFRP reinforcement as alternative to steel to avoid the degradation of the color of the concrete due to the corrosion. All the specimens, except the unreinforced one, after curing period, were cracked to accelerate the reinforcement deterioration process. The crack was made by notching and loading the specimen in bending . The surface of color observation was limited to 1 in. from each

of the two sides of the crack times the width of the beam (4 in.). The strength for each concrete mixture was evaluated at 28 days with three cylinders with 6 in. diameter and 12 in height.

4.5.2. PARAMETERS AND RESULTS

Three series of conditioning (A, B, C) were used in the investigation. The three series simulated different levels of environment: (A) highly aggressive, (B) controlled highly aggressive, (C) lightly aggressive.

For series A, the specimens were immersed in the sea, in a position where the changing of the tide naturally simulated the immersing–drying cycles. The coupons were located at the Rosenstiel School of Marine and Atmospheric Science Campus of the University of Miami on the east shore of Virginia Key. Color and pH were monitored with the following schedule: every week from the beginning of the conditioning for the first two months, every two weeks for the third month and every four weeks for the remaining time. The conditioning was stopped after 6 months. The pH was evaluated collecting a 5 g concrete sample from the top surface of the beam. The sample was pulverized and mixed with distilled water. The pH of the mixture was measured with pH strips following ASTM F710-08.

For the controlled highly aggressive environment (Series B), immersion-drying conditioning was conducted. The schedule of each cycle for all the specimens was the following:

1. Immersion in 3.5% NaCl solution for 4 hours,

2. Drying at 68°F for 1 hour
3. Drying at 140°F for 19 hours.

Fifty cycles were conducted. At the beginning of the test and every 10 cycles, pH and color were monitored.

The objective of Series C was to evaluate the behavior of the specimens in a lightly aggressive environment to define the benchmark of the test. The specimens were located away from the sea water, but in the same condition of weather (temperature, weather, sun exposure, etc.). The specimens were left in the open air outside the Structural Lab of the Coral Gables campus of the University of Miami for 6 months. The same monitoring previously described for Series A and B was conducted at the beginning of the test and every four weeks.

For practical reasons, the collection of the data was conducted at distinct slot. For this reason the rate of variation of the color in not definable, however the trend described by the curve seems to give a good approximation of the behavior of the sample.

The HunterLab spectrophotometer was used to measure the color and its variations following the CIELab color scale. The instrument was programmed and was calibrated as in Phase I. The color values were expressed in terms of L*, a*, b*, DE*, DL*, Da*, and Db*. Mould or other entities could certainly invalidate the reading of the color, for this reason before every reading the specimen's surface was wiped over with a 50% water and bleach solution. The color of the specimens was taken directly on the surface in five randomly chosen locations, within the observation area (1 x 4 in.). For each location the average of five readings was recorded as a sample measurement. Therefore, each beam is represented by twenty-five measurements of color.

To evaluate the strength of the batch at the beginning of the conditioning, three cylinders for each batch were tested in compression following standard ASTM 39. Table 4-2 shows the results of the compression test of each batch.

Fig. 4-7 to Fig. 4-9 show the evolution of the color change over time in terms of L*, a*, b*, and DE* for each series. Each graphic is the average of the results in terms of color and time for each type of sample. The nomenclature used consisting of a letter B that stays for batch, a number (0, 7.5, 15) which represents the percentage of WPC replaced, and a letter, N, G, and S indicating the type of reinforcement used. In particular, N stays for not reinforced, G for GFRP reinforced, and S for steel reinforced. The results are divided per batch and series.

4.5.2.1 SERIES A

The results indicate that Series A is characterized by a wide variation with respect to all the three parameters. It was noticed that color changes were highly influenced by the constant formation of algae during the sea conditioning. Even though the color measurements were taken after surface cleaning, some of the algae would leave green stain on the concrete surface. The presence of the green spots increased with an increasing number weeks of testing. After approximately two months the green coloring occurred homogeneously over the surface, as the standard deviation of the averaged results demonstrates (Fig. 4-7 (d), Fig. 4-8 (d), and Fig. 4-9 (d)). In fact, since the sample were taken randomly on the surface, when the surface has variation of the color concentrated in a small area, the standard deviation is high, however when the color is

homogeneous, the standard deviation is close to zero. From Fig. 4-7 (d), Fig. 4-8 (d), and Fig. 4-9 (d) it can also be notice that the samples reinforced with steel are the only one with high predominance of a* in the positive direction (red). This indicates the presence of iron on the surface, due to the corrosion of the steel embedded in the concrete. In the other two types of samples (unreinforced and GFRP reinforced) the variation in color is mainly due to the formation of algae. The results also show that there is a correlation between the percentage of RHA used in the concrete mixture and the color degradation due to both steel corrosion and algae. A previous study (Study No. 2) indicate that the incorporation of R180 (in Study No. 2 coded as OWRHA) delays the corrosion of the steel reinforcement. In particular, the initiation of the corrosion is delayed the most substituting 15% by weight of R180 to white portland cement. The resistance to corrosion of concrete under conditioning is significantly improved in comparison to that of the portland cement concrete. The current study proves that the change in color due to the corrosion decreases with the incorporation of R180. B7.5 and B15 show that the variation in terms of a* is delayed with respect to the other samples. This indicates not only less corrosion (red), but also less formation of algae (green). The development of the corrosion of the steel reinforcement is also confirmed by a lower decreasing pH level of the concrete (Fig. 4-7 (d), Fig. 4-8 (d), and Fig. 4-9 (d)).

The differences observed for the rate of algae growing could be attributed to differences in the intrinsic bioreceptivity of the concrete. Rough surfaces with a high micro- and macro-porosity present a higher number of anchoring sites for microorganisms [95]. As such, algae were more rapidly retained on the specimens without R180. Study No. 2 demonstrated that the porosity of the concrete decreases with

the increase in percentage of R180 incorporated, which explains the difference in the rate of colonization between samples with and without R180. Furthermore, each set of samples tested showed a similar behavior after a comparable time, indicating the reproducibility of the test setup.

4.5.2.2 SERIES B

The use of distilled water for the conditioning of Series B did not allow the growing of algae, so that he variation in color in this series was mainly caused by chemical reaction and corrosion of the steel reinforcement. After 30 cycles, the sample with no R180 and reinforced with steel presented rust bleeding. The bleeding was concentrated at the cracks and area and the dimensions of the spot were in the range of 0.4 ÷0.6 in., which explain the high value of the standard deviation (Fig. 4-10 (d)). The dimension of the spot increased progressively with the number of cycles. At 50 cycles, the product of steel corrosion penetrated through the concrete cracks covered homogeneously the area of observation. The results showed that, the incorporation of R180 reduces the variation of color due to the steel corrosion. The development of the corrosion of the steel reinforcement is also confirmed by the trend of the concrete pH level (Fig. 4-10 (d), Fig. 4-11 (d), Fig. 4-12 (d)). The other two sets of samples (unreinforced and GFRP-reinforced), did not show any significant variation in terms of a* and b*. However, a slight variation in the whiteness (L*) occurred for the sample without R180. This behavior might be caused by a phenomenon named efflorescence [96]. Efflorescence is a white powdery deposit that can form on the surface of concrete.

When dissolved calcium hydroxide dissipates to the surface, it combines with atmospheric carbon dioxide and precipitates as low solubility product calcium carbonate producing lime efflorescence. This phenomenon happens when moisture dissolves salts in concrete and carries them via capillary action to the surface. When the moisture evaporates, it leaves behind a mineral deposit [97]. On ordinary gray or white concrete, the white deposit frequently goes unnoticed at the naked eye. However, since the deposit can have the effect of lightening or fading of the surface color, this product was detected by the spectrophotometer. Efflorescence is usually avoided minimizing the entry of moisture into concrete, this explains the absence of this phenomenon in the samples with R180. Also in this series, each set of tested samples showed a similar behavior after a comparable time, indicating the reproducibility of the test setup.

4.5.2.3 SERIES C

Series C, as expected, shows the lowest level of color variation, in particular due to steel corrosion. None of the steel reinforced samples showed any rust bleeding, and the stability of the pH level confirms that no corrosion was developing in the system. Almost all samples without R180 showed an analogous trend in the variation of whiteness (Fig. 4-13). The trend can be divided into three stages: 1) stationary, 2) whiteness increasing, and 3) whiteness decreasing. The first stage can be considered as a steady state in terms of colors. There is no major reaction happening on the surface or immediately under it that can cause color variation. In the second stage, efflorescence happens and causes a localized increase in the whiteness. In the third stage, probably pollution in the air and/or

rain causes a slight darkening of the surface. Samples made with R180 did not show any efflorescence (Fig. 4-14-Fig. 4-15). Furthermore, also in this series, each set of samples tested showed a comparable behavior, indicating the reproducibility of the test setup.

4.5.3. OBSERVATIONS

The use of three environment setups made it possible to recognize separately the different phenomena that can cause color variation in concrete. Series B and C allowed the identification of the time dependent efflorescence phenomena under both controlled and uncontrolled conditioning. Series B allowed for the detection of color degradation due to the corrosion of the steel reinforcement, and how this varies with the incorporation of R180. Series A evidenced the effect of the algae growing, and the implication that R180 has on this event. Fig. 4-16 to Fig. 4-18 show the influence that reinforcement and percentage of rice husk ash have on the total color variation (DE*). These graphic plot the total variation of the color for each series, as function of the reinforcement type used, and the percentage of RHA180 in the mixture. All three series confirm that steel reinforced concrete without R180 and steel reinforced have the highest variation of color mainly due to the corrosion of the embedded steel. The color analysis based on the CIELab color space allowed for both the distinction of the events and the area interested by those events. The use of the average value of five measurements taken at randomly chosen locations allowed defining the extension of the event on the white surface.

4.6. CONCLUSIONS

From the results obtained in Phase I and II, the following conclusions are drawn:

1. The residual carbon present in the RHA has a negative linear effect on the whiteness of the powder.
2. The linear relationship between whiteness and carbon content, found for the powders, remains also for the hardened mortar. The increase in RHA percentage increases the surface darkness in terms of L*. This effect is strongly reduced at increasing residence time, till it become negligible for R180.
3. Among the different types of RHA under investigation, R180 (lowest carbon content) showed to be the best supplementary cementitious material to retain the white concrete color. R180 was chosen to be used as the SCM to be studied in Phase II.
4. The consistency of the results obtained with three types of conditioning validates the reproducibility of the setup and of the methodology used for the monitoring.
5. Aggressive environment facilitates the corrosion of the steel embedded in the concrete, which highly influences surface color degradation. The incorporation of R180 retards the steel corrosion, and so the damaging of the concrete aesthetics.
6. The intrinsic bioreceptivity of the concrete influences the algae growing and is strictly related to its porosity. By reducing the porosity of the concrete, the incorporation of R180 delays the algae formation which is a major reason for concrete staying in marine environment.

7. The presence of R180 in the mixture reduces the penetration of moisture into the concrete and eliminates the efflorescence effect that causes alteration of the surface color, such as lightening or fading.
8. If white concrete requires reinforcement, the combination of GFRP and R180 appears to be the most promising solution for the prevention of white color degradation.
9. The CIELab color space allowed a clear distinction among three major phenomenon that can cause alteration of white concrete aesthetics: corrosion, algae growing, and efflorescence. The methodology employed in the study, enabled to evaluate the extension of the surface area interested by such phenomena.

Table 4-1– Powder color measurements

Sample ID	Residence Time [min]	Carbon [%]	L*	a*	b*	ΔE*	Standard Deviation
WPC	N/A	N/A	92.38	-1.87	5.76	0.00	-
R15	15	0.46	23.16	0.41	0.79	69.44	0.32
R30	30	0.40	28.80	0.27	1.08	63.79	0.24
R45	45	0.36	36.07	0.18	1.04	56.55	0.31
R60	60	0.26	46.72	0.23	2.23	45.85	0.25
R90	90	0.05	65.87	0.85	5.26	26.65	0.33
R120	120	0.04	70.24	1.13	6.54	22.36	0.35
R150	150	0.03	71.67	1.13	5.90	20.92	0.21
R180	180	0.01	73.79	1.42	6.30	18.89	0.22
Fine aggregates	N/A	N/A	90.25	-1.65	5.61	2.15	0.24
Coarse Aggregates	N/A	N/A	84.55	-1.32	5.12	7.88	0.33

Table 4-2: Mix proportion

Code	OWRHA (%)	Quantities lb/ft^3					w/c[2]	Average Compressive Strength		
		Cement	OWRHA	Sand	Coarse aggregates	Water		psi	Normalized	COV
W0	0	29.4	0					5,236	100	2%
W7.5	7.5	27.2	2.2	74.5	29.2	13.2	0.44	5,947	113	1%
W15	15	24.9	4.3					6,034	115	1%

[2] Water/Cementitious Ratio

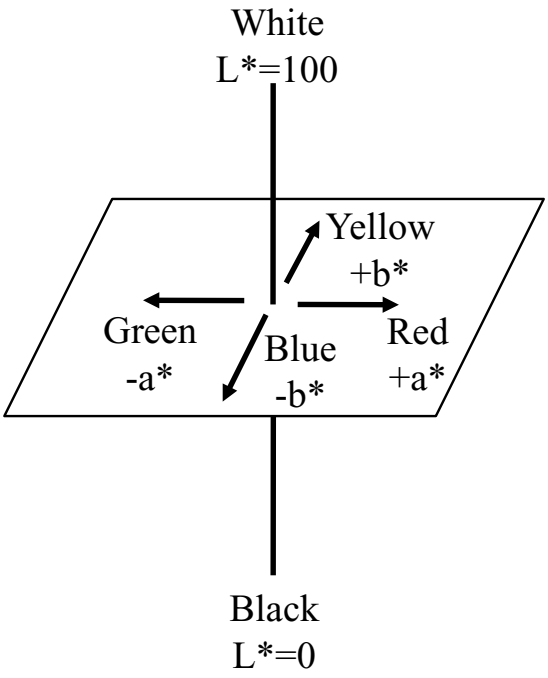

Fig. 4-1– CIELab color space diagram

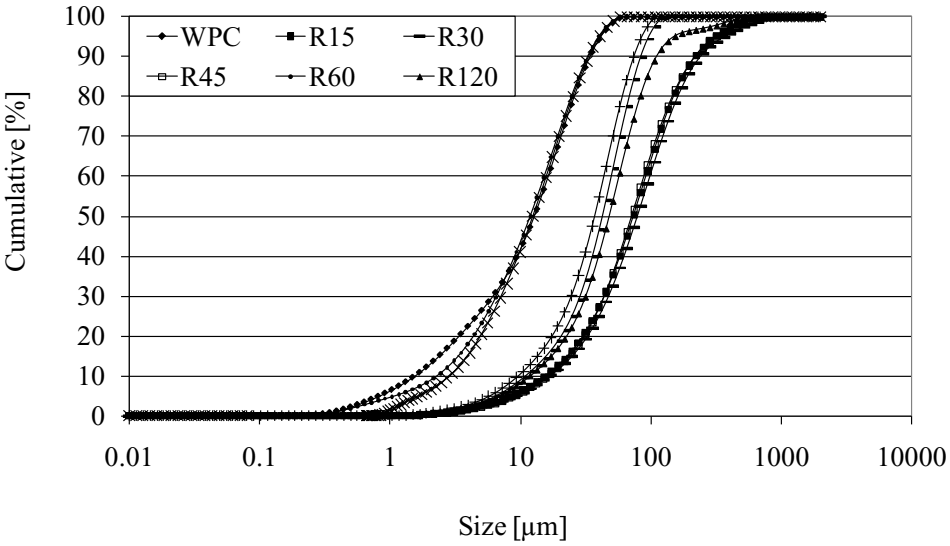

Fig. 4-2 – Particle size distribution for cement and RHA at different furnace residence time

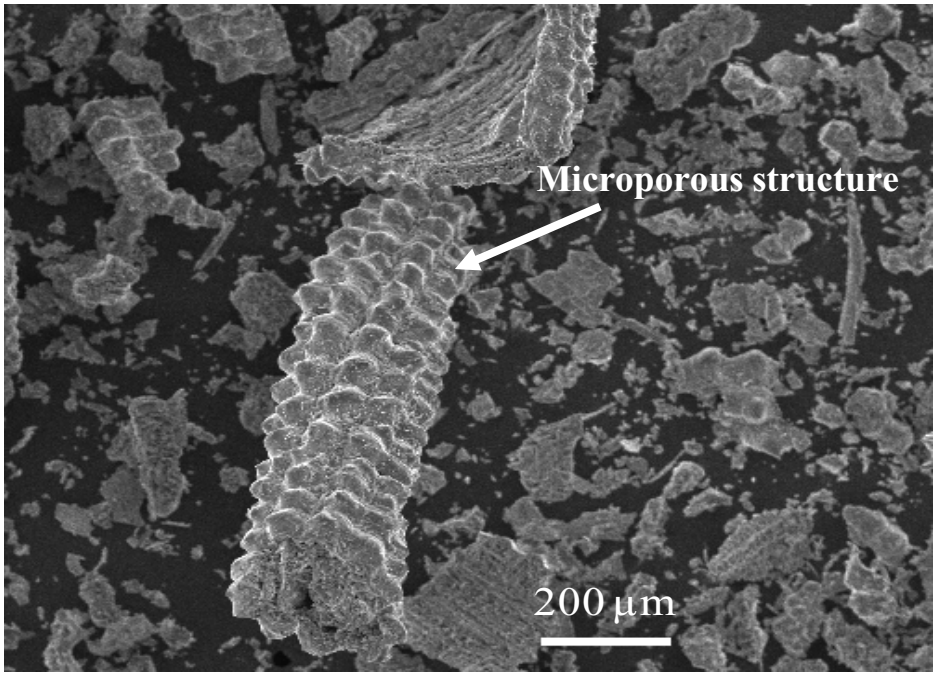

Fig. 4-3 – Scanning electron microscope (SEM) of RHA

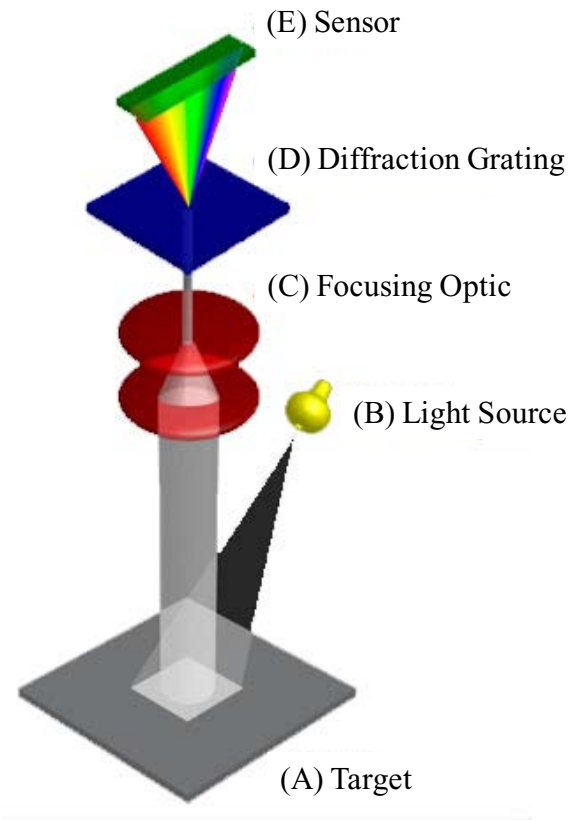

Fig. 4-4 – Diagram illustrating operation of spectrophotometer

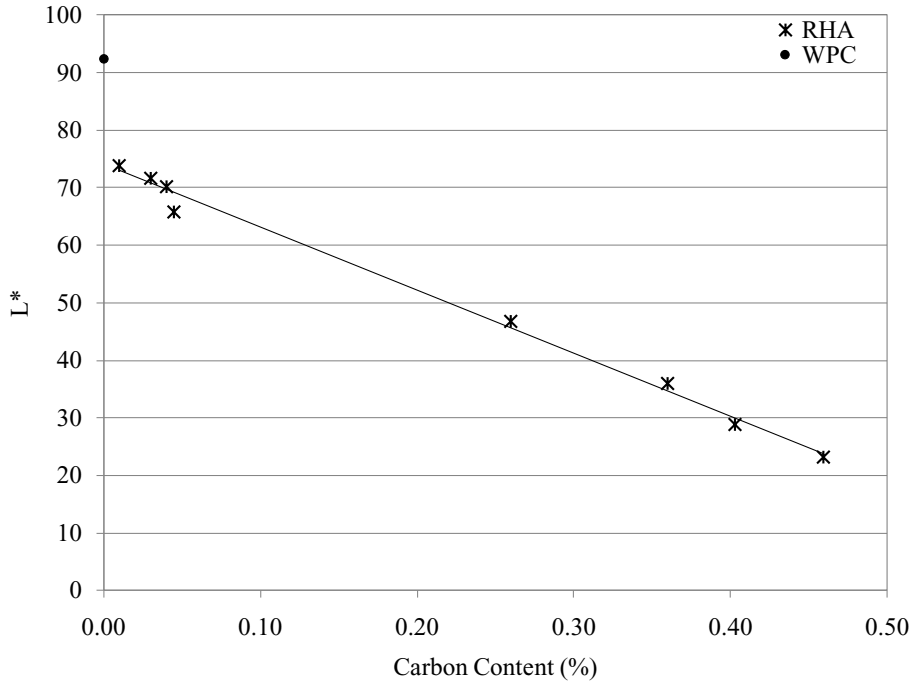

Fig. 4-5 – Whiteness versus residual carbon content of RHA (powder)

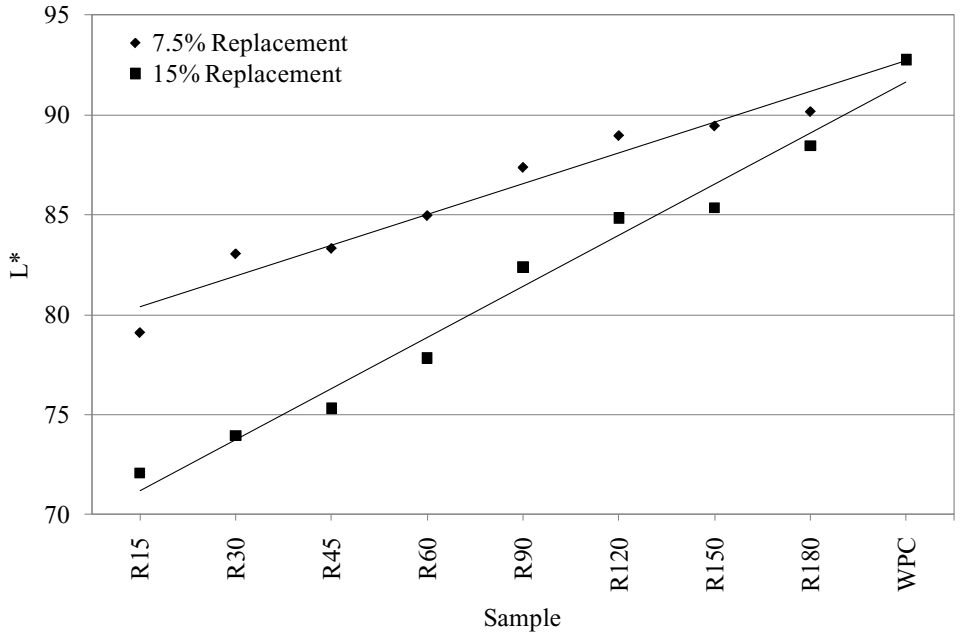

Fig. 4-6– Whiteness of hardened white concrete at different RHA replacement percentage and furnace residence time

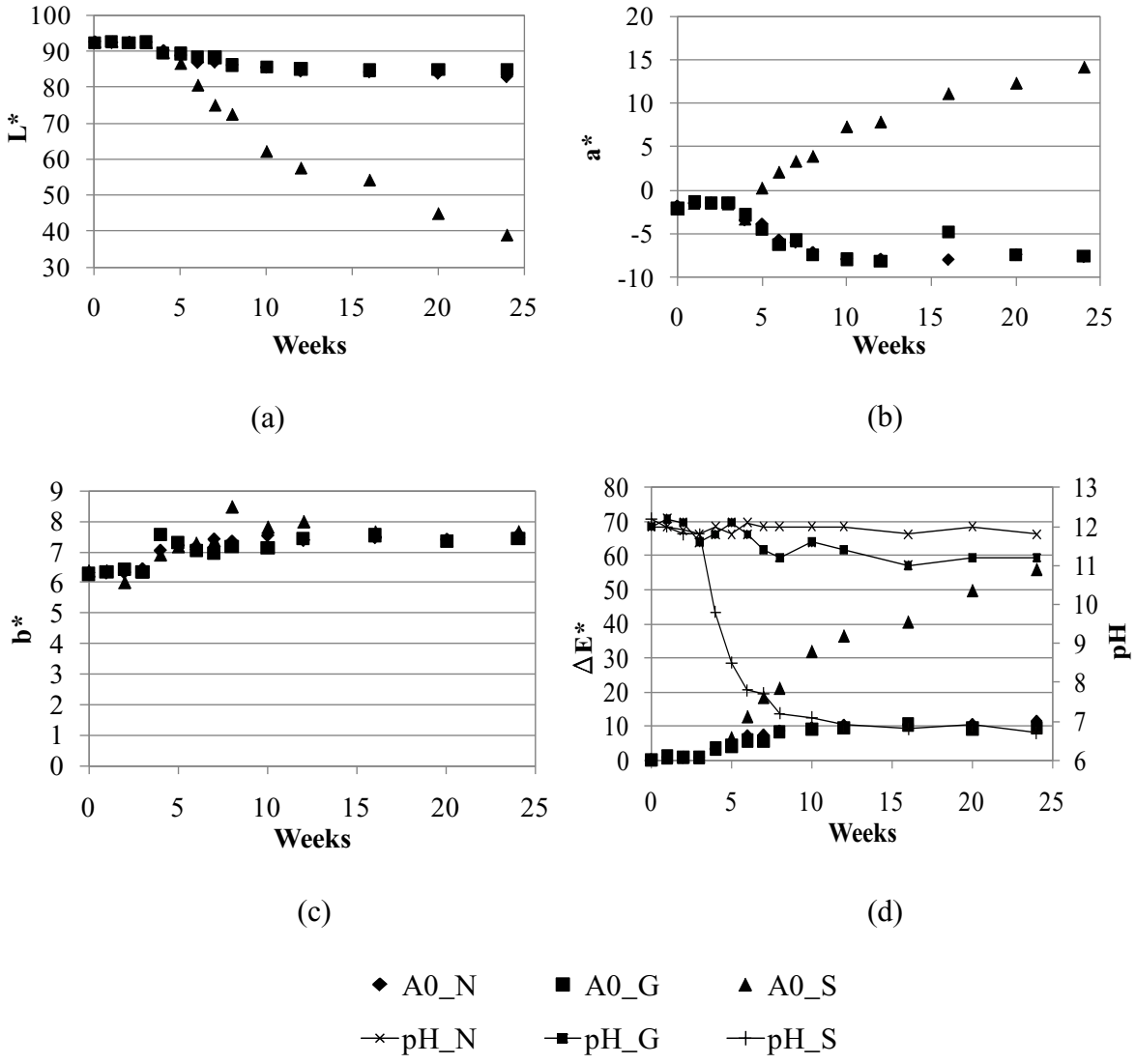

Fig. 4-7 – Color measurements for Series A – concrete with 0% RHA

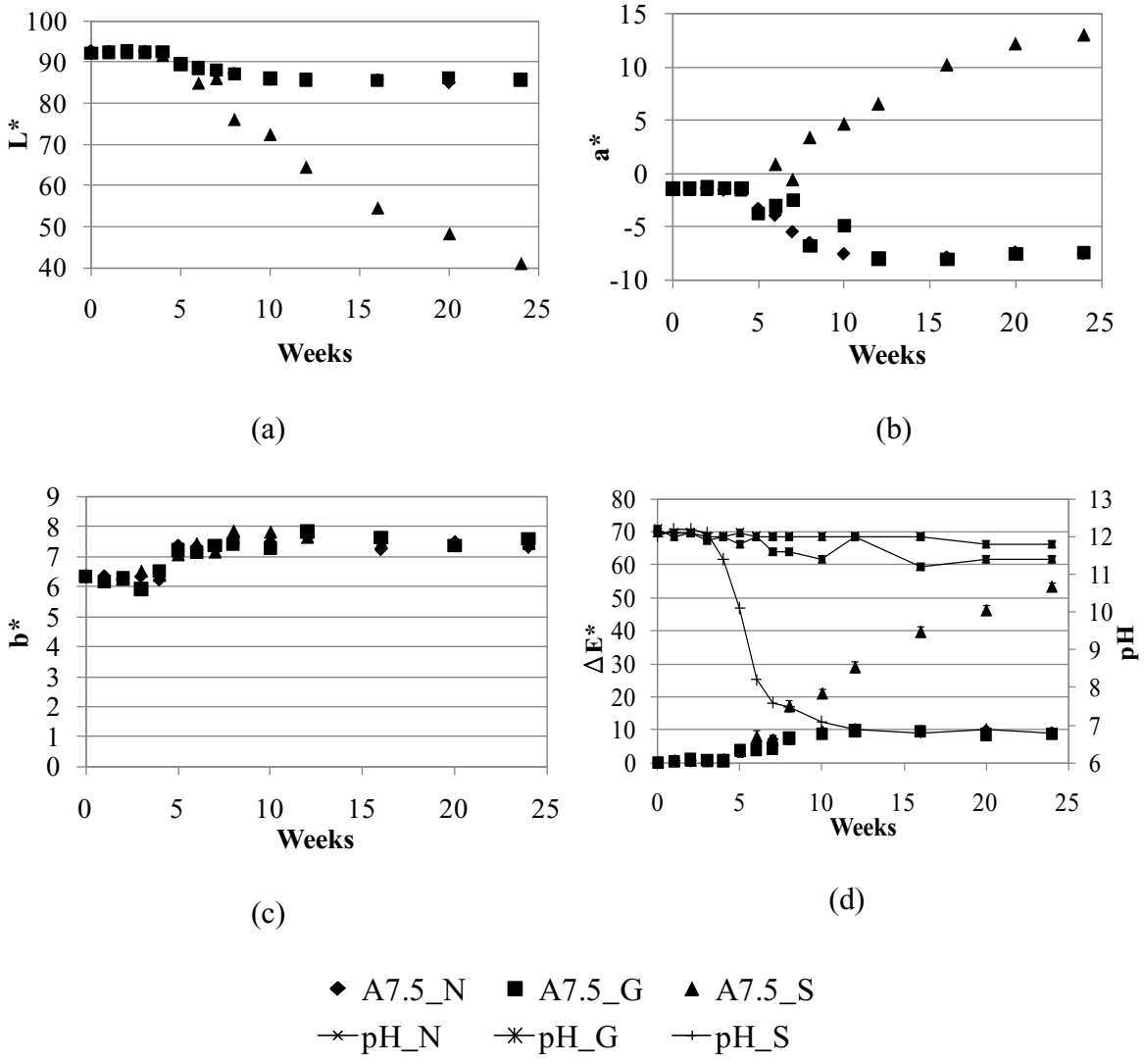

Fig. 4-8 – Color measurements for Series A – concrete with 7.5% RHA

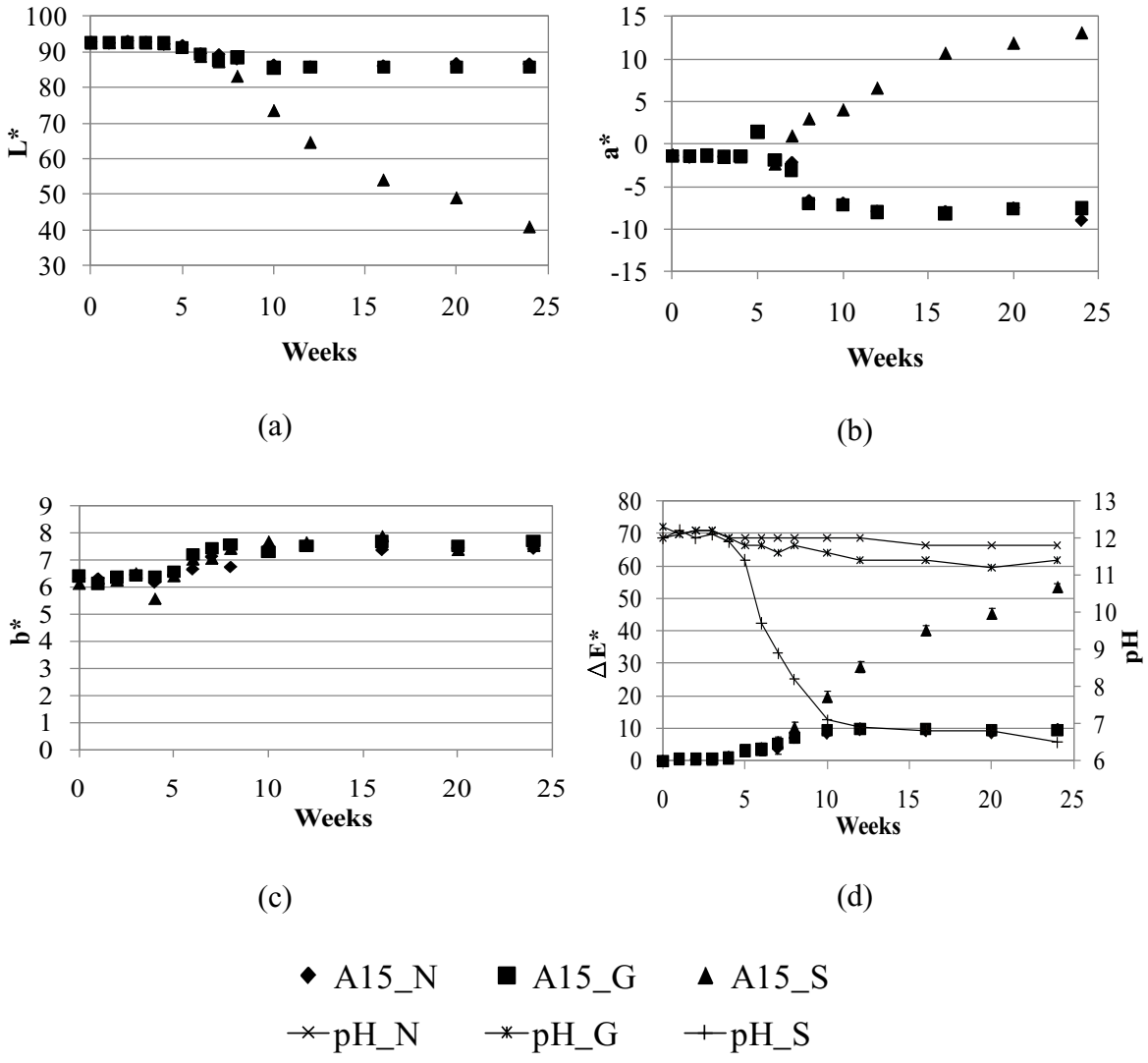

Fig. 4-9 – Color measurements for Series A – concrete with 15% RHA

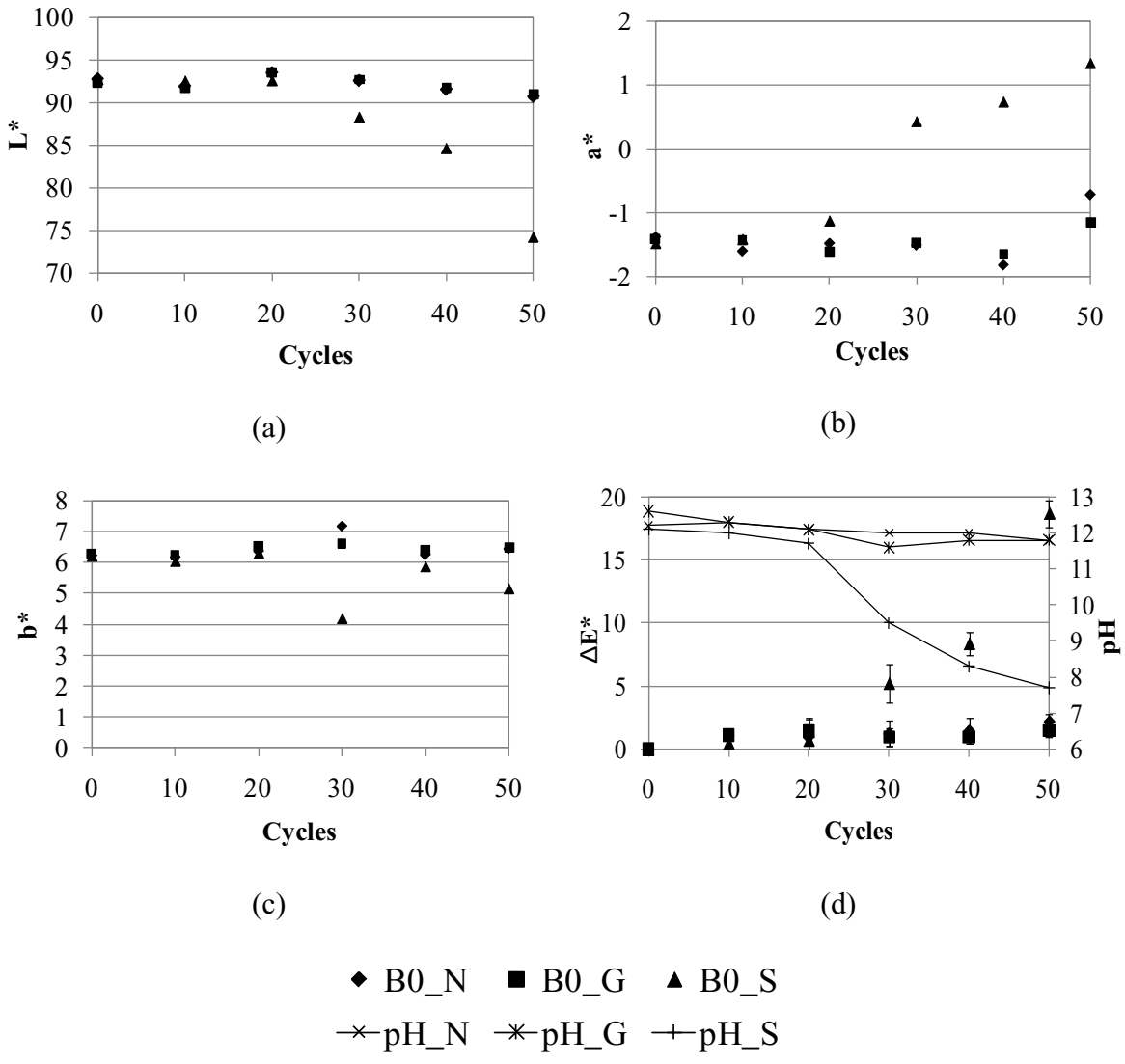

Fig. 4-10 – Color measurements for Series B – concrete with 0% RHA

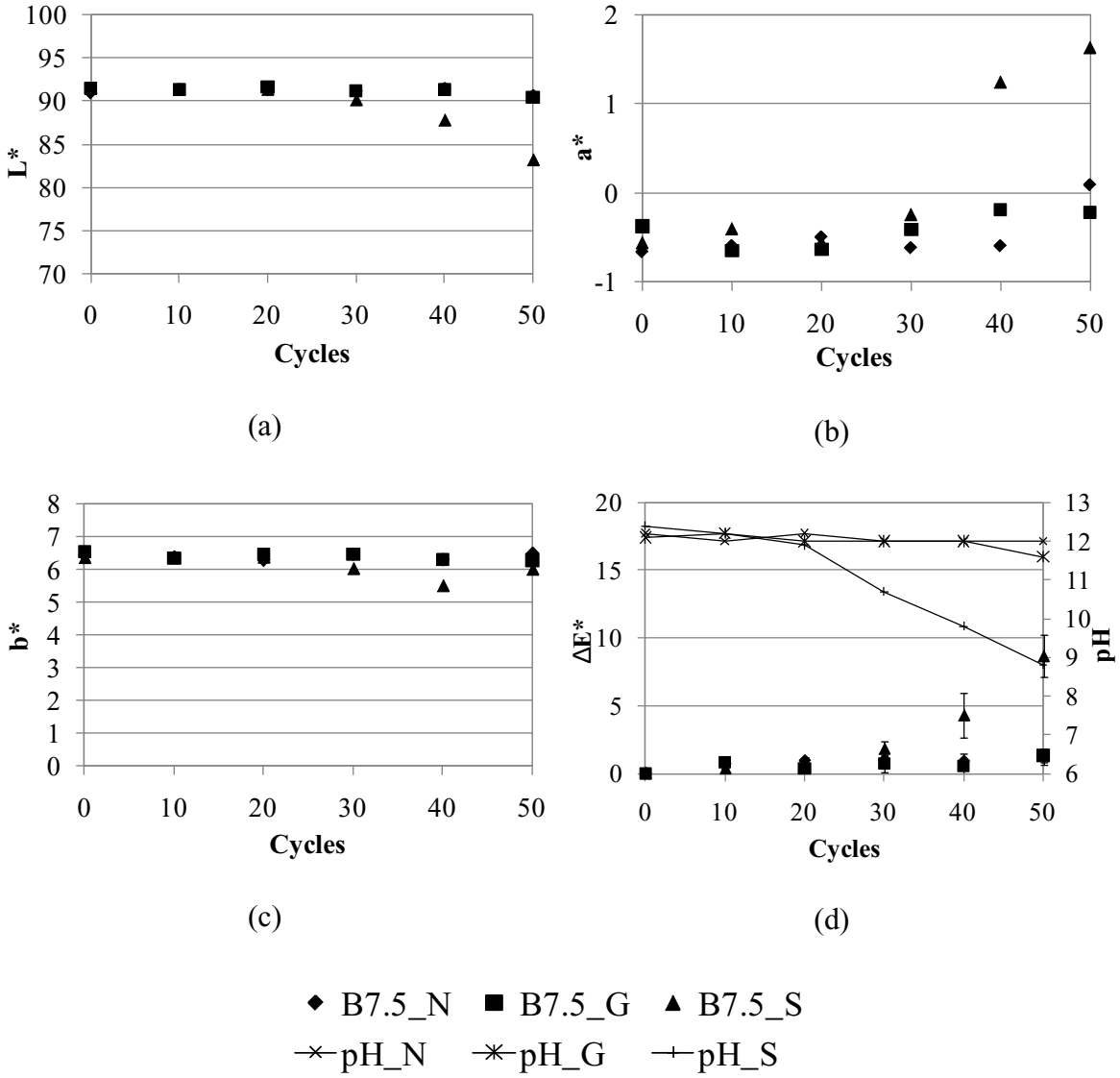

Fig. 4-11 – Color measurements for Series B – concrete with 7.5% RHA

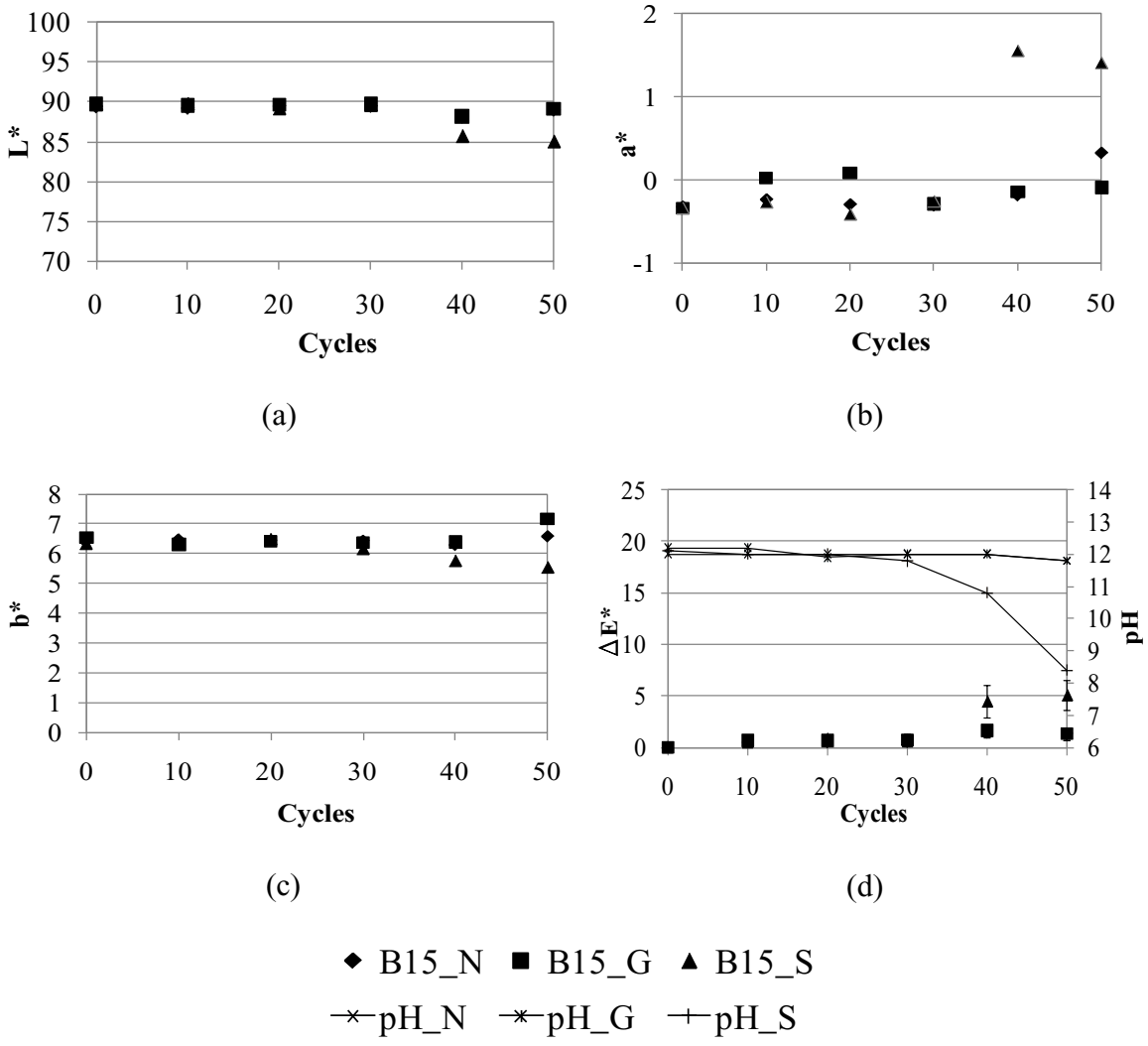

Fig. 4-12 – Color measurements for Series B – concrete with 15% RHA

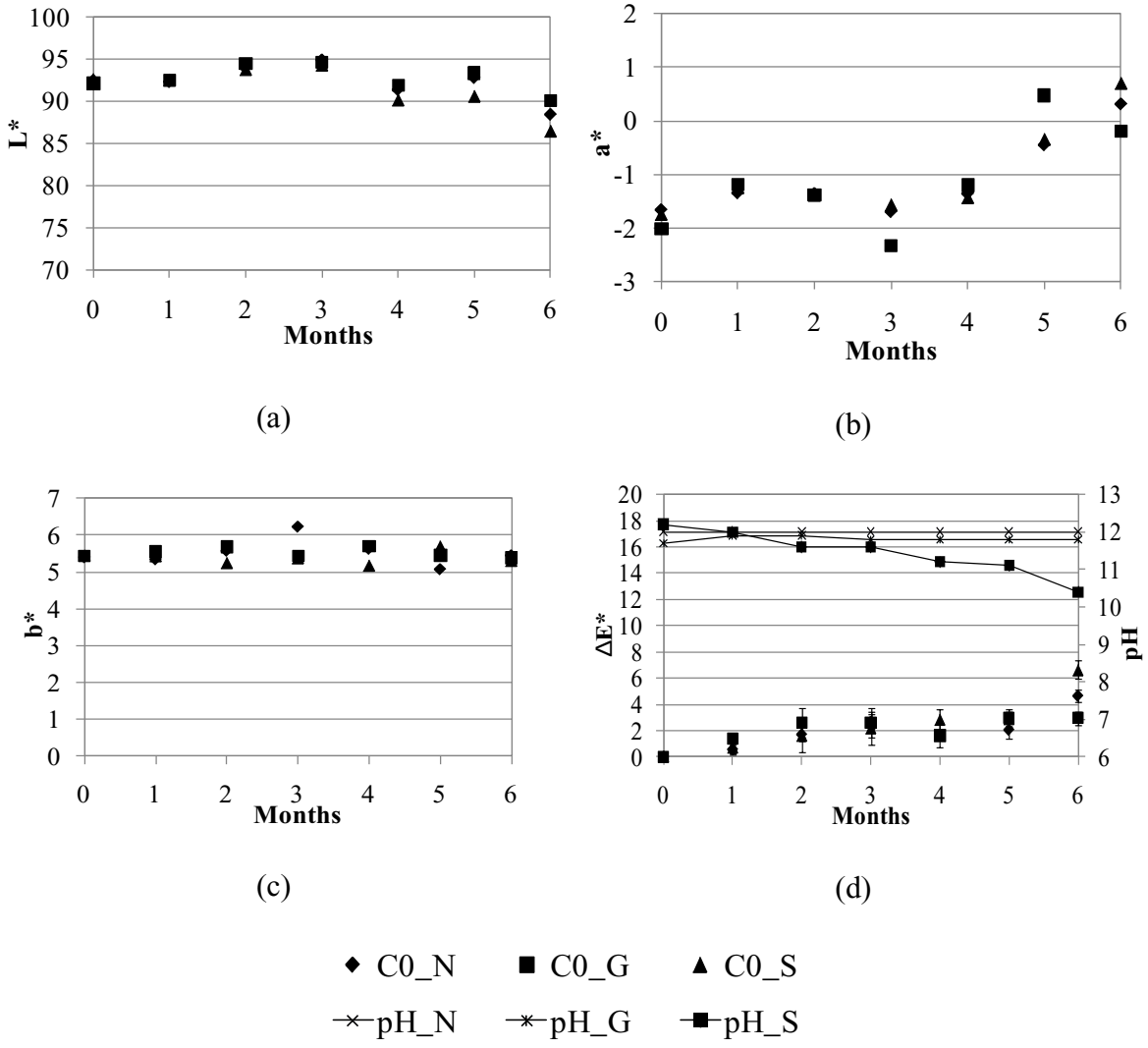

Fig. 4-13 – Color measurements for Series C – concrete with 0% RHA

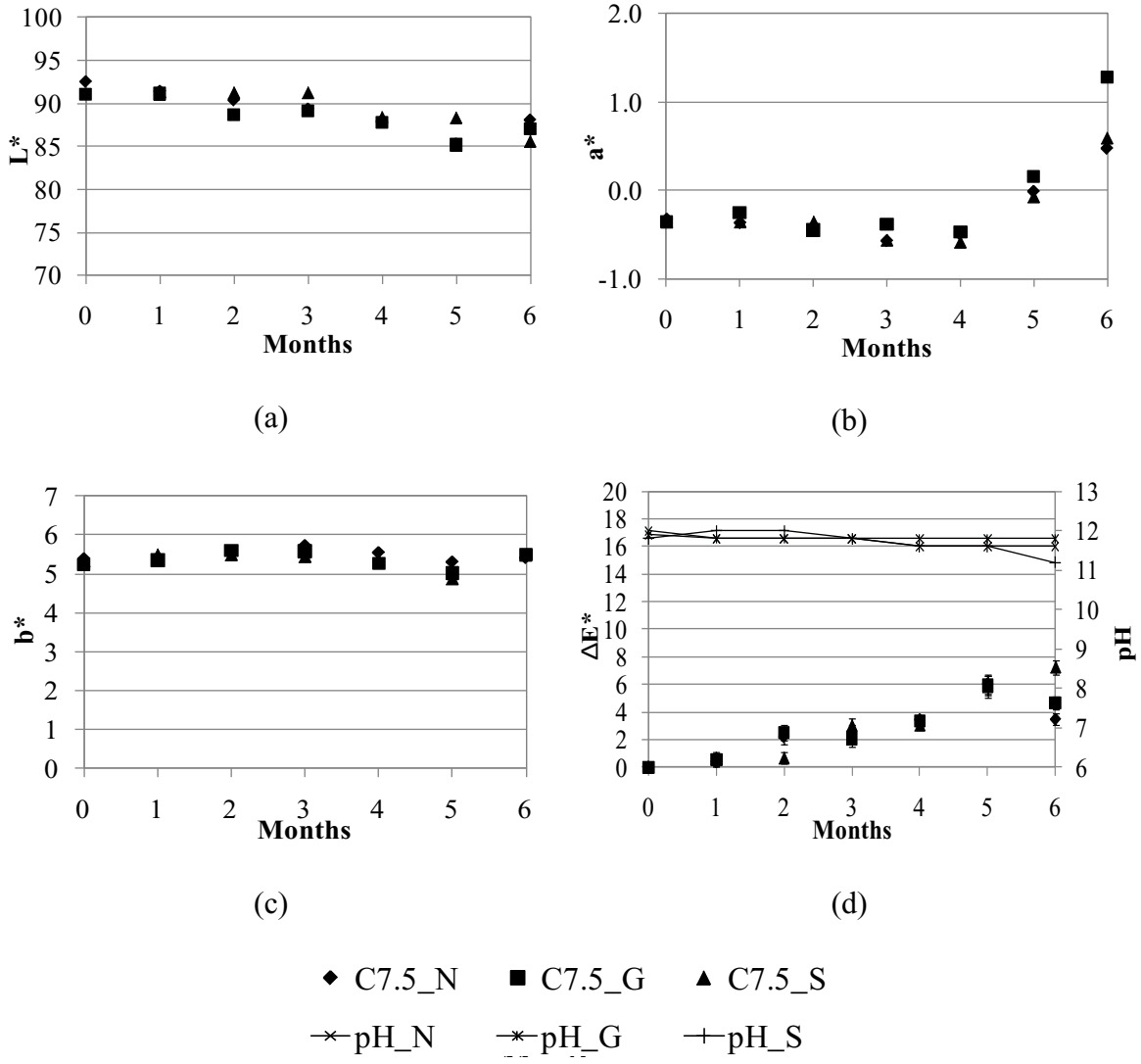

Fig. 4-14 – Color measurements for Series C – concrete with 7.5% RHA

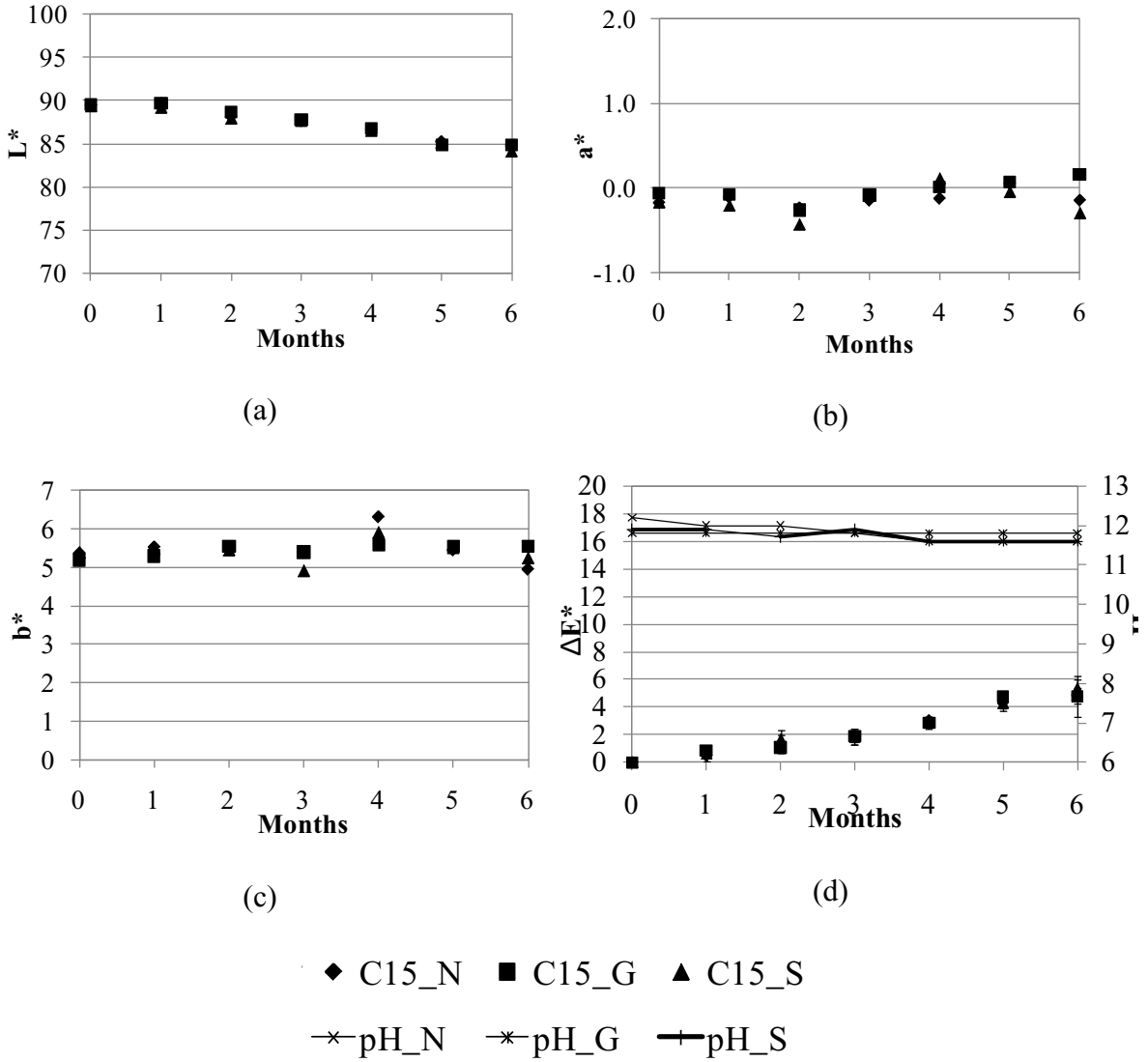

Fig. 4-15 – Color measurements for Series C – concrete with 15% RHA

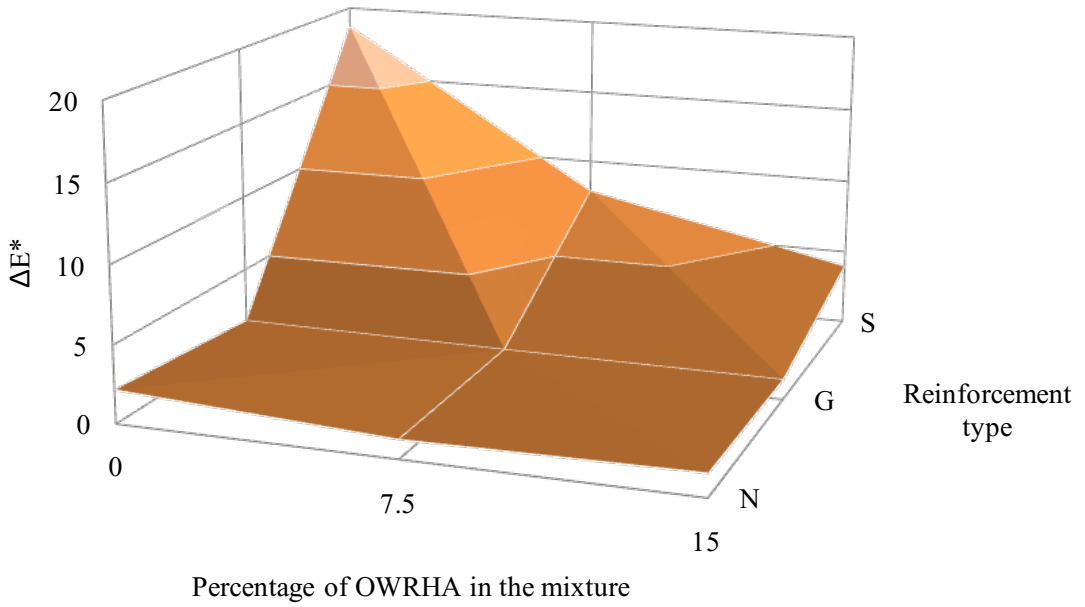

Fig. 4-16 –Relation between ΔE*, reinforcement type and percentage of R180 in concrete for Series A

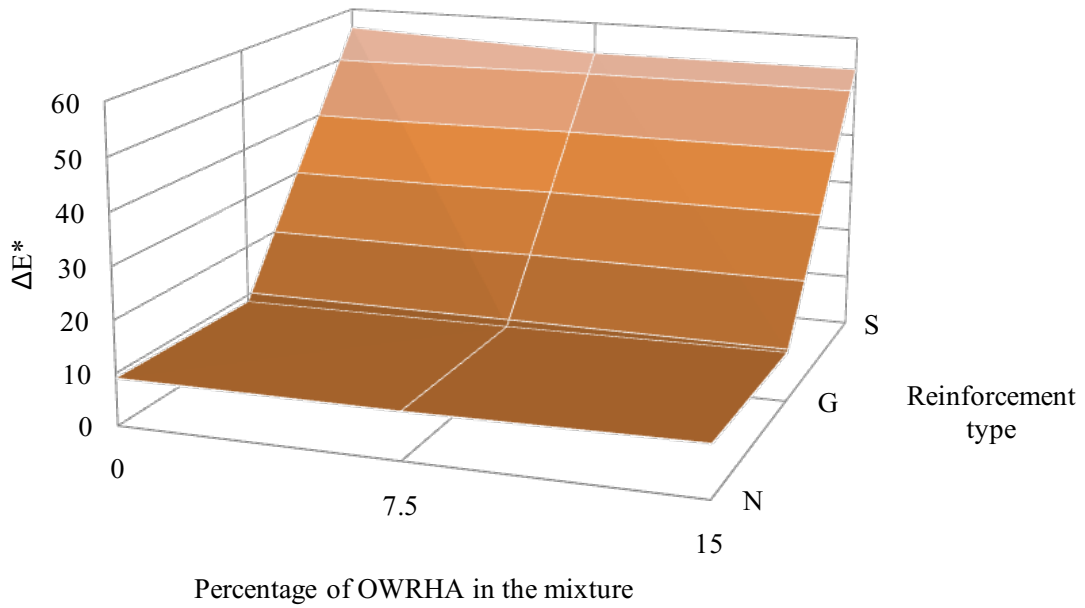

Fig. 4-17 –Relation between ΔE*, reinforcement type and percentage of R180 in concrete for Series B

Fig. 4-18 –Relation between ΔE*, reinforcement type and percentage of R180 in concrete Series C

Chapter 5

5. CONCLUSIONS

5.1. DISCUSSION

This thesis was initiated with the aim of introducing a new sustainable material system in the area of new construction. This material system is the final product of an integration of white concrete and off-white rice husk ash. In previous studies, white concrete demonstrated its effectiveness in the sustainable construction arena. Thanks to its high reflectivity, it reduces temperature fluctuation and so energy need, resulting in a reduction of the heat island effect. Additionally, the use of OWRHA increases the environmental benefit related to disposal of waste material reduces the carbon oxidation emission, and the need of cement in the concrete mixture.

In terms of energy, this system reduces the energy required for the production of the primary materials, decreases the energy needed for heating and cooling a building, and increases the life of the structure it reduces the energy usage for material disposal. In order to demonstrate the validity of this system, three main studies were conducted. In the first study, the properties of OWRHA and its use as pozzolanic material were proved. Since durability effects occupy an important position in this scenario, the second study was conducted on this aspect. If the system is durable, less maintenance is needed to keep the functionality of the system, which translates in a reduction of the consumption of

non-renewable resources. During this study an innovative methodology was developed to improve the accuracy of determination of the beginning of the corrosion mechanism in reinforced concrete. This third study addressed the influence of OWRHA on the reflectivity of the white concrete. Given that the sustainable activity of white concrete is related to the color, which allows a high solar reflectivity, a great deal of attention had to be devote to the influence that OWRHA has on this property. Also, in this case durability effects played a fundamental role, and so a color degradation study was carried out. A new methodology was designed to investigate the color of the concrete and the its evolution due to the primary material used to compose the material, and the different environment in which the system can be located. OWRHA is highly amorphous, with high percentage of silica, and almost negligible amount of residual carbon. Unlikely most of the other pozzolanic materials, OWRHA particles do not need to be extremely fine. This is because the source of high surface area in rice husk is in the microporous structure of individual particles. This propriety reduces the energy need to manufacture the RHA associated with the grinding.

5.2. OBJECTIVE I

The first goal of this thesis was to realize a high performance sustainable system. The material would combine the advantages of white concrete in terms of aesthetic, safety and energy savings to the effects that RHA produce in concrete in terms of high durability and strength. In order to address this objective the pozzolanic activity of OWRHA and the effect that this product has on white concrete in terms of strength and durability had to be studied. The first study presented in this dissertation, demonstrated

the effectiveness of OWRHA as pozzolanic material. The results prove that this material is perfectly in line with the standard related to supplementary cementitious materials and that it can increase the mechanical properties of white concrete, and so of grey concrete, as much as RHA tested in previous studies.

5.3. OBJECTIVE II

The second goal of this thesis was to develop a new methodology to determine the beginning of the corrosion process of steel in concrete and the difference in effect when OWRHA is used. The time of the first crack was estimated together with porosity and coefficient of water absorption. In order to evaluate the time of first crack, different parameters were measured during the conditioning of the samples and a correlation with respect to time was made after the end of the test. Acoustic Emission (AE) detected the first crack before current measurement and visual inspection. The parameters measured with the AE during the conditioning, such as amplitude, duration, hits and energy allowed for identification of the crack event. By its waveform, it became possible to identify the type of damage occurred; in this case cracking of concrete due to the corrosion/expansion process of the embedded steel. The corrosion current measurements were able to detect not only the time of cracking of the concrete, but also the difference in resistance, and so conductivity of the concrete made with different amounts of OWRHA. This material reduces the porosity of the concrete and so the migration of water and ions in it. This phenomenon retards the deterioration of the concrete due to steel corrosion. The consistency in the results obtained, proves that the methodology designed, is a valid tool

applicable in the area of corrosion of steel in concrete not only to predict the beginning of the process but also to evaluate the effect of the concrete mixture on it.

5.4. OBJECTIVE III

One of the biggest challenges faced in this thesis was the development of a test methodology that could allow to first identify the color of the concrete and its components, and then its evolution due to the exposure to different environments. To overcome this problem a color analysis technique mainly used in the food engineering was borrowed, the spectrophotometry. The use of three different environments, with increasing level of aggressiveness allowed a clear distinction among three major phenomena that can cause alteration of white concrete aesthetics: corrosion, algae growth, and fluorescence. The methodology employed in this study, also enables to evaluate the extension of the surface area interested by such phenomena. The consistency of the results obtained with three types of conditioning validates the reproducibility of the setup and of the methodology used for the monitoring. The incorporation of OWRHA in the concrete mixture determined a reduction of 1) corrosion of embedded steel, 2) algae growing, and 3) fluorescence development, resulting in an increase in the color durability of the concrete. Furthermore, the use of GFRP reinforcement in the concrete demonstrated to eliminate the problem of the corrosion without alternating the high reflectivity of the white surfaces.

5.5. OVERALL CONCLUSIONS

From the results obtained in the three studies presented, it can be concluded that the approach used in this thesis effectively helped to achieve the objectives of the research. This thesis demonstrates the effectiveness of white concrete incorporating OWRHA for sustainable, safety, and architectural applications. The use of this material system allows to reduce the energy related to the material production, and structure conditioning. From an economical stand point this material reduces costs of maintenance because of the high durability, energy because of the reduction in temperature fluctuation of the structure, and may allow the building to earn credits for LEED Certification. But the use of OWRHA is not restricted only to white concrete. OWRHA can become a SCM also for grey concrete that can compete with the product on the market, such as silica fume or fly ash. These materials contain a considerable percentage of heavy metals, known to be detrimental to health in sufficient quantities, but until the 2008, the United State Environmental Protection Agency (EPA) considered unnecessary to regulate these materials as a hazardous waste. However, in June 2008, the U.S. House of Representatives held an oversight hearing on the Federal government's role in addressing health and environmental risks of fly ash. The interest in this direction increased, in particular after the events of December 22nd 2008, in Tennessee. This change in direction will progressively reduce the use of fly ash, and new materials, such as OWRHA, will be needed to overcome this increasing demand.

The two new methodologies developed in this thesis represent a valid support in the area of construction. The ability to determine the beginning of the process of corrosion in concrete can allow evaluating, in a fast and precise way, the effect that

additives, SCMs, or new mixtures can have on the corrosion process of the embedded steel. The introduced color analysis has potential to become the standard for defining color of concrete, predicting the final color of the mixture based on the colors of the primary components, or for quality control applications.

5.6. SCIENTIFIC CONTRIBUTION

The concept of reinforced concrete made with white cement and off-white rice husk had been developed and added to the existing body of scientific knowledge of sustainable construction. The methodology used to test the initiation of the corrosion process of steel reinforcing concrete in more detail, provides a new tool to add to the generally recognized practices. This research also contributed to fill the lack of knowledge related to the influence that composition and/or environment have on the whiteness of concrete. The set up used for conditioning of samples together with the adopted color monitoring procedure represents a new useful technology that can become a useful tool to the extension of existing methods and theories.

5.7. FURTHER INVESTIGATIONS

This dissertation represents an important step towards the use of and eco-friendly material in a wide range of applications. However, the work embodied in this dissertation is not without limitations. A great deal of work can be undertaken to overcome the following limitations and improve the capabilities of the results:

- Based on the previous work on RHA, this research analyzed only two percentage of OWRHA in concrete (7.5 and 15 %). The optimization of the amount of OWRHA is necessary.
- The effect of the fineness of the pozzolanic material should be conducted using OWRHA processed at different levels of grinding. The nature of the pozzolanic effect of OWRHA is mainly related to the internal specific surface, but perhaps a more fine powder could allow the material to increase its filling effect.
- The study allowed eliminating the degradation of the color due to corrosion of steel reinforcement. However, the algae growth could only be retarded. Surface treatments to decrease the bio-receptivity and to comprise the application of water repellents and/or biocides could be tested to eliminate this phenomenon.
- Previous results validate the effectiveness of white concrete as reflective material. However, more investigation of the conductivity of this material should be conducted in order to verify the real energy reduction for building conditioning.
- The actual technique for the spectrophotometry is punctual, and the only way to test a big surface is to statistically select a number of samples and locations considered representative of the total area. However different solutions can be used to improve the system and allow evaluating the color of an entire building surface. If a constant relationship between picture elements (pixels) and color exist, it would be possible to take pictures of a surface and analyze them afterwards. In this case the labor for this work would be minimal, and data could collect and analyzed more easily at anytime.

REFERENCE

1. Mora E.P., "Life Cycle, Sustainability and the Transcendent Quality of Building Materials," *Building and Environment,* 42, 2007, pp. 1329–1334.

2. Grace K.C.D., "Sustainable Construction-The Role of Environmental Assessment Tools," *Journal of Environmental Management,* 86, 2008, pp. 451–464.

3. Hurd M.K., "Tips for Coloring Concrete, Concrete Construction," 38 (5), 1993, pp. 345-351.

4. Portland Cement Association - News From PCA 2008. "Architectural and Decorative Concrete," (Hitting the headlines article) [Online]. (Updated Apr. 21, 2008) Available at: http://www.cement.org [accessed May 27, 2008].

5. LEED New Construction Version 2.2 Reference Guide. Second Edition September 2006.

6. Melchers R.E., Li C.Q., Lawanwisut W., "Probabilistic Modeling of Structural Deterioration of Reinforced Concrete Beams Under Saline Environment Corrosion," *Structural Safety,* 30, 2008, pp.447–460.

7. Ballim Y., Reid J.C., and Kemp A.R., "Deflection of RC Beams Under Simultaneous Load and Steel Corrosion," *Magazine of Concrete Research*, 53 (3), 2001, pp.171–81.

8. Derrien F., Chahbazian G., Carpio J.J., and Raharinavio A., "Cathodic Polarization Behavior of Steel in Solutions Simulating Concrete," *Cement and Concrete Research* (20), 1990, pp.636-643.

9. Raharinaivo J.P., Guilbauda G., Chahbazianb, and Derrien F., "The Electrochemical Behavior of Steel Under Polarization in Porous Media Simulating Concrete," *Corrosion Science*, 33, 1992, pp. 1607-1616.

10. Fejardo G., Valdez P., and Pacheco J., (in press), "Corrosion of Steel Rebar Embedded in Natural Pozzolan Based Mortars Exposed to Chlorides," *Construction and Building Materials.*

11. Poursaee C., and Hansson M., "The Influence of Longitudinal Cracks on the Corrosion Protection Afforded Reinforcing Steel in High Performance Concrete," *Cement and Concrete Research*, (38), 2008, pp.1098-1105.

12. Vempati R.K., "Composition and Method of Forming Low-Carbon, Amorphous Siliceous Ash From Siliceous Waste Material," US Patent No.6,44,186 B1 (2002a).

13. Vempati R.K., Borade R., Hegde R.S., and Komarneni S., "Template Free ZSM-5 From Siliceous Rice Hull Ash With Varying C Contents," *Microporous and Mesoporous Material*, 93, 2006, pp. 134-140.

14. Hurd M.K., "Tips for Coloring Concrete," *Concrete Construction*, 38 (5), 1993, pp. 345-351.

15. Beagle E., "Rice Husk Conversion to Energy," Agricultural Service Bulletin 31, Food and Agricultural Organization, Rome, Italy (1978).

16. Nehdi M., Duquette J., and El Damatty A., "Performance of Rice Husk Ash Produced Using a New Technology as a Mineral Admixture in Concrete," *Cement and Concrete Research*, 33 (8), 2003, pp. 1203-1210.

17. Spire S., Elefthriou S.S.K., and Siludom S., "Durability of Concrete Containing Rice Husk in an Additive," Proc., Exploiting wastes in concrete, Creating with Concrete, Dundee, 1999.

18. Jauberthie R., Rendella F., Tambab S., and Cisseb I., "Origin of the Pozzolanic Effect of Rice Husks," *Construction of Building Material*, 14, 2000, pp. 419-423.

19. Moayad N.A. , and Yousif H.A., "Use of Rice Husk Ash in Concrete," *International Journal of Cement Composites and Lightweight Concrete*, 6 (4), 1984, pp. 241-248.

20. Nair D.G., Fraaija A., Klaassenb A.A.K., and Kentgens A.P.M., "A Structural Investigation Relating to the Pozzolanic Activity of Rice Husk Ashes," *Cement and Concrete Research*, 38 (8), 2008, pp. 61-869.

21. Mehta P. K. "Siliceous Ashes and Hydraulic Cements Prepared Therefrom." U.S. Patent 4105459, 1978.

22. Mehta P.K. "Siliceous Ashes and Hydraulic Cements Prepared Therefrom." Belgium Patent 802909, 1973.

23. Pitt N., "Process for Preparation of Siliceous Ashes," U.S. Patent 3959007, 1976.

24. FAO, (2009) "FAO Statistical Databases," <http://faostat.fao.org/site/567/default.aspx>, (April 3, 2009).

25. Beagle E., "Rice Husk Conversion to Energy." Agricultural Service Bulletin 31, Food and Agricultural Organization, 1978, Rome, Italy.

26. Nair D.G., Fraaija A., Klaassenb A.A. K., and Kentgens A.P.M., "A Structural Investigation Relating to the Pozzolanic Activity of Rice Husk Ashes," *Cement and Concrete Research*, 38, 2008 pp. 861-869.

27. Mehta P. K. (1978). "Siliceous Ashes and Hydraulic Cements Prepared Therefrom." U.S. Patent 4105459.

28. Spire S., Elefthriou S.S.K., and Siludom S., "Durability of Concrete Containing Rice Husk in an Additive." Proc., Exploiting wastes in concrete, Creating with Concrete, Dundee, 1999.

29. Metha P.K., "The Chemistry and Technology of Cement Made from Rice Husk Ash," Proc., Workshop on Rice Husk Ash Cement, Regional Center for Technology Tranfer, Bangalor India, 1979, pp. 113-122.

30. Jauberthie R., Rendella F., Tambab S., and Cisseb I., "Origin of the Pozzolanic Effect of Rice Husks," *Construction and Building Materials*, 14, 2000, pp. 419-423.

31. Ganesan K., Rajagopal K., and Thangavel K., "Rice Husk Ash Blended Cement: Assessment of Optimal Level of Replacement for Strength and Permeability Properties of Concrete," *Construction and Building Materials*, 22, 2008, pp. 1675-1683.

32. Mehta P.K. "Rice Husk Ash – a Unique Supplementary Cementing Material." Proc., Int. Symp. on Advances in Concrete Technology, Athens, Greece, 1992, pp. 407-430.

33. Mehta P.K. "Siliceous Ashes and Hydraulic Cements Prepared Therefrom." Belgium Patent 802909, 1973.

34. Pitt N. "Process for Preparation of Siliceous Ashes." U.S. Patent 3959007, 1976.

35. Zhang M.H., Lastra R., and Malhotra V.M., "Rice Husk Ash Paste and Concrete: Some Aspect of Hydration and of the Microstructure of the Interfacial Zone Between the Aggregates and the Paste," *Cement and Concrete Research*, 26 (6), 1996, pp. 963-977.

36. Quijun Y.K., Sawayama S., Sugita S., Shoya M., and Isojima Y., "The Reaction Between Rice Husk Ash and $Ca(OH)_2$ Solution and the Nature of its Product," *Cement and Concrete Research*, 29, 1999, pp. 37-43.

37. Vempati R.K., Borade R., Hegde R.S., and Komarneni S., "Template free ZSM-5 from Siliceous Rice Hull Ash With Varying C Contents," *Microporosity and Mesoporosity Materials*, 93, 2006, pp. 134-140.

38. Boateng A.A., Fan L.T., Walawender W.P., and Chee C.S., "Morphological and Development of Rice Hulls Derived Charcoal in a Fluidized Bed Reactor," *Fuel*, 70, 1991, pp. 995-1000.

39. Savant N.K., Snyder G.H., and Datnoff L.E., "Silicon Management and Sustainable Rice Production," *Advanced Agronomy*, 58, 1997, pp. 151-199.

40. Krainwood K., Chain J., Smith S., and Seksun C., "A Study of Ground Course Fly Ashes with Different Finenesses from Various Sources as Pozzolanic Materials," *Cement and Concrete Composites*, 23, 2001, pp. 335-343.

41. Paya J., Monzo J., Peris-Mora E., Borrachero M.V., Tercero R., and Pinillos C., "Early-Strength Development of Portland Cement Mortars Containing Air Classified Ashes," *Cement and Concrete Research*, 25 (2), 1995, pp. 449-456.

42. Paya J., Monzo J., Peris-Mora E., Borrachero M.V., Peris E., and Gonzales-Lopez E., "Mechanical Treatment of Fly Ashes. Part III: Sstudies on Strength Development on Ground Fly Ash Cement Mortars," *Cement and Concrete Research*, 27 (9), 1997, pp. 1365-1377.

43. Kamath S.R. , and Proctor A., "Silica Gel from Rice Hull Ash: Preparation and Characterization, " *Cereal Chemistry*, 75, 1998, pp. 484-487.

44. Rukzon S., and Chindaprasirt P., "Strength of Ternary Blended Cement Mortar Containing Portland Cement, Rice Husk Ash and Fly Ash," *Journal of the Engineering Institute* of *Thailand*, 17, 2006, pp. 33.

45. Rukzon S., Chindaprasirt P., and Mahachai R., "Effect of Grinding on Chemical and Physical Properties of Rice Husk Ash," *International Journal of Mining and Mineral*, 16, (2), 2009, pp. 242.

46. Jauberthie R., Rendell F., Tamba S. and Cissé I.K., "Properties of Cement – Rice Husk Mixture," *Construction and Building Materials*, 17, 2003, pp. 239-243.

47. Zang M.H., and Malhotra V.M., "High-Performance Concrete Incorporating Rice Husk Ash as a Supplementary Cementing Material," *ACI Material Journal*, 93, (6), 1996, pp. 629-636.

48. Saraswathy V., and Song H. W., "Corrosion Performance of Rice Husk Ash Blended Concrete," *Construction and Building Materials*, 21, 2006, pp. 1779-1749.

49. Sakr K., "Effects of Silica Fume and Rice Husk Ash on the Properties on Heavy Weight Concrete," *Journal of Material for Civil Engineering*, 18 (3), 2006, pp. 367-376.

50. Rodriguez de Sensale G., "Strength Development of Concrete with Rice-Husk Ash," *Cement and Concrete Composites*, 28, 2006, pp. 158-160.

51. Melchers R.E., Li C.Q., and Lawanwisut W., "Probabilistic Modeling of Structural Deterioration of Reinforced Concrete Beams Under Saline Environment Corrosion," *Structural Safety*, 30, 2008, pp. 447–460.

52. Mehta P.K., "Durability—Critical Issues for the Future," Concrete International, 19, 7, July 1997, pp. 27-33.

53. Oh B.H., and Jang B.S., "Chloride Diffusion Analysis of Concrete Structures Considering the Effects of Reinforcements," *ACI Materials Journal*, 100, (2), Mar.-Apr. 2003, pp. 143-149.

54. Broomfield, J. P. "Corrosion of Steel in Concrete: Understanding, Investigation and Repair," E&FN Spon, London, Great Britain, 2007, pp. 277.

55. Gjory O.E., and Vannesland O., "Sea Salts and Alkalinity of Concrete," *ACI Journal*, 72, 42, pp. 512.

56. Bentur A., Diamond S., and Berke N.S., "Steel Corrosion in Concrete," Chapman & Hall, London, 1997.

57. Derrien F., Chahbazian G., Carpio J. J., and Raharinavio A., "Cathodic Polarization Behavior of Steel in Solutions Simulating Concrete," *Cement and Concrete Research*, 20, 1990, pp. 636-643.

58. Raharinaivo A., Guilbauda J. P., Chahbazianb G., and Derrien F., "The Electrochemical Behavior of Steel Under Polarization in Porous Media Simulating Concrete," *Corrosion Science*, 33, 1992, pp. 1607-1616.

59. Alonso C., Anndrade C., Castellote M., and Castro P., "Chloride Threshold Values to Depassivate Reinforcing Bars Embedded in a Standardized OPC Mortar," *Cement and Concrete Research*, 55, 2, April 2003, pp. 1047-1055.

60. Corrosion Cost (2009), U.S. Department of Transportation Federal Highway Administration, www.corrosioncost.com, (October 3, 2009).

61. Cook D. J., "Cementitious Materials Based on Rice Husk Ash," Proc., Workshop on Rice Husk Ash Cement, Regional Center for Technology Transfer, Bangalor, India, 1979, pp.162-173.

62. Chan W.W.J., and Wu C.M.L., "Durability of Concrete with High Cement Replacement," *Cement and Concrete Research*, V. 30, No. 6, 2000, pp. 865–879.

63. Moyad N., Khalaf A., and Yousif Hana A., "Use of Rice Husk Ask in Concrete," *International Journal of Cement Composite and Light Weight Concrete*, 6, 1987, pp. 241-248.

64. Nehdi M., Duquette J., and El Damatty A., "Performance of Rice Husk Ash Produced Using a New Technology as a Mineral Admixture in Concrete," *Cement and Concrete Research*, 33, 8, August 2003, pp. 1203-1210.

65. Vempati R.K., "Composition and Method of Forming Low-Carbon, Amorphous Siliceous Ash from Siliceous Waste Material," US Patent No.6,44,186 B1 (2002a).

66. Krainwood K., Chain J., Smith S., and Seksun C., "A Study of Ground Course Fly Ashes with Different Finenesses from Various Sources as Pozzolanic Materials," *Cement Concrete Composite*, 23, 2001, pp. 335-343.

67. Malhotra V.M., "Effect of Curing on the Compressive Strength, Resistance to Chloride-Ion Penetration and Porosity of Concretes Incorporating Slag, Fly Ash or Silica," *Cement Concrete Composite*, 17, 1995, pp. 125-133.

68. Soulioti D., Barkoula N.M, Paipetis A., Matikas T.E., Shiotani T., and Aggelis D.G., "Acoustic Emission Behavior of Steel Fibre Reinforced Concrete Under Bending," *Construction and Building Materials*, 23, 2009, pp. 3532–3536.

69. Yuyama S., Kishi T., and Hisamatsu Y., "Effect of Environment, Mechanical Conditions, and Materials Characteristics on AE Behavior During Corrosion Fatigue Processes of an Austenitic Stainless Steel," *Nuclear Engineering and Design*, 81, 2, September 1984, pp .345-355.

70. Kumar R., and Bhattacharjee B., "Porosity, Pore Size Distribution and in Situ Strength of Concrete," *Cement and Concrete Composite*, 33, 2003, pp. 155-164.

71. Vodák F., Trtík K., Kapicková O., Hosková S., and Demo P., "The Effect of Temperature on Strength – Porosity Relationship for Concrete," *Construction and Building Materials*, 18, 2004, pp. 529-534.

72. Paya J., Monzo J., Peris-Mora E., Borrachero M.V., Tercero R., and Pinillos C., "Early-Strength Development of Portland Cement Mortars Containing Air Classified Ashes," *Cement and Concrete Research*, 25, 2, 1995, pp. 449-456.

73. Paya J., Monzo J., Peris-Mora E., Borrachero M.V., Peris E., and Gonzales-Lopez E., "Mechanical Treatment of Fly Ashes. Part III: Studies on Strength Development on Ground Fly Ash Cement Mortars," *Cement and Concrete Research*, 27, 9, 1997, pp. 1365-1377.

74. Powers T.C., "Properties of Fresh Concrete," John Wiley & Sons Publisher, New York, 1968.

75. Chindaprasirt P., and Rukzon S., "Strength, Porosity and Corrosion Resistance of Ternary Blend Portland Cement, Rice Husk Ash and Fly Ash Mortar," *Construction and Building Materials*, 22, 8, August 2008, pp. 1601-1606.

76. Idrissi H., and Limam A., "Study and Characterization by Acoustic Emission and Electrochemical Measurements of Concrete Deterioration Caused by Reinforcement Steel Corrosion," *NDT&E International*, 36, 2003, pp.563-569.

77. Assouli B., Simescu F., Debicki G., and Idrissi H., "Detection and Identification of Concrete Cracking During Corrosion of Reinforced Concrete by Acoustic Emission Coupled to the Electrochemical Techniques," *NDT&E International*, 38, 2005, pp. 682-689.

78. Saraswathy V., and Song H.W., "Corrosion Performance of Rice Husk Ash Blended Concrete," *Construction and Building Materials*, 21, 2007, pp.1779-1784.

79. Chindaprasirt P., Homwuttiwong S., Jaturapitakkul C., "Strength and Water Permeability of Concrete Containing Palm Oil Fuel Ash and Rice Husk-Bark Ash," *Construction and Building Materials*, 21, 2007, pp. 1492-1499.

80. Fajardo G., Valdez P., and Pacheco J., "Corrosion of Steel Rebars Embedded in Natural Pozzolan Based Mortars Exposed to Chlorides," *Construction and Building Materials*, 23, 2, February 2009, pp. 768-774.

81. Andrade C., and Alonso C., "Corrosion Rate Monitoring in the Laboratory and On-Site," *Construction and Building Materials*, 10, 5, 1996, pp.315-328.

82. Böhni, H., "Corrosion in Reinforced Concrete," Woodhead Publishing, Cambridge, 2005.

83. LEED New Construction Version 2.2 Reference Guide. Second Edition September 2006.

84. Hurd M.K., "Tips for Coloring Concrete," *Concrete Construction*, 38 (5), 1993, pp. 345-351.

85. Zhang M.H., Lastra R., and Malhotra V.M., "Rice Husk Ash Paste and Concrete: Some Aspect of Hydration and of the Microstructure of the Interfacial Zone Between the Aggregates and the Paste," *Cement and Concrete Research*, 26 (6), 1996, pp. 963-977.

86. Quijun Y.K., Sawayama S., Sugita S., Shoya M., and Isojima Y., "The Reaction Between Rice Husk Ash and $Ca(OH)_2$ Solution and the Nature of its Product," *Cement and Concrete Research*, 29, 1999, pp.37-43.

87. Krainwood K., Chain J., Smith S., and Seksun C., "A Study of Ground Course Fly Ashes with Different Finenesses from Various Sources as Pozzolanic Materials," *Cement and Concrete Composites*, 23, 2001, pp. 335-343.

88. Boateng A.A., Fan L.T., Walawender W.P., and Chee C.S., "Morphological and Development of Rice Hulls Derived Charcoal in a Fluidized Bed Reactor," *Fuel*, 70, 1991, pp. 995-1000.

89. Savant N.K., Snyder G.H., and Datnoff L.E., "Silicon Management and Sustainable Rice Production," *Advanced Agronomy*, 58, 1997, pp. 151-199.

90. Tiwari B.K., Muthukumarappan K., and O'Donnell C.P., Cullen P.J., "Modeling Color Degradation of Orange Juice by Ozone Treatment Using Response Surface Methodology," *Journal of Food Engineering*, 88, 2008, pp. 553-560.

91. Niamnuy C., Devahastin S., Soponronnarit S., and Raghavan G.S.V., "Kinetics of Astaxanthin Degradation and Color Changes of Dried Shrimps During Storage," *Journal of Food Engineering*, 87, 2008, pp. 591-600.

92. Ferreira S.L.C., Ferreira H.S., de Jesus R.M., Santos J.V.S., Brandao G.C., and Souza A.S., "Development of Method for the Speciation of Inorganic Iron in Wine Samples," *Analytica Chimica Acta* (602), 2007, pp. 89-93.

93. CIE Publication 15.2 (1986) Colorhnetry (second edition) Section 4.2.2.

94. Nanni, A., "Flexural Behaviour and Design of RC Members Using FRP Reinforcement," *Journal of Structural Engineering*, AXE, 119 ST11, 1993, pp. 3344-3359.

95. De Muynck W., Ramirez A.M., De Belie N., and Verstraete W., "Evaluation of Strategies to Prevent Algal Fouling on White Architectural and Cellular

Concrete," *International Biodeterioration & Biodegradation*, 63, 2009, pp. 679-689.

96. Dow C., and. Glasser F.P, "Calcium Carbonate Efflorescence on Portland Cement and Building Materials," *Cement and Concrete Research*, 33 (1), 2003, pp. 147-154.

97. Paris N., and Chusid M., "Colour in Concrete - Beauty and Durability," *Concrete International*, 1, 1999, pp. 60-63.

APPENDIX I: STUDY II – ACCELERATED CORROSION TEST WITH IMPRESSED VOLTAGE

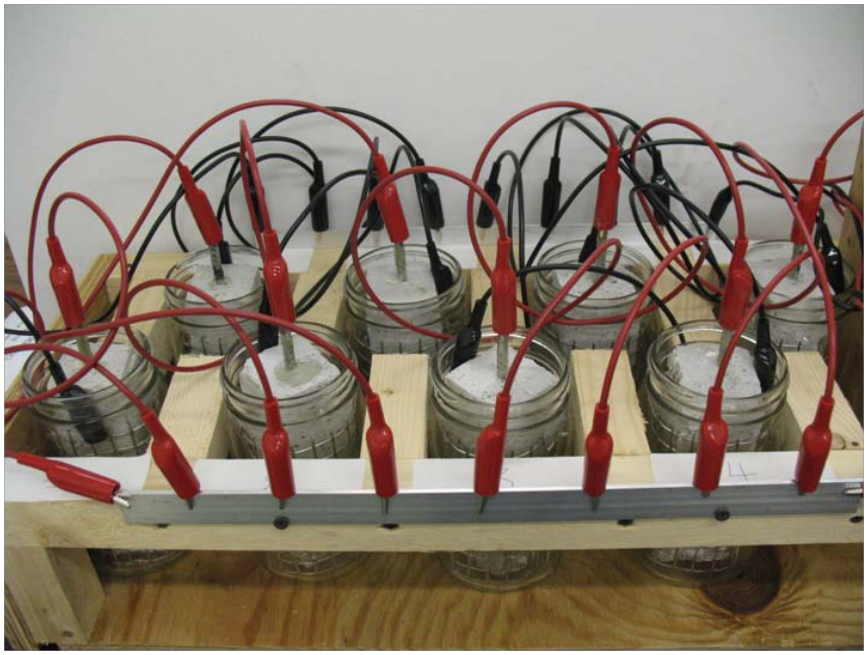

Fig. A.1- 1– ACTIV set-up

Fig. A.1- 2– DC Source used to impose constant voltage on the sample

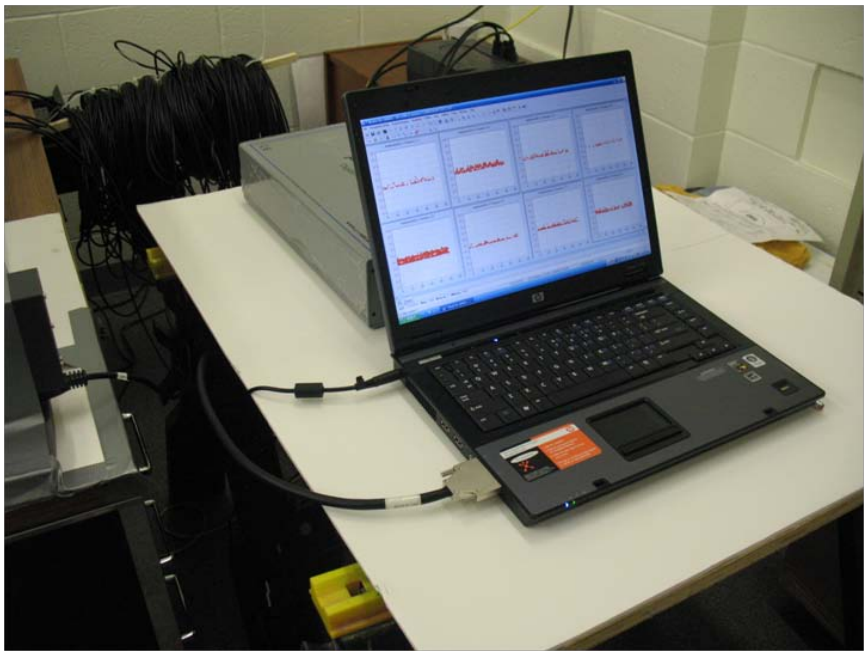

Fig. A.1- 3– Portable digital data acquisition system for acoustic emission

Fig. A.1- 4– Samples tested with ACTIV

Fig. A.1- 5– Interior view of sample tested with ACTIV

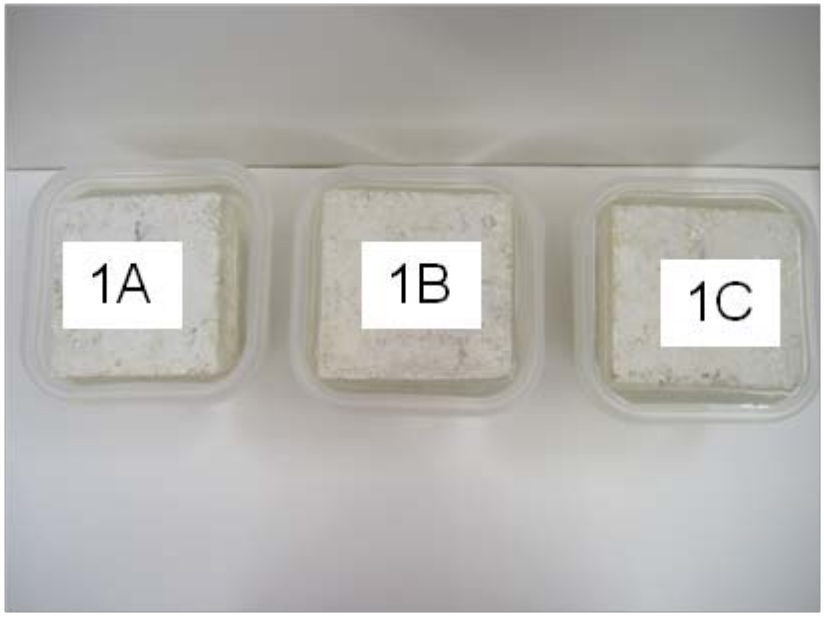

Fig. A.1- 6– Absorption test set-up

APPENDIX II: STUDY III - SCANNER ELECTRON MICROSCOPY OF RHA WITH DIFFERENT PERCENTAGE OF CARBON CONTENT

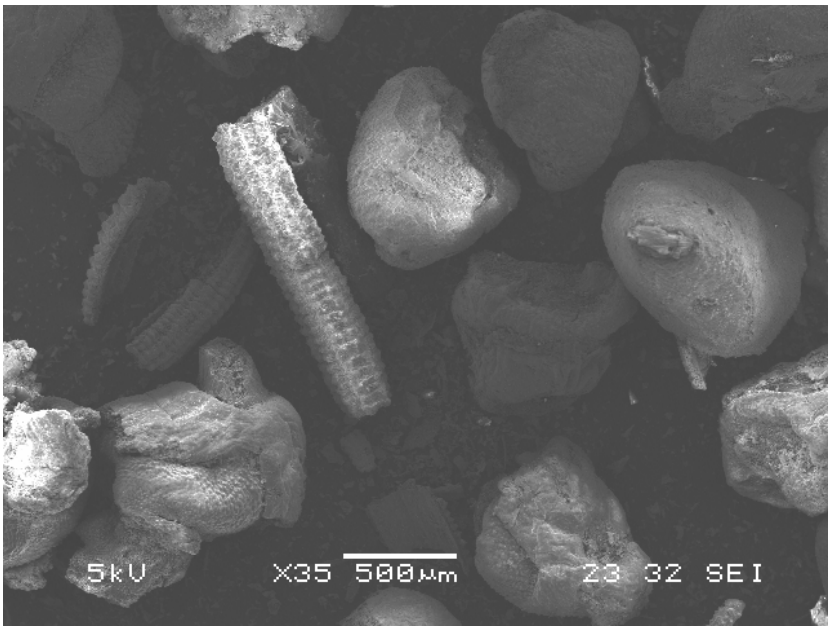

Fig. A.2 - 1– SEM of R15

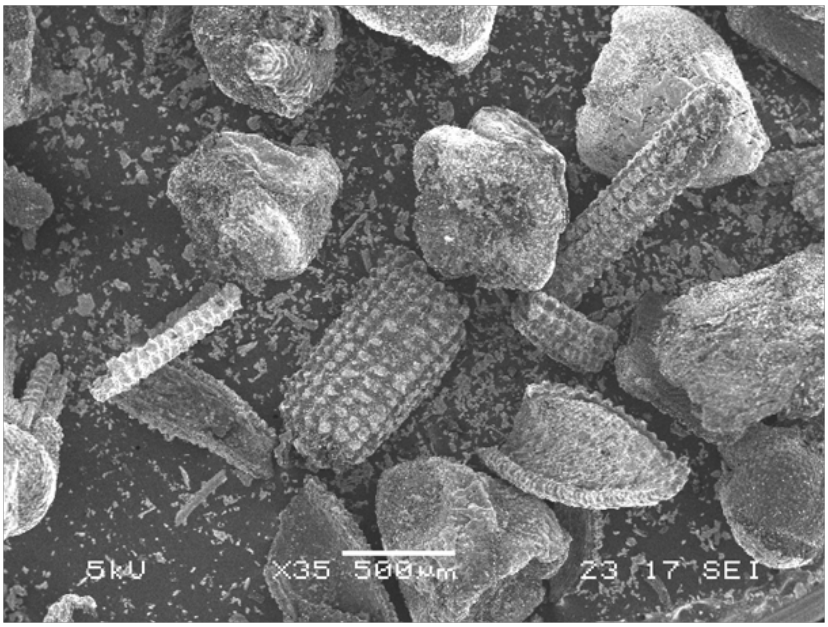

Fig. A.2 - 2– SEM of R30

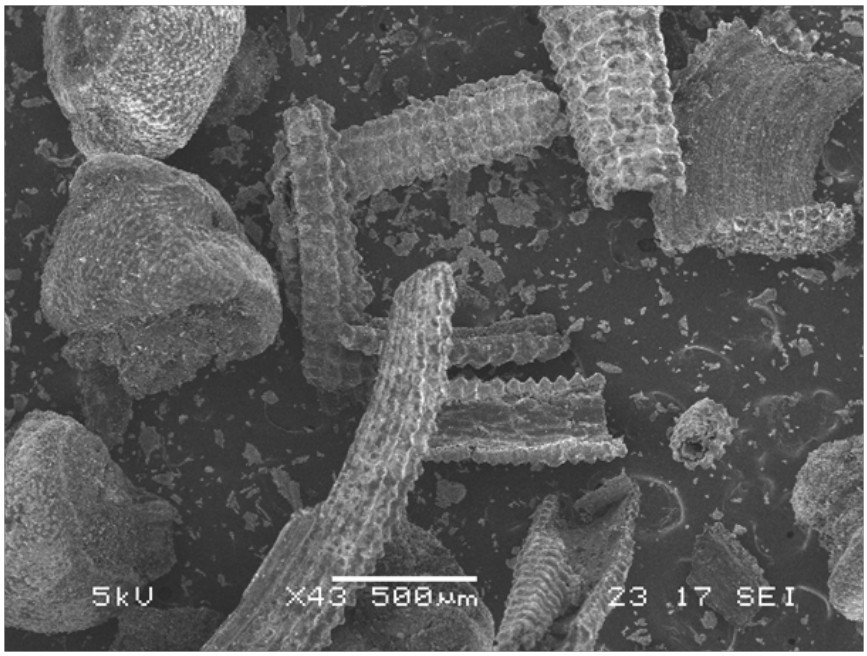

Fig. A.2 - 3– SEM of R45

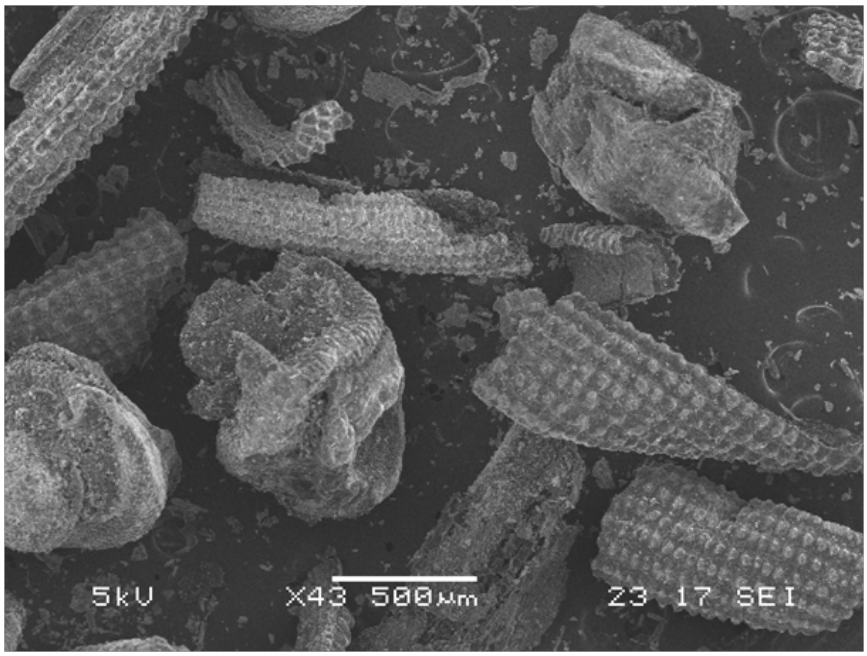

Fig. A.2 - 4– SEM of R60

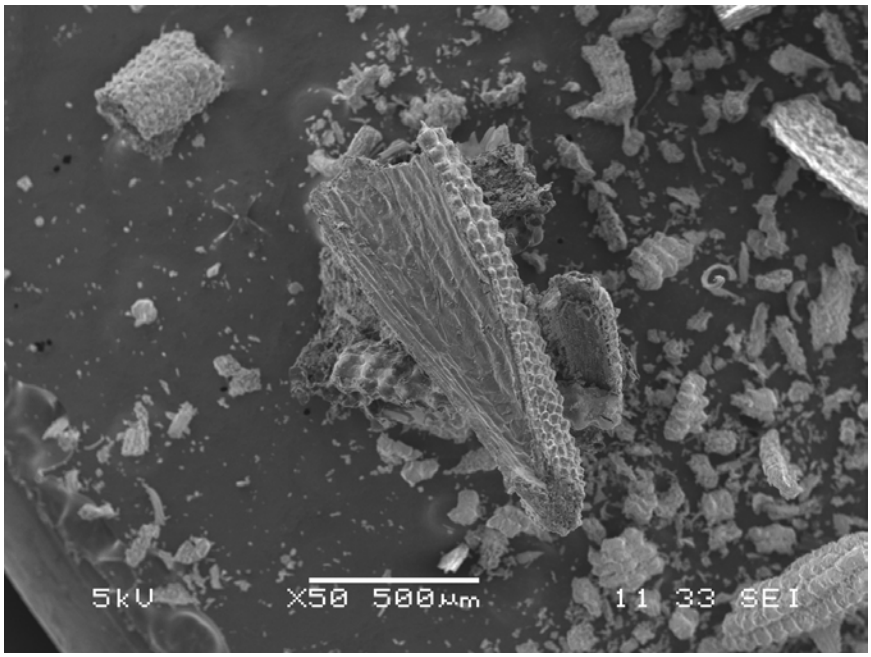

Fig. A.2 - 5– SEM of R90

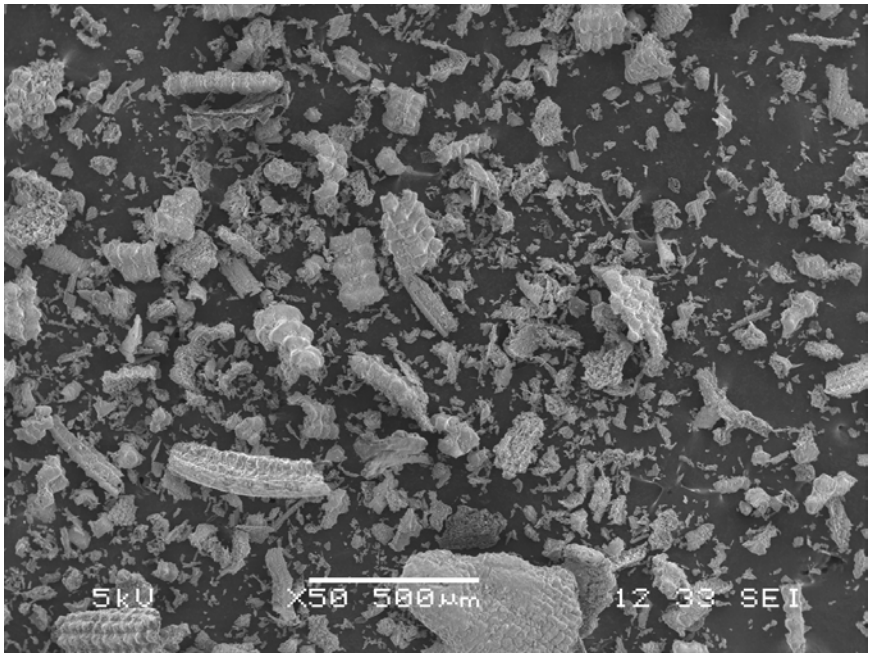

Fig. A.2 - 6– SEM of R120

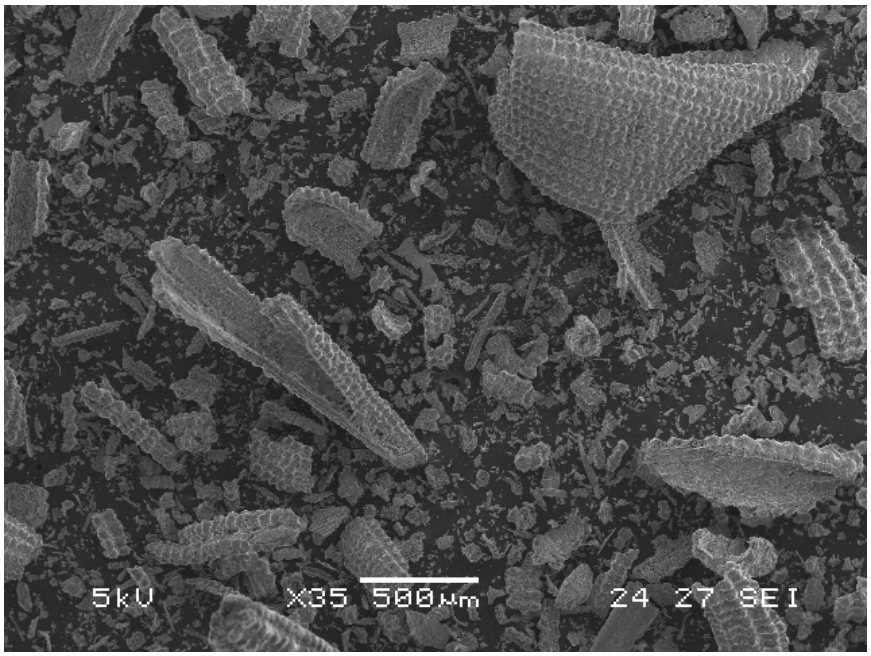

Fig. A.2 - 7– SEM of R150

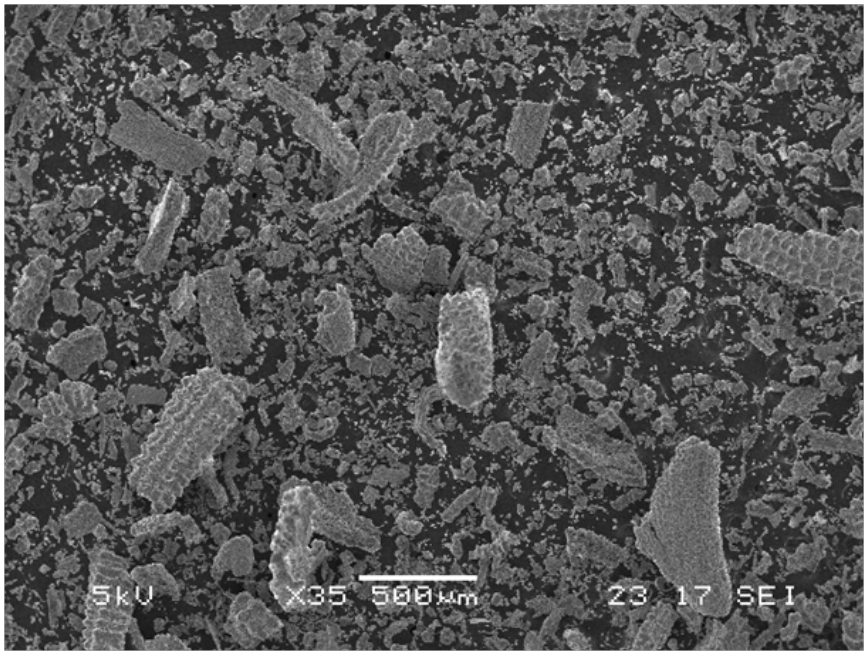

Fig. A.2 - 8– SEM of R180

APPENDIX III: STUDY III – RHA WITH DIFFERENT PERCENTAGE OF CARBON CONTENT

Fig. A.3 - 1– R15

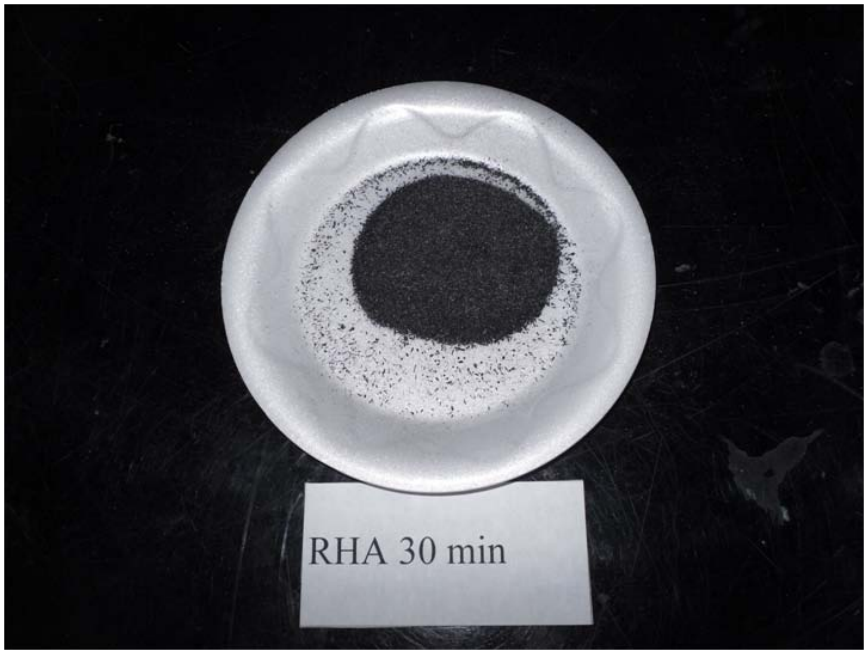

Fig. A.3 - 2– R30

Fig. A.3 - 3– R45

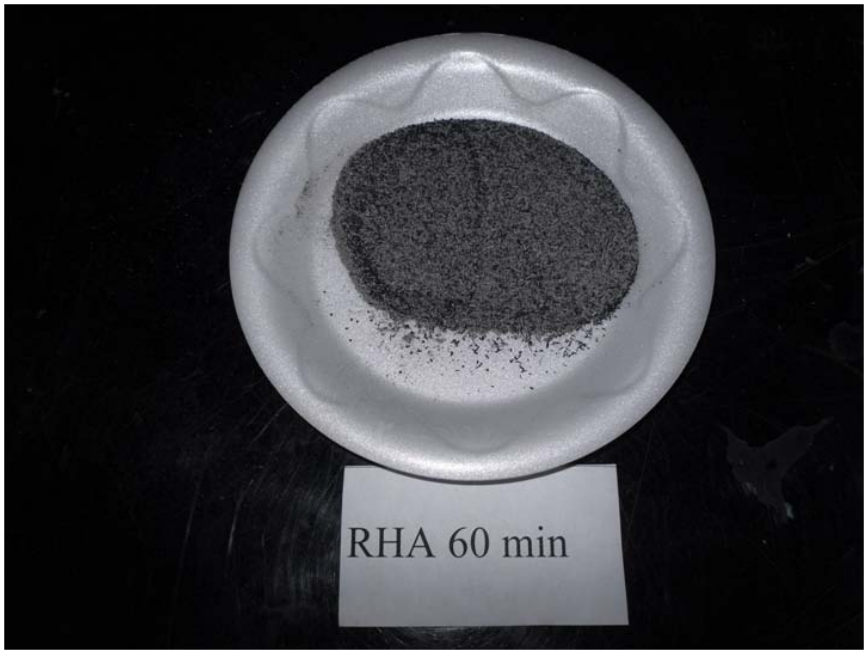

Fig. A.3 - 4– R60

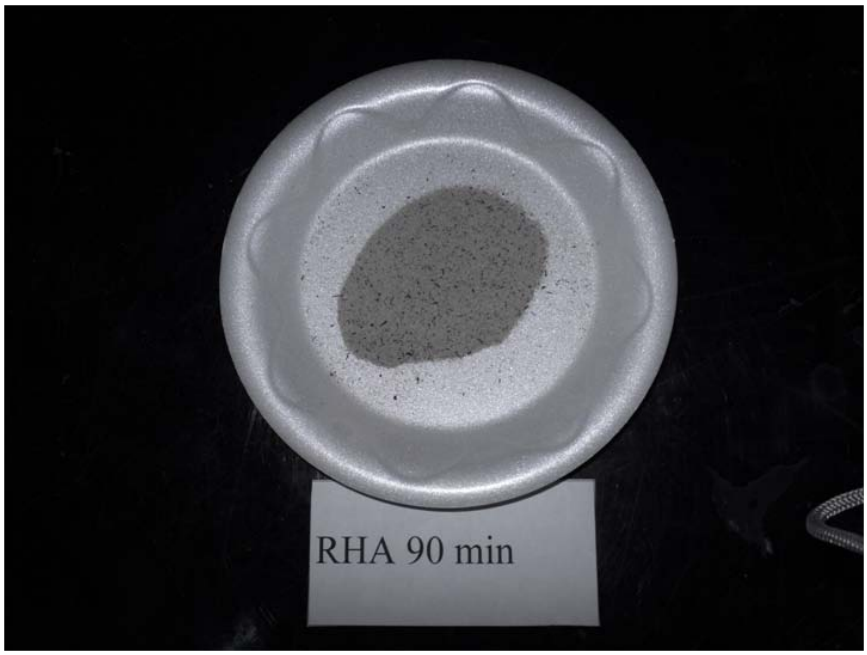

Fig. A.3 - 5– R90

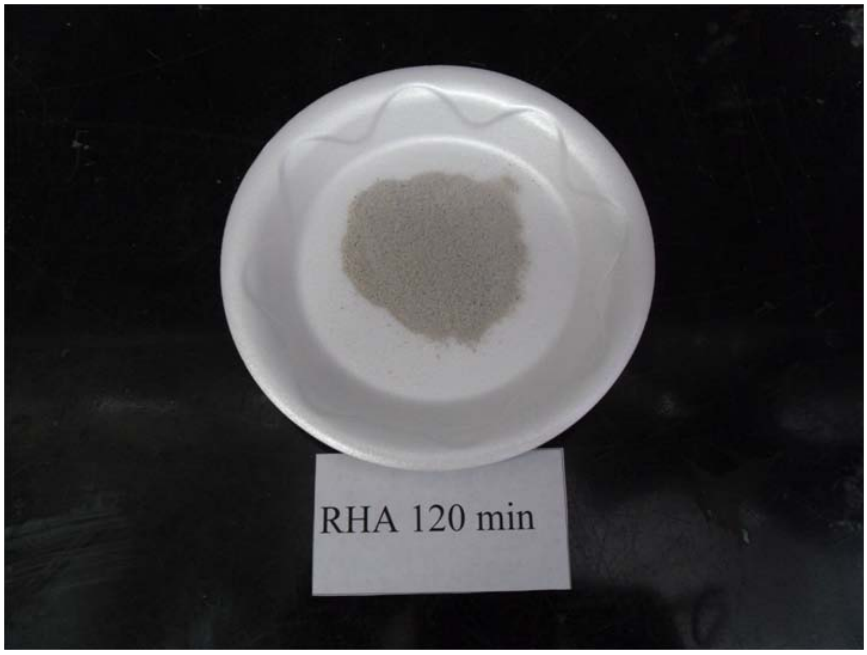

Fig. A.3 - 6– R120

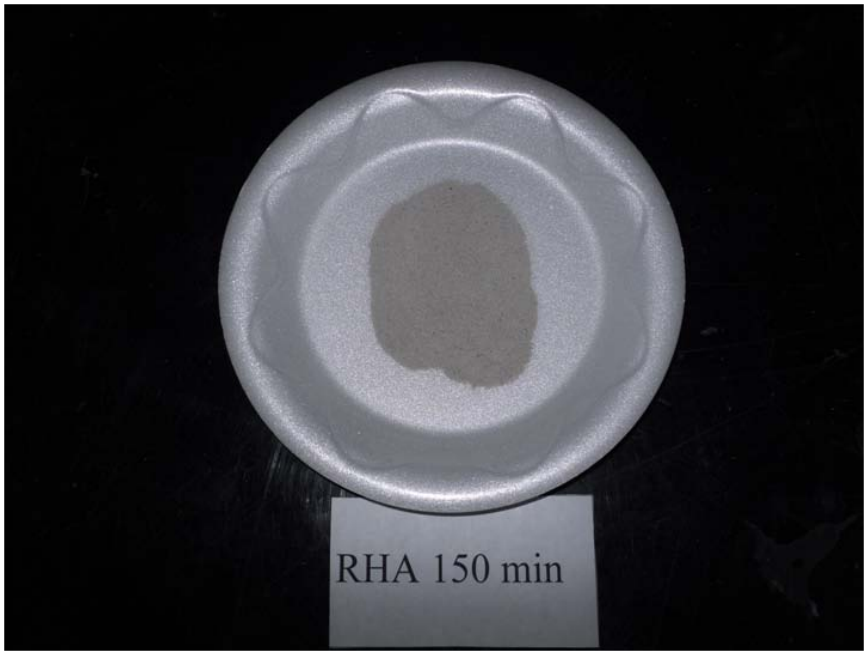

Fig. A.3 - 7– R150

Fig. A.3 - 8– R180

APPENDIX IV: STUDY III – COLOR DEGRADATION ANALYSIS

Fig. A.4 - 1– Three point bending set-up for sample cracking

Fig. A.4 - 2– Series A set-up

Fig. A.4 - 3– Series B set-up

Fig. A.4 - 4– Series C set-up

Fig. A.4 - 5– Spectrophotometer

Fig. A.4 - 6– Spectrophotometry of powder sample

Fig. A.4 - 7– Spectrophotometry of hardened sample